IL
NUOVO CIMENTO
ORGANO DELLA SOCIETÀ ITALIANA DI FISICA
SOTTO GLI AUSPICI DEL CONSIGLIO NAZIONALE DELLE RICERCHE

VOL. XI, N. 4 *Serie decima* 16 Febbraio 1959

Coloration of Biotites by α-Particles in Pleochroic Haloes - II.

S. DEUTSCH (*)

Laboratoire de Physique Nucléaire, Université Libre de Bruxelles - Bruxelles

P. JANSSENS

Institut Technique Supérieur de l'Etat pour les Industries Nucléaires - Bruxelles

(ricevuto il 16 Giugno 1958)

Summary. — The coloration of biotites by α particles has been investigated as a function of the number of displaced atoms. These number has been calculated by means of the theory of F. Seitz. The coloration increases, saturates and diminishes with increasing number of ions.

Amongst the effects caused in solids by the radiation emitted from naturally occurring radioelements, the phenomena of pleochroic haloes is one of the most remarkable.

JOLY [1] has shown that the coloration of the biotite, under the action of α particles, was due, in major part, to the ionization of the atoms of this mineral. The study of the ring structure of haloes with minute inclusions [2]

(*) From the Institut Interuniversitaire des Sciences Nucléaires.

(1) J. JOLY: *Phil. Mag.*, **16**, 381 (1907); **18**, 577 (1909); **19**, 327 (1910).

(2) G. H. HENDERSON and S. BATESON: *Proc. Roy. Soc.*, A **145**, 263 (1934).

and of the artificial coloring of biotites by means of experimental irradiation [3] has confirmed this fact.

The curve of coloration, up to its inversion as a function of the dose of α (in arbitrary units), was obtained by JEDRZEJOWSKI [4] (Fig. 1). The inversion of the coloration has been attributed [5] to the progressive metamictization of the biotite, the α, at the end of their paths displacing the atoms from their lattice sites.

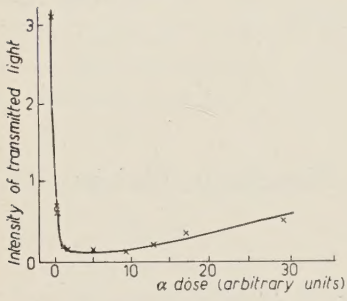

Fig. 1. – Blackening of a biotite of pegmatite by the action of the α-particles (after H. JEDRZEJOWSKJ).

The determination of the quantitative relation existing between the halo colour and the α irradiation doses, which is the object of this note, presents an interest both for an understanding of the phenomena of coloration and in the application of the haloes for an estimation of the ages of rocks [6].

This determination has become possible only since the perfection of the technique of photographic emulsions used in nuclear research, which permits an evaluation of the very low concentrations of uranium and thorium (of the order of $(10^{-10} \div 10^{-13})$ uranium) contained in the radioactive minerals (inclusions) around which the haloes are formed.

Using microphotometric measurements, we have deduced this relation from the study of the coloration of the halo profiles in rocks of known ages [6].

The photoregistered profiles of the haloes give the relation between the intensity of the light transmitted across the irradiated biotite and that across the non irradiated biotite as a function of the distance from the inclusion. The increase in optical density at any point across the halo is easily deduced, being evaluated across a thickness of 30 μm, which is the mean thickness of the thin sections of rock used.

The variation of ΔD across a profile is parallel to and explained by the variation of the number of ions per unit of volume as a function of distance from the inclusion.

For our study, we have chosen haloes with inclusions which may be considered as thick layers (> 40 μm), in order that the coloration be independent of the form and size of the inclusion.

---

[3] G. KURTI: *Ber.*, IIa, **174** (Wien, 1938), p. 401.

[4] H. JEDRZEJOWSKI: *Compt. Rend.*, **135**, (1928).

[5] P. HURLEY and H. FAIRBAIRN: *Bull. Geol. Soc. Am.*, **64**, 659 (1953).

[6] S. DEUTSCH, D. HIRSCHBERG and E. PICCIOTTO: *Bull. Soc. Belg. Géol.*, **65**, 267 (1956); S. DEUTSCH, P. KIPFER and E. PICCIOTTO: *Nuovo Cimento*, **6**, 796 (1957).

1. – The variation of the number of ions with respect to distance from the source.

The variation of the number of ions with respect to the distance from the source, in α-thick layer emission may be calculated after EVANS (7). Fig. 2 gives the distributions p_x^{x+5} of the number of ions formed in 5 μm thick bands of biotite (~ 1 cm air) as a function of their distance from a source containing either one of the U or Th families in equilibrium, or a mixture of the two families in the ratio Th/U = 3.4. Bragg's law has here been considered valid for solids, which implies that the total number of ions formed by the α-particles, as well as their distribution, are the same in the biotite and in the air, taking into account the relative α-stopping power of biotite to air which is of the order of 2 000.

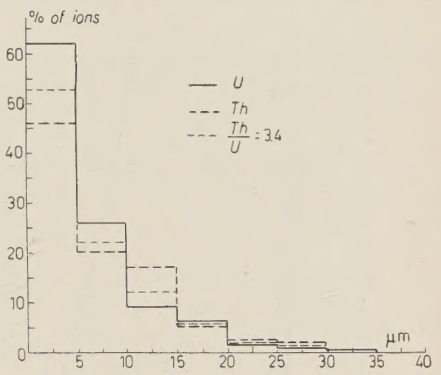

Fig. 2. – Distribution of the number of ions P, formed in the biotite as a function of their distance from an α-thick radioactive source.

2. – The curves of ΔD with respect to the number of ions per unit volume.

The halo profiles having been divided into 5 μm wide bands, the mean optical density increase ΔD has been evaluated for every band. The total number of α per unit surface being known (Q_T), the number of ions N_i per unit volume follows:

$$N_i = 2 \cdot 10^3 \cdot P_x^{x+5} \cdot q \cdot Q_T \ \text{cm}^{-1} ,$$

q is the mean total number of ions formed per α emitted from a thick layer, being of the order of 10^5 for Th/U = 3.4. The factor $2 \cdot 10^3$ cm^{-1} appears in the equation due to the fact that the number of ions has been calculated for a band of 5 μm.

Fig. 3 gives ΔD as a function of N_i for the biotites of the dated granites of Kalule (Congo, 1 000 My.), Allt Mhoille (Scotland, 310 My.), St. Amarin, S^{te} Marie (Vosges, 230 My.), La Bresse (Vosges, 340 My.) and Elba (Italy,

(7) R. EVANS: *Phys. Rev.*, **45**, 29 (1934).

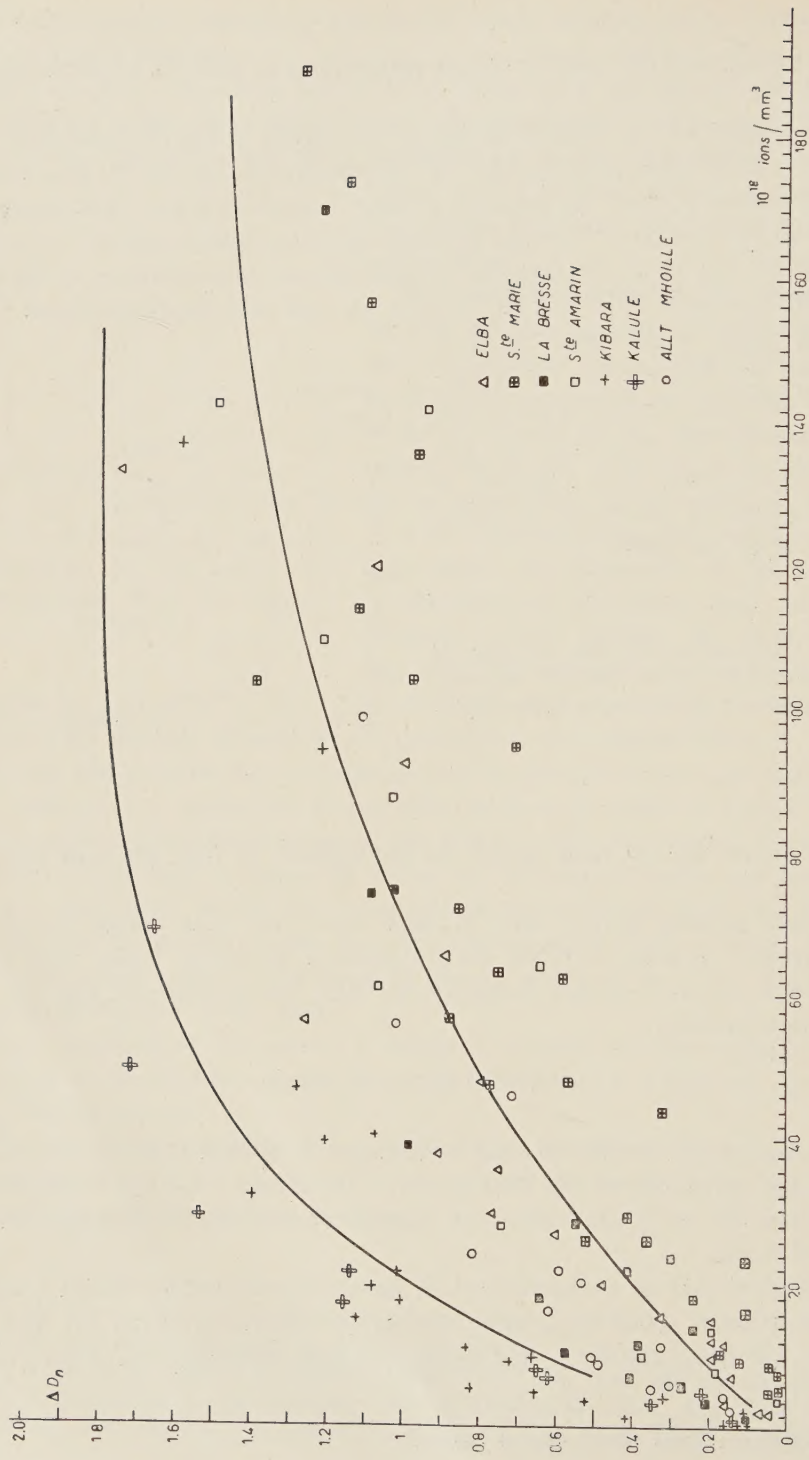

Fig. 3. – Increase in optical density of the haloes as a function of the number of ions per mm³.

30 My.), which have been previously studied ([6]). The various sets of points thus obtained fall in the vicinity of curves of the form

$$\Delta D = \Delta D_{\max}(1 - \exp[-\varrho N_i]),$$

where $\Delta D_{\max}$ is the optical density corresponding to saturation of the coloration, this value being easily deduced from saturated haloes, ϱ is the fraction of the total number of colour centers formed per ion per unit volume.

A parameter S may be introduced where $S = 0.69/\varrho$ is the number of ions necessary in order to obtain an increase in density equal to $\Delta D = \Delta D_{\max}/2$.

Table I gives the values of this parameter for the biotites in question.

TABLE I. – *The parameters ϱ, S and $\Delta D_{\max}$ for the curves of increasing optical density as a function of the number of ions per unit volume in the haloes.*

Rock	$\Delta D_{\max}$	ϱ 10^{-20} mm³/ions	S 10^{18} ions/mm³
Kalule Kibara	1.8	4	18
Allt Mhoille	1.2	3.7	20
St-Amarin Ste Marie	1.4	1.4	50
La Bresse	1.5	1.7	40
Elba	1.8	1.9	36

It is noted that the higher the values of $\Delta D_{\max}$ and ϱ, the higher is the sensitivity of the biotite to α irradiation. The commencement of the coloration appears for doses of the order of 10^{18} ions/mm³. The values set out cannot be given more precisely because:

1) The ratio Th/U of the inclusion is not measurable.

2) The uncertainties in the α activity and in the age of the rocks are, at best, of the order of 10%.

3) A part of the coloration is due to the displacement of the atoms at the end of the α-particle path, when the particle has ceased to cause ionization.

The distribution of the α path endings, with respect to their distance from a α-thick source, may be calculated after FINNEY and EVANS ([8]) (Fig. 4). The

([8]) G. FINNEY and R. EVANS: *Phys. Rev.*, **48**, 503 (1935).

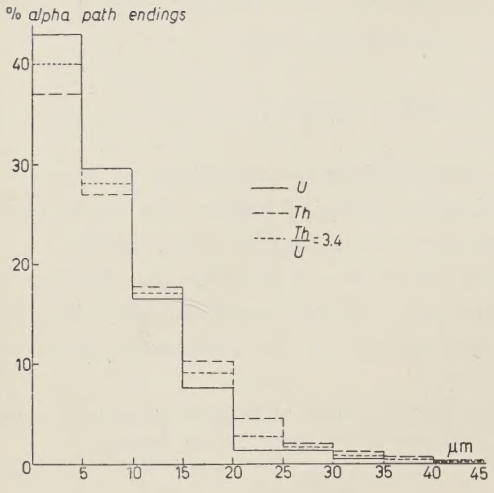

Fig. 4. – Distribution of the number of α-particles V ending in the biotite as a function of their distance from an α-thick radioactive source.

ratio of the number of α endings to the number of ions per unit volume remains relatively constant for all distances from the source; the α path ending effect cannot, therefore, be evaluated from a study of the profiles of non-annular haloes.

The biotites thus indicate different sensitivities to α irradiation, the order of sensitivity being Congo > Allt Mhoille > Elba > Bresse > St. Marie. In Fig. 3, two curves only have been traced in order to demonstrate this more clearly: the curve corresponding to the granites of the Congo, and a mean curve for the other biotites.

3. – Inversion of the coloration.

An analysis of the profiles of inversed haloes gives us information on the curve of the coloration of the biotite, with respect to the ionization caused by strong doses of α, an inversed halo being a halo which presents an inversion of coloration, at least at the beginning of its radius.

Fig. 5 presents the typical appearance of the profile of an inversed halo. The halo itself is shown in the Fig. 6, which is focussed on the biotite, through the nuclear emulsion, the α-particles emitted by the inclusion being visible as well.

It has been shown (6) that approximately 10^{17} α/cm² are necessary in order

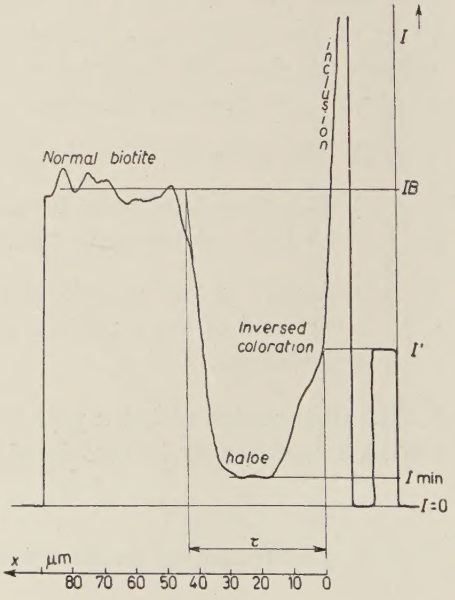

Fig. 5. – Photoregistered profile of the inversed haloe shown in photo 6.

Fig. 6.

to form an inversed halo in the case of rocks from the Vosges and from Scotland.

Figs. 7*a* and 8*a* show the increase in optical density ΔD with respect to

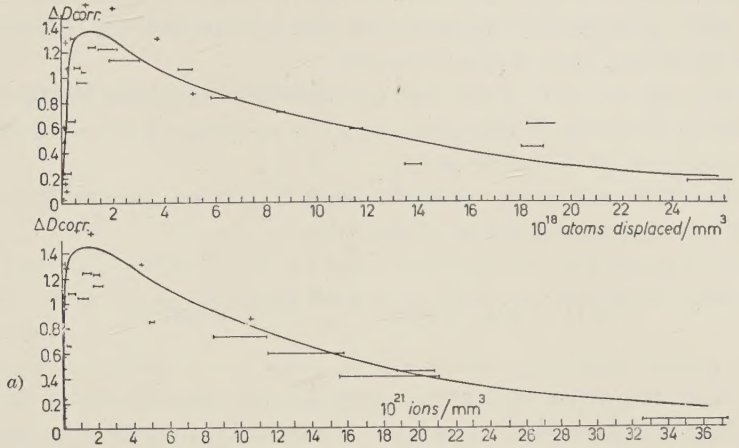

Fig. 7*a*, *b*. – *a*) Increase in optical density as a function of the number of ions produced per mm³, after the inversed haloes of La Bresse; *b*) Increase in optical density as a function of the number of atoms displaced per mm³ after the inversed haloes of La Bresse.

the number of ions per unit volume for the granites of La Bresse and St. Amarin; haloes of a radius > 40 μm have been considered as due to either Th/U = 3.4 or Th alone.

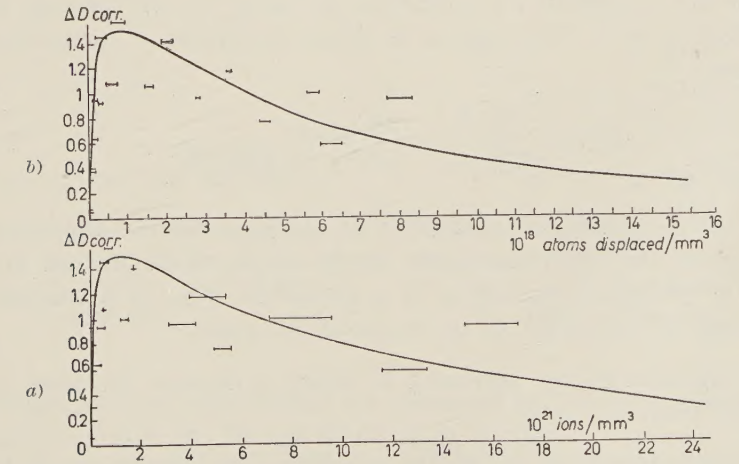

Fig. 8*a*, *b*. – *a*) Increase in optical density as a function of the number of ions produced per mm³, after the inversed haloes of St. Amarin; *b*) Increase in optical density as a function of the number of atoms displaced per mm³ after the inversed haloes of St. Amarin.

A halo with a radius $r = 36$ (RaC') was attributed to the action of the α-particles due to the uranium family alone.

ΔD with respect to the number of ions per unit volume shows a rapid increase, which is studied in detail in the case of non inversed haloes, followed by a saturation and then a slow decrease.

The value of the ratio U/Th has an important influence on the value of N_i, and the uncertainty in this ratio prohibits anything but a numerical order of the importance of N_i to be given.

The saturation exists for doses of from $2 \cdot 10^{20}$ to $2.4 \cdot 10^{21}$ ions/mm^3 according to an exponential curve of the type

$$\Delta D = \Delta D_{max} \exp\left[-\frac{0.69}{S'} N_i + 0.166\right],$$

where S' is of the order of 10^{22} ions/mm^3 for the biotites of La Bresse and St. Amarin. This dose corresponds to a diminution of the optical density $\Delta D = \Delta D_{max}/2$, obtained after the saturation. The inversion of the coloration in the biotite is a slower phenomenon than the coloration which explains the paucity of totally inversed haloes.

The shape of the coloration curve of the granitic biotites deduced from their haloes is seen to resemble the curve obtained by the experimental irradiation of the biotites of pegmatite by JEDRZEJOWSKI.

4) *a*) An approximative evaluation of the number of atoms displaced by an α-particle of energy E, penetrating into a solid, may be carried out according to the theoretical considerations of SEITZ (9). We use his notations in the following text. The number of atoms displaced by an incident α-particle is thus:

$$\text{(I)} \qquad N_{(E)} = \frac{R_d \cdot E_c}{\sqrt{E \cdot E_d}} = \left(\frac{E_c}{E_d}\right) \sqrt{\frac{\overline{E}}{E_d}} \cdot \frac{1}{\log E/E^*},$$

where E_c is the amount of energy lost by the α-particle in displacing atoms. E_c depends on the mean ionization energy of the medium and on ε_t, the threshold of electronic excitation, of a numerical order of a fraction of the lowest energy of excitation of the material traversed.

E_d: the minimum energy necessary in order to displace an atom from his lattice site;

E^*: the minimum energy which the α-particle can transmit to an atom;

$\overline{E}$: the mean kinetic energy transmitted to a displaced atom.

(9) F. SEITZ: *Disc. Farad. Soc.*, **5**, 271 (1949).

Certain parameters which can be determined with great difficulty intervene in the expression for $N_{(E)}$. In order to indicate the extreme limits of the values, we have calculated (I) for an ensemble of values for these parameters, in the case of the biotite E lying between 0.5 and 10 MeV and $E_d = 10$, 25, 50 eV.

It appears that the second factor

$$\sqrt{\frac{E}{E_d}} \cdot \frac{1}{\log E/E^*},$$

remains practically constant in the region considered, and has a value of 0.16.

On the other hand, the first factor depends on the three values E, E_d, E_c or ε_t.

We have determined the value of the mean ionization energy from the path-energy relation of the α-particles in the biotite, and found it to be 240 eV. The energy ε_t is difficult to determine, we have chosen the values 0.1, 0.25, 0.50, 0.75, 1.0 and 1.50 eV in our calculations.

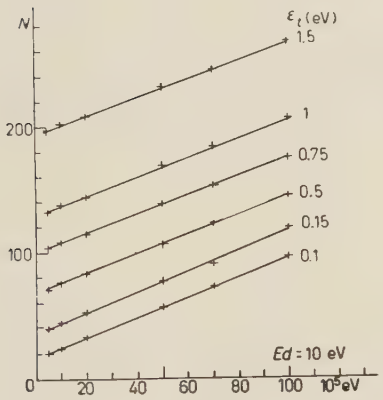

Fig. 9. – Number of the displaced atoms as a function of the energy of the α for $E_d = 10$ eV and different values of ε_t.

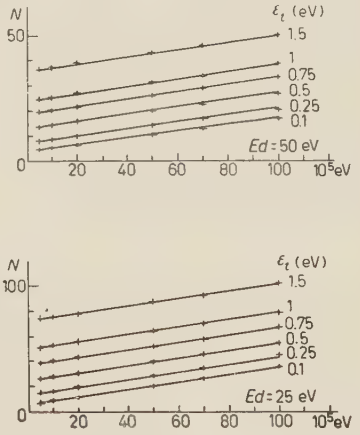

Fig. 10. – Number of the displaced atoms as a function of the energy of the α for $E_d = 50$ eV and 25 eV and different values of ε_t.

The results of these calculations are presented in the three graphs relative to the values of $E_d = 10$, 25 and 50 eV (Figs. 9, 10).

We have, here, shown N as a function of E for the different values of ε_t.

It will be noted that, for a certain medium (E_d and ε_t remaining constant), the number of atoms ejected increases in proportion to the energy E of the particle.

On the other hand, N depends on the values of E_d and ε_t, the former of which depends essentially on the composition of the medium, the latter, on its structure also.

By comparison with analogous elements, the most reasonable values appear to be $E_d = 25$ eV and $\varepsilon_t = 0.75$ eV, which, for α of 5 MeV in the biotite gives a value of N equal to

$$N = (55 \pm 25) \text{ displaced atoms}.$$

b) ΔD may be evaluated as a function of the number of atoms displaced in every 5 μm thick band of the inversed haloes (from the number of α endings). The Figs. 7*b* and 8*b* show such a function for the biotites of La Bresse and St. Amarin. It is seen that S_d, the number of atoms displaced corresponding to an inversion of the coloration such as $\Delta D = \Delta D_{\max}/2$, is of the order of $0.5 \cdot 10^{19}$ displaced atoms per mm³, or, in other words, about $1.5 \cdot 10^{18}$ atoms per milligram of biotite. As 1 mg of biotite contains $9 \cdot 10^{19}$ atoms, the fraction of atoms displaced is of the order of 2%. The same line of reasoning applied *to the almost complete effacement of the coloration, which is due to the displacement of about* $2 \cdot 10^{19}$ *atoms per mm³*, attributes this effacement to the displacement of about 10% of the total number of atoms. Such a small fraction of displaced atoms invalidates an explanation of the inversion of the coloration as a result of the phenomenon of metamictization, which only appears when at least 25% of the atoms have been displaced. This reasoning concords with the approximate evaluations of PELLAS ([10]).

4. – Conclusions.

The microphotometric study of the haloes, and the measurement of the activity of the inclusions, in rocks of known age, has enabled the determination of a quantitative law governing the increase in the coloration of the biotite as a function of the number of ions formed. The curve of the optical density increase ΔD consists of three parts:

1) An increasing part: the coloration increases according to an approximate law of the form

$$\Delta D = \Delta D_{\max}\left(1 - \exp\frac{-0.69 N_i}{S}\right),$$

where N_i is the number of ions formed per mm³.

([10]) P. PELLAS: *Bull. Soc. Fr. Min. et Crist.*, **77**, 447 (1954).

S is the number of ions per mm^3 necessary in order to obtain an increase in optical density equal to

$$\Delta D = \frac{\Delta D_{max}}{2},$$

ΔD_{max} is the increase in density corresponding to the saturation of the coloration.

The coloration commences after the formation of about 10^{18} ions/mm^3.

The parameters S and ΔD_{max} vary from one biotite to another; S being of the order of 10 to $50 \cdot 10^{18}$ ions/mm^3, and ΔD_{max} lying between 1.2 and 1.8 for a photometered thickness of 30 μm.

2) A horizontal part: the coloration being saturated for doses from $2 \cdot 10^{20}$ to $2.4 \cdot 10^{21}$ ions/mm^3.

3) A decreasing part: the coloration diminishing for doses from $2.4 \cdot 10^{21}$ to $7 \cdot 10^{22}$ ions/mm^3. This inversion cannot be explained as a metamictisation of the biotite as the inversion of the coloration is almost complete with only about 10% of the lattice atoms having been displaced.

* * *

We are indebted to Mr. P. Kipfer and E. Picciotto for many helpful discussions.

RIASSUNTO (*)

È stata esaminata la colorazione delle biotiti da parte delle particelle α come funzione del numero di atomi dislocati. Tale numero è stato calcolato in base alla teoria di F. Seitz. La colorazione aumenta, si satura e diminuisce con numero crescente di ioni.

(*) *Traduzione a cura della Redazione.*

IL NUOVO CIMENTO Vol. XI, N. 4 16 Febbraio 1959

An Experimental Analysis of Two Large Cosmic Ray Jets.

F. A. Brisbout and C. B. A. McCusker (*)

The F.B.S. Falkiner Nuclear Research and Adolph Basser Computing Laboratories, School of Physics (**), The University of Sydney - Sydney N.S.W.

(ricevuto il 2 Ottobre 1958)

Summary. — The true primary energy of two large jets has been estimated from a study of the secondary interactions and the electromagnetic cascades resulting from the decay of π^0-mesons. This is compared with the energy estimated from $\gamma_p = 2/\mathrm{tg}^2\,\eta$ and found, in both cases, to be much greater. However, good agreement with the estimate of primary energy obtained using the tunnel theory of jets is found.

1. – Introduction.

One of the predictions of the tunnel theory (1) of cosmic ray jets is that, in many cases (particularly those where a central collision with silver and bromine has occurred), the true primary energy will be much greater than the energy estimated from formulae (such as $\gamma_p = 2/\mathrm{tg}^2\,\eta$) which assume nucleon-nucleon collisions. Until about 1955 the only way in which this prediction could be in any way verified was by the good fit obtained on a $\log f$-$\log E$ diagram (see ref. (1)) of all jets, or the comparison of events at the same γ_p such as the Bristol jets, 0+4p and 0+28p at $\gamma_p = 2\,000$. With the coming of larger stacks however the possibility arose of getting an independent esti-

(*) Visiting Professor from the Institute for Advanced Studies, Dublin.

(**) Also supported by the Nuclear Research Foundation within the University of Sydney.

(1) F. C. Roesler and C. B. A. McCusker: *Nuovo Cimento*, **10**, 127 (1953).

mate of the true primary energy either from relative scattering of the secondaries or from a study of the secondary interactions or the electromagnetic cascades. The first method was possible with the Turin jet ([2,3]). The second method is applied to two large jets in this paper. The jets are of the type 18+56p, $\gamma_p = 2500$ (P_4) and 23+152p $\gamma_p = 7000$ (P_8). Because of the importance of the correct derivation of the primary energy in the study of the jets themselves, in the verification of the tunnel theory, and in the study of the cosmic ray energy spectrum, the methods used are given in some detail.

2. – Selection of events.

In order to determine the primary energy with some accuracy by a study of the electromagnetic cascades and of the secondary interactions, it is necessary to select events which have as large a number of cascades and interactions as possible. This means, in practice, that the method is applicable to jets with a large number of shower particles which themselves traverse a considerable quantity of emulsion. It is a fortunate circumstance that jets of large n_s are most likely to arise from central collisions with silver or bromine, for in this case the discrepancy between the energy estimated assuming a nucleon-nucleon collision and the true primary energy will be greatest and also the effects of a possibly large elasticity in the individual nucleon-nucleon collisions will be greatly reduced.

Two of the available jets, namely P_4 and P_8 ([4]) satisfied these criteria.

3. – The angular distribution of the shower tracks.

The angular distributions of the shower tracks for P_4 and P_8 are shown in Fig. 1 and 2. Target diagrams for the more centrally emitted tracks are given in Fig. 3 and 4. The values of γ_p, calculated from the median angle using

$$\gamma_p = \frac{2}{\mathrm{tg}^2\,\eta},$$

are 2500 for P_4 and 7000 for P_8.

([2]) A. Debenedetti, C. M. Garelli, L. Tallone and M. Vigone: *Nuovo Cimento*, **4**, 1142 (1956).

([3]) C. B. A. McCusker and F. C. Roesler: *Nuovo Cimento*, **5**, 1136 (1957).

([4]) F. A. Brisbout, C. Dahanayake, A. Engler, Y. Fujimoto and D. H. Perkins: *Phil. Mag.*, **1**, 605 (1956).

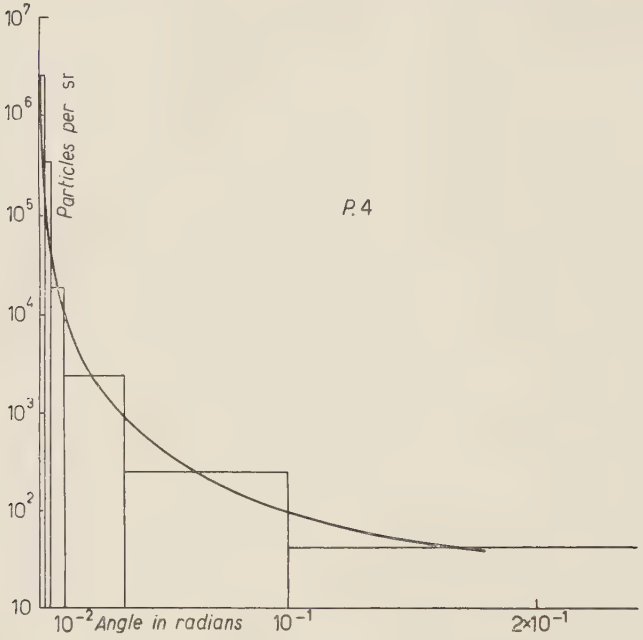

Fig. 1. – The angular distribution of the shower tracks in P_4.

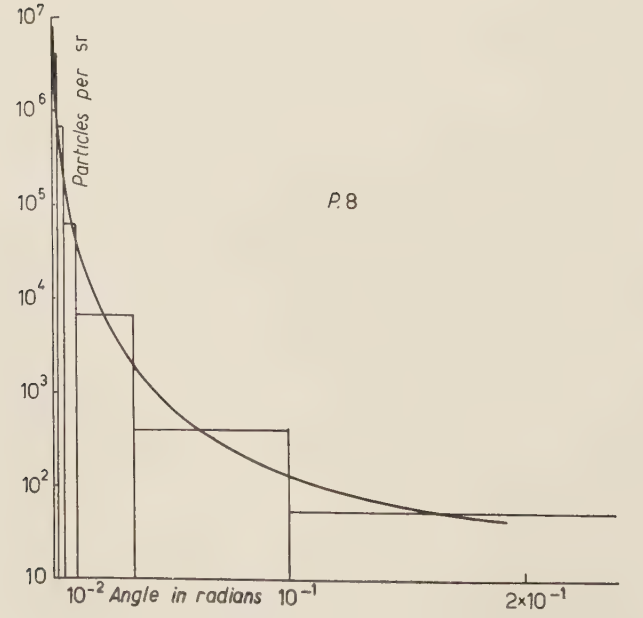

Fig. 2. – The angular distribution of the shower tracks in P_8.

Fig. 3. – Target diagram for P_4.

It is of interest to compare these two jets with others of similar γ_p. For instance DANIEL *et al.* (5) found two jets with $n_s = 7$ and γ_p respectively 2200

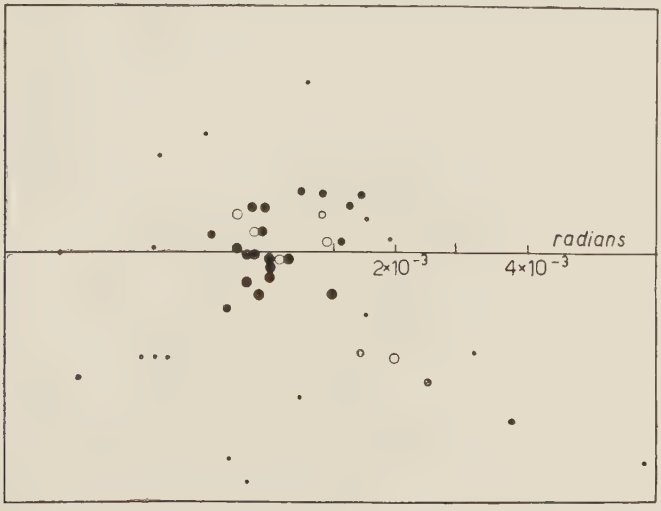

Fig. 4. – Target diagram for P_8. Open circles correspond to particles producing a secondary interaction. The size of the circle is a rough indication of the energy of the particle.

(5) R. R. DANIEL, J. H. DAVIES, J. H. MULVEY and D. H. PERKINS: *Phil. Mag.*, **43**, 753 (1952).

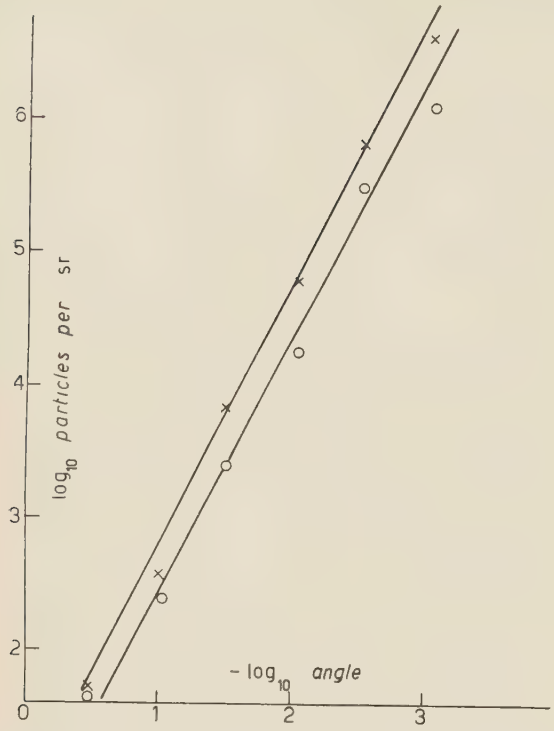

Fig. 5. – A double logarithmic plot of the angular distributions in P_4 and P_8. The lines represent a law of the form Density $\propto 1/\theta^2$.

and 2300 and KAPLON and RITSON (6) found a jet with $n_s = 14$ and $\gamma_p = 7200$.

It can be seen from Fig. 5 that the number of tracks per steradian falls off approximately as the inverse square of the angle of emission in both cases. The average energy of the particles, as will be shown later, also falls off rapidly with the angle of emission. In such circumstances, if one wishes to get a reasonably accurate value for the total energy by estimating an average and then multiplying this by the number of particles, one must split the target diagram into a number of annuli, carry out this procedure separately for each and then sum the separate values.

For this reason the target diagram in both cases was subdivided as shown in Fig. 6

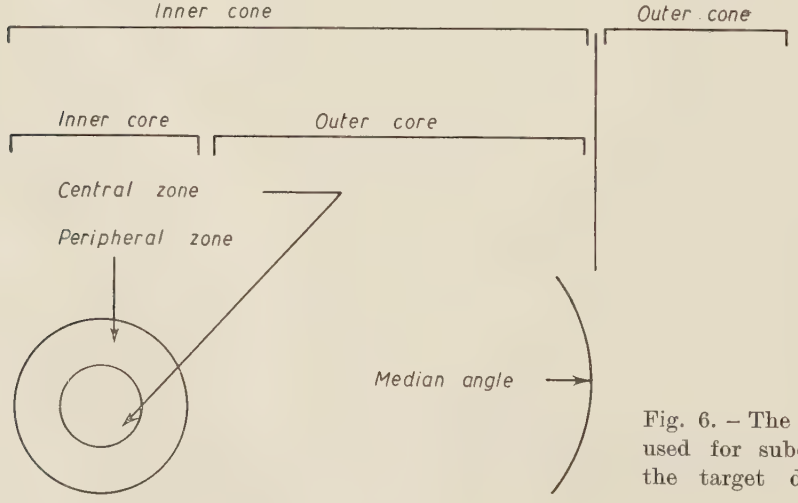

Fig. 6. – The method used for subdividing the target diagram.

(6) M. F. KAPLON and D. RITSON: *Phys. Rev.*, **88**, 386 (1952).

The median angle is used to define two areas known as the inner and outer cones. The inner cone was then further subdivided into the inner and outer cores on the basis of the observed density of tracks. The inner core was then split into the central and peripheral zones, the central zone containing the particles of very high energy. Inspection of the average energies of the particles in the various annuli in Table I will make it obvious that this rather involved procedure is necessary.

TABLE I. – *This gives the angle of emission and γ_s for the various secondary interactions of jets P_4 and P_8 and the average γ_s for the various zones.*

Jet	Annulus	Secondary interaction	Angle of emission in rad	γ_s	Average γ_s
P_4	*Inner Core* Central zone	P_4S_{26}(5+23p)	$2 \cdot 10^{-4}$	2400	1000
		P_4S_{27}(4+34p)	$4 \cdot 10^{-4}$	400	
		P_4S_{29}(12+20p)	$6 \cdot 10^{-4}$	300	
	Peripheral zone	P_4S_{20}(13+ 8p)	$2.0 \cdot 10^{-3}$	900	400
		P_4S_{22}(15+10p)	$2.1 \cdot 10^{-3}$	200	
		P_4S_{24}(10+15p)	$2.6 \cdot 10^{-3}$	100	
	Outer Core	P_4S_{36}(0+ 5p)	$1.7 \cdot 10^{-2}$	30	—
P_8	*Inner Core* Central zone	P_8S_{11}(11+14p)	$0.5 \cdot 10^{-4}$	5000	2800
		P_8S_R(x+> 7p)	$1 \cdot 10^{-4}$	> 1000	
		P_8S_{10}(x +23p)	$3 \cdot 10^{-4}$	500	
	Peripheral zone	P_8S_7 (16+32p)	$8 \cdot 10^{-4}$	300	200
		P_8S_5 (3+25p)	$9 \cdot 10^{-4}$	200	
		P_8S_8 (23+25p)	$9 \cdot 10^{-4}$	100	
		P_8S_9 (8+ 9p)	$2.3 \cdot 10^{-3}$	3000	3000
	Outer Core	P_8S_6	$2.3 \cdot 10^{-3}$	80	—
		P_8S_3	$3.9 \cdot 10^{-3}$	40	—

4. – The determination of the primary energy from the secondary interactions.

The inner cones of jets P_4 and P_8 were scanned for secondary interactions using the methods of BRISBOUT *et al.* (1). It is essential that only second gene-

ration interactions be included. For events produced by charged shower particles one can make sure of this by tracing back the primary. For interactions produced by neutral particles this is not so and hence these were excluded. Table I shows the various interactions observed, the angles of emission of their primaries, their γ_s and the average γ_s for the various annuli. Two of the secondary interactions require some comment. The interaction P_8S_R occurred in an emulsion sheet which was destroyed when the stack landed. The shower tracks of the inner core were observed in the next emulsion and an estimate of γ_s was made from there, and also by means of relative scattering measurements on the primary tracks of P_8S_R and P_8R_{11}.

Event P_8S_9 occurred near the very noticeable « side core » seen at the target diagram shown in Fig. 7. It is of anomalously high energy for a track at such an angle and has been classed as being in the central zone.

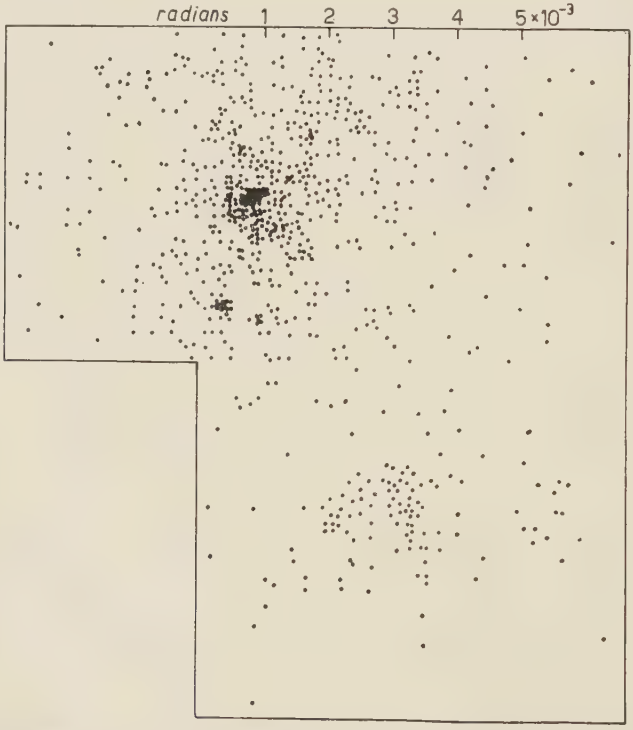

Fig. 7. – Diagram showing the development of the electromagnetic cascade in P_8 at a distance of about four cascade units from the origin.

Having obtained the average energy of the particles in each annulus it is then necessary, if one wishes to obtain the total energy, to multiply these averages by the number of particles in each annulus. Since only the charged

particles leave visible tracks, the number of charged particles in each annulus must be multiplied by a factor to allow for the neutral particles. The total number of shower particles n_T is given by

$$n_T = n_s \{1 + 0.4 + 0.25\} \approx 1.7\, n_s ,$$

where the second and third factors give the numbers of neutral pions and non pions respectively.

Using this factor and the values for $\langle \gamma_s \rangle$ given in Table I then, the primary energies of P_4 and P_8 are calculated in Table II.

TABLE II. – *The table shows the number of shower particles, their average γ_s and the total energy for each annulus. The total energy for the two jets is also given. The particles in the outer cone are neglected because of their very low average energy.*

Jet	Annulus	n_s	$\langle \gamma_s \rangle$	$1.7 n_s \langle \gamma_s \rangle$
P_4	Central zone	6	1 000	10 200 GeV
	Peripheral zone	9	400	6 100
	Outer core	13	20	440
			Total	16 740
P_8	Central zone	7+1	2 800	38 100
	Peripheral zone	16	200	5 400
	Outer core	54	50	4 600
			Total	48 100

5. – The determination of the primary energy from the electromagnetic cascades.

For each jet target diagrams of all tracks were made at intervals of about one conversion length (~ 4 cm). One target diagram for P_8 is shown in Fig. 7. In the case of P_4 and the outer core of P_8 each cascade was traced back to *its parent electron pair* (*). The cascades from the parent electron pairs in P_4

(*) This method of detecting parent electron pairs was checked against that of BRISBOUT *et al.* and found to be 100% efficient.

which materialized before the first secondary interactions were analyzed with respect to their lateral spreads (7), using a radius of about 50 μm and suitable background corrections. The γ-ray energies thus obtained are shown in Table III. It proved to be impossible to treat P_8 in this detailed manner, because the cascades intermixed at too early a stage.

TABLE III. – *This gives the γ-ray and π^0-meson energies for ten cascades of P_4. The average energy for each annulus is also given.*

Jet	Annulus	Cascade	γ-ray energy		π^0-meson energy	Weighted mean zone energy	Minimum π-meson energy from spatial angle between pairs
	Central zone	1	500÷600 GeV	paired	(1 000÷ ÷1 200) GeV		1 000 GeV
		2	500÷600 GeV				
		3	400 GeV	paired	600 GeV	800	500 GeV
		4	200 GeV				
P_4	Peripheral zone	5	200 GeV	paired	300 GeV	—	200 GeV
		7	100 GeV				
		6	100 GeV	unpaired	200 GeV taken as twice γ-ray energy	250	—
		8	100 GeV	unpaired	200 GeV	—	—
	Outer core	9	low energy 15 GeV	unpaired	30 GeV	20	—
		10	low energy 5 GeV	unpaired	10 GeV		—

Once again the average energy of a particle in each annulus must be multiplied by the total number of particles in the annulus in order to get the total energy. As before, n_s, the number of charged shower particles must be multiplied by 1.7 to allow for the unseen neutral particles. It is worth noting, that the total energy obtained in this case will probably be an underestimate for there is some evidence that the average energy carried off by pions is less than that carried off by non pions. (8). Table IV shows the experimental results for P_4.

It is, perhaps, worth saying a little more about the cascade development in P_8. It can be seen from Fig. 7 that there is a very marked « side shower »,

(7) K. PINKAU: in the press.

(8) B. EDWARDS, J. LOSTY, D. H. PERKINS, K. PINKAU and J. REYNOLDS: *Phil. Mag.*, **3**, 237 (1958).

TABLE IV. - *This gives n_s the number of shower particles and their average energy for each annulus for jet P_4 and the estimated total energy of the jet.*

Jet	Annulus	n_s	$\langle E_{\pi^0} \rangle$	$1.7 n_s \langle E_{\pi^0} \rangle$
P_4	Central zone	6	800	8 250 GeV
	Peripheral zone	9	250	3 820 GeV
	Outer core	13	8	170 GeV
			Total	12 240 GeV

that is, there are two *spatially* separated regions of high electron density in the target diagram. The smaller of these regions appear to be associated with the secondary interaction $P_8 S_9$ of anomalously high energy which was previously noted. If phenomena such as this occur at higher energies, they might explain some of the peculiar air shower distributions which have been noted [9,10] from time to time.

6. - Determination of the primary energy using tunnel theory.

In determining the primary energy using any cascade theory one must first ascertain, as far as possible, the path length of the cascade through nuclear matter. A very simple method of doing this is given in detail in ref. [1] and [3]. Briefly, one takes the two experimental parameters n_s and γ_p and, using the formula given by the theory, one computes f, the multiplicity parameter, and E', the primary energy on each of the two extreme assumptions, that the event was a nucleon-nucleon collision and that the event was a central collision with silver. From the positions of the two points on a log f-log E' plot, the path length through nuclear matter can be estimated. The calculation takes about five minutes.

Treating P_4 in this way one finds that it was due to a central or near central collision with silver. According to the theory the primary energy is then given by

$$E'_{\text{GeV}} = 5.76\, \gamma_p = 14\,400 \text{ GeV} .$$

[9] T. E. CRANSHAW and W. GALBRAITH: *Proc. Oxford Conf.* (1956), A.E.R.E. Report.
[10] C. CLARK, J. EARL, W. KRAUSHAAR, J. LINSLEY, B. ROSSI and F. SHERB: *Nature*, **180**, 353 (1957).

The position with regard to P_8 is rather more complicated. The $\log f$-$\log E'$ diagram suggests that the path length through nuclear matter was greater than that across the diameter of a silver nucleus. This, of course, is assuming that the primary particle was a proton with the usual geometric interaction cross-section. Two ways out of this difficulty suggest themselves:

a) One can assume that at an early stage in the cascade a particle was scattered at an anomalously wide angle, resulting in the formation of a side tunnel, or an enlargement in one direction of the diameter of the main tunnel or

b) One can assume that the primary was a deuteron ([11]).

Alternative *b*) is attractive because on this assumption one obtains an excellent fit on the $\log f$-$\log E'$ diagram. The possibility of deuterons occurring as the primaries of jets has been envisaged by DILWORTH *et al.* Indeed it seems very likely that the proportion of deuterons in the primary cosmic ray beam is much higher than in the universe as a whole. Deuterons can be found as fragmentation products of heavy nuclei ad α-particles in collisions both with interstellar matter and with the atmosphere above the balloon flight level. The proportion of deuterons and tritons in singly charged particles from stars in emulsion is ~ 30 percent ([12]). Assuming that the primary particle was a deuteron, its primary energy per nucleon is given by

$$\tfrac{1}{2} E'_{\mathrm{GeV}} = 5.29\, \gamma_{\mathrm{p}}$$

that is, the total energy was 74 000 GeV. This is considerably higher than the estimate from the secondary interactions, but it must be remembered that this last may well be an underestimate.

7. – Conclusions.

For jet P_4 the primary energy estimated assuming a nucleon-nucleon collision was 2 500 GeV. The energy estimated from a study of the secondary interactions was 16 740 GeV and from a study of the electromagnetic cascades was 12 200 GeV. An application of the Tunnel Theory of jets suggested that the event was a central collision with silver and gave an estimate of 14 400 GeV for the primary energy. The good agreement in the last three cases is obvious.

For P_8 the energy estimated assuming that it was a nucleon-nucleon col-

---

([11]) C. C. DILWORTH, S. J. GOLDSACK, T. F. HOANG and L. SCARSI: *Nuovo Cimento*, **10**, 1261 (1953).

([12]) U. CAMERINI, W. O. LOCK and D. H. PERKINS: *Progr. in Cosmic Ray Phys.*, vol. **1**.

lision is 7 000 GeV. The estimate from the study of the secondary interactions is 48 100 GeV and from the Tunnel Theory, assuming that the primary is a proton, 49 000 GeV. In both cases, therefore, it is very difficult to get agreement with the assumption that the events are nucleon-nucleon collisions, but good agreement can be obtained with the energy estimates based on the Tunnel Theory for a central collision with silver.

* * *

We are grateful to Professor H. MESSEL for the hospitality of his laboratories and to Dr. A. J. HERZ for many interesting discussions.

Also one of us (F. B.) wishes to thank Professor POWELL (H. H. Wills Physical Laboratory, Bristol) for the hospitality of his laboratory and Mrs. HERMAN for technical assistance in the analysis of the interactions and electromagnetic cascades.

RIASSUNTO (*)

L'energia primaria vera di due grandi getti è stata ricavata dallo studio delle interazioni secondarie e delle cascate elettromagnetiche risultanti dal decadimento dei mesoni π^0. Si confronta il risultato con l'energia ricavata dalla formula $\gamma_p = 2/\mathrm{tg}^2\,\eta$ e si trova, per ambo i getti, che essa è molto maggiore. Si ha, tuttavia, un buon accordo col valore dell'energia primaria ottenuto in base alla teoria del tunnel applicata ai getti.

(*) *Traduzione a cura della Redazione.*

IL NUOVO CIMENTO Vol. XI, N. 4 16 Febbraio 1959

On Extended Conformal Transformations of Spinors and Spinor Equations.

H. A. Buchdahl (*)

Physics Department, University of Tasmania - Hobart

(ricevuto il 27 Ottobre 1958)

Summary. — This paper deals in the first place with the behaviour of spinors of arbitrary valence, and of their first derivatives, under transformations of the extended conformal group C, whose elements are basically the transformations of the metric according to ${}'g_{kl}=\lambda g_{kl}$, where λ is an arbitrary positive function of the coordinates. The results obtained are applied to certain relativistic equations for fields associated with particles of arbitrary spin S. It is shown that: (i) if the mass-scalar $\varkappa$ which occurs in them is taken to be a conformal invariant, then the equations cannot be invariant under C for *any* value of S; (ii) if $\varkappa$ is taken to be a conformal covariant, then the equations can be invariant under C only if they are reflection-invariant and S is half-odd integral, and the subsidiary equations are imposed *after* transformation, *i.e.* they are not themselves required to be invariant; (iii) if the conformal invariance of the subsidiary equations also is required then the only equations which can be invariant under C are Dirac's equations ($S=\frac{1}{2}$) with conform-covariant mass-scalar, the subsidiary equations being absent in this case.

1. – Introduction.

The conformal behaviour of relativistic wave equations has been considered previously on a number of occasions, *e.g.* by Dirac (1), Bhabha (2), McLennan (3,4), Gürsey (5), Pauli (6), Bludman (7), *et al.* Most of these papers,

(*) Present address: Institute for Advanced Study, Princeton, N. J.

(1) P. A. M. Dirac: *Ann. Math.*, **37**, 429 (1936).

(2) H. J. Bhabha: *Proc. Camb. Phil. Soc.*, **32**, 622 (1936).

(3) J. A. McLennan jr.: *Nuovo Cimento*, **3**, 1360 (1956).

(4) J. A. McLennan jr.: *Nuovo Cimento*, **5**, 640 (1957).

(5) F. Gürsey: *Nuovo Cimento*, **3**, 988 (1956).

(6) W. Pauli: *Helv. Phys. Acta*, **13**, 204 (1940).

(7) S. A. Bludman: *Phys. Rev.*, **107**, 1163 (1957).

in particular the first five of those just referred to, deal with the *restricted* conformal group C_0, which consists of all transformations of co-ordinates which are such that they transform the galilean metric tensor η_{kl} into a metric tensor γ_{kl} whose components differ from those of the former only by a common factor, *i.e.*

$$\gamma_{kl} = \lambda\eta_{kl}\,, \tag{1.1}$$

where λ may be a function of the co-ordinates. As discussed by McLennan ([4], § 4) all the transformations of C_0 can be obtained from the space and time reflections together with the transformations of the restricted proper conformal group C_0^+. The latter is defined by its fifteen independent infinitesimal transformations

$$\left|\begin{array}{ll} {}'x^k = x^k + \beta^k & \\ {}'x^k = x^k + \omega^k{}_l x^l & (\omega_{(kl)} = 0) \\ {}'x^k = (1+\nu)x^k & \\ {}'x^k = (1 + 2\alpha_l x^l)x^k - \alpha^k x_l x^l\,, & \end{array}\right. \tag{1.2}$$

β^k, $\omega^k{}_l$, ν and α^k being infinitesimal parameters.

In the context of relativistic wave equations the extended conformal group C seems to have been considered rather more rarely. In particular Pauli ([6]) has examined the behaviour of Dirac's equations under C; that is, the effect on the equation of the replacement of η_{kl} by $\lambda\eta_{kl}$, where λ is an *arbitrary* (positive) function of the co-ordinates. Given $\lambda({}'x)$, there will of course in general be no transformation of co-ordinates ${}'x = f(x)$ such that $\gamma_{kl}({}'x) = \lambda({}'x)\eta_{kl}$. In the present paper I consider the conformal behaviour under C of spinors of arbitrary valence and their first derivatives, and of certain general wave equations constructed from them. For this purpose the spinor analysis of Infeld and van der Waerden ([8]) will be used (*), since with it the introduction of non-flat metrics is particularly straightforward. More explicitly, let ζ (indices suppressed) be a spinor field of arbitrary valence, defined in a given Riemann space V_4 (of signature -2), whose metrical tensor is $g_{kl}(x)$. Further, let a certain real number r, called its conformal weight, be associated with ζ; whilst $q(x)$ shall be an arbitrary real function of the co-ordinates. If now Ω (indices suppressed) is a spinor formed of $\gamma_{\mu\nu}$, $\sigma^{k\dot{\alpha}\beta}$, and the covariant derivative of ζ, then what is to be investigated in the first place

([8]) L. Infeld and B. L. van der Waerden: *Sitzber. Preuss. Akad. Wiss.*, 380 (1933).
(*) Their notation will be adhered to except where otherwise indicated.

is the conformal transform $'\Omega$ of Ω, *i.e.* the form of the quantity $'\Omega$ which results under a transformation T of C:

$$\sigma^{k\dot{\mu}\nu} \to {}'\sigma^{k\dot{\mu}\nu} = \sigma^{k\dot{\mu}\nu}\,, \tag{1.3}$$

$$\gamma_{\mu\nu} \to {}'\gamma_{\mu\nu} = e^{-a}\gamma_{\mu\nu}\,, \tag{1.4}$$

$$\zeta \to {}'\zeta = e^{\nu a}\zeta\,. \tag{1.5}$$

(The condition that the metric must be initially galilean has been relaxed for the time being.) If $'\Omega = e^{\alpha a}\Omega$, where α is a real number, then Ω will be said to be conformally covariant, or «a conformal covariant», the term «conformal invariant» being reserved for the special case $\alpha = 0$. It will be noted that the choice of (1.3, 4) ensures that under T $'g_{kl} = e^{2a}g_{kl}$ (cf. EISENHART (9)). No greater generality would have been obtained by choosing (with b real)

$$'\sigma^{k\dot{\mu}\nu} = e^{ba}\sigma^{k\dot{\mu}\nu}\,, \qquad '\gamma_{\mu\nu} = e^{-(b+1)a}\gamma_{\mu\nu}, \tag{1.6}$$

for (1.6) results from (1.3, 4) through the spin transformation

$$\Lambda^{\mu}{}_{\nu} = \delta^{\mu}{}_{\nu}e^{\frac{1}{2}ba}\,. \tag{1.7}$$

Once the effect of conformal transformations on the linear spinor connexion is known (Section **2**), one may easily investigate the formation of conformally invariant fundamental spinors on the one hand (Section **3**), and the effect of such transformations on a general derived spinor Ω on the other (Section **4**). This in turn allows one to examine systematically sets of field equations, linear or quasi-linear, constructed from spinors ξ, η and their first derivatives (Sections **5** and **6**), leading to the general results announced in the summary at the beginning of this paper.

2. – The linear connexion.

If the basic hermitian vector spinor $\sigma^{k\dot{\mu}\nu}$, and the metric spinor $\gamma_{\mu\nu}$ be associated with the Riemann space V_4 whose metric tensor is g_{kl}, one has the fundamental relations

$$\gamma_{\dot{\mu}\dot{\alpha}}\gamma_{\nu\beta}\sigma^{k\dot{\mu}\nu}\sigma^{l\dot{\alpha}\beta} = g^{kl}\,, \tag{2.1}$$

$$\sigma^{k\dot{\mu}\nu}{}_{;l} = 0\,, \tag{2.2}$$

$$\gamma_{\alpha\beta;l} = 0\,, \tag{2.3}$$

(9) L. P. EISENHART: *Riemannian Geometry* (Princeton, 1926), chap. II, § 28.

where subscripts following a semicolon indicate covariant differentiation, the latter being defined with respect to the linear connexion Γ^s_{kl} (*i.e.* the Christoffel symbols od V_4) and the linear spinor connexion $\Gamma^{\mu}_{\nu l}$ and its complex conjugate $\Gamma^{\dot\mu}_{\dot\nu l}$. It may be noted that (2.3) has been adopted in place of the weaker equation

$$(\gamma_{\dot\mu\dot\alpha}\gamma_{\nu\beta})_{;l} = 0\,. \tag{2.4}$$

The former destroys the phase-invariance of the theory, whereas the latter does not. Electromagnetic interactions are however here taken to be absent in any case, for it is known ([10]) that their presence brings with it special difficulties in the context of fields for particles of spin $S \geqslant 1$, and with that problem this paper is not concerned.

Now let $'V_4$ be a space in conformal correspondence with V_4, *i.e.*

$$'g_{kl} = e^{2q} g_{kl}\,, \tag{2.5}$$

where q is an arbitrary real function of the co-ordinates. If $'\sigma^{k\dot l\nu}$, $'\gamma_{\alpha\beta}$ be the corresponding basic spinors given by (1.3) and (1.4) one has the fundamental relations

$$'\gamma_{\dot\mu\dot\alpha}\,'\gamma_{\nu\beta}\,'\sigma^{k\dot\mu\nu}\,'\sigma^{l\dot\alpha\beta} = {}'g^{kl}\,, \tag{2.6}$$

$$'\sigma^{k\dot\mu\nu}{}_{;l} = 0\,, \tag{2.7}$$

$$'\gamma_{\alpha\beta;l} = 0\,, \tag{2.8}$$

the colon indicating covariant differentiation with respect to the transformed linear connexions $'\Gamma^s_{kl}$ and $'\Gamma^{\mu}_{\nu l}$. It is convenient to write for either connexion

$$\Delta = {}'\Gamma - \Gamma\,, \tag{2.9}$$

(indices suppressed). Then it follows from $'g_{kl:s} = 0$ as usual that

$$\Delta^s_{kl} = \delta^s_k q_{,l} + \delta^s_l q_{,k} - g_{kl} g^{st} q_{,t}\,. \tag{2.10}$$

Now, identically,

$$'\sigma^{k\dot\mu\nu}{}_{;l} = \sigma^{k\dot\mu\nu}{}_{;l} + \Delta^k_{tl}\sigma^{t\dot\mu\nu} + \Delta^{\dot\mu}_{\dot\lambda l}\sigma^{k\dot\lambda\nu} + \Delta^{\nu}_{\lambda l}\sigma^{k\dot\mu\lambda}\,,$$

$$e^q({}'\gamma_{\mu\nu})_{;l} = e^q(e^{-q}\gamma_{\mu\nu})_{;l} - \Delta^{\lambda}_{\mu l}\gamma_{\lambda\nu} - \Delta^{\lambda}_{\nu l}\gamma_{\mu\lambda}\,,$$

the second equation effectively constituting only a single equation for each

([10]) *E.g.* M. Fierz and W. Pauli: *Proc. Roy. Soc.*, A **173**, 211 (1939).

value of l. Using (2.2, 3) and (2.7 ,8)

$$\Delta^{k}{}_{lt}\sigma^{t\dot{\mu}\nu} + \Delta^{\dot{\mu}}{}_{\dot{\lambda}l}\sigma^{k\dot{\lambda}\nu} + \Delta^{\nu}{}_{\lambda l}\sigma^{k\dot{\mu}\dot{\lambda}} = 0\,, \tag{2.11}$$

$$q_{,l} + \Delta^{\lambda}{}_{\lambda l} = 0\,. \tag{2.12}$$

Multiplying (2.11) throughout by $\sigma_{k\dot{\mu}\varrho}$ and using (2.12) it follows easily that

$$\Delta^{\nu}{}_{\varrho l} = -\tfrac{1}{2}\sigma_{k\dot{\mu}\varrho}\sigma^{t\dot{\mu}\nu}\Delta^{k}{}_{lt}\,. \tag{2.13}$$

Inserting (2.10) on the right and making use of the identity

$$2\sigma^{(k}{}_{\dot{\mu}\varrho}\sigma^{l)\dot{\mu}\nu} = \delta^{\nu}{}_{\varrho}\,g^{kl}\,, \tag{2.14}$$

eq. (2.13) becomes simply

$$\Delta^{\mu}{}_{\nu l} = -\sigma_{l\dot{\alpha}\nu}\sigma^{t\dot{\alpha}\mu}q_{,t}\,. \tag{2.15}$$

It is sometimes convenient to introduce the spinor

$$q^{\dot{\alpha}\beta} = \sigma^{k\dot{\alpha}\beta}q_{;k}\,. \tag{2.16}$$

Then (2.15) reads simply

$$\Delta^{\mu}{}_{\nu l} = -\sigma_{l\dot{\alpha}\nu}q^{\dot{\alpha}\mu}\,. \tag{2.17}$$

With this result the investigation of the behaviour of derived spinors under transformations of C becomes quite straightforward.

3. – The conformal curvature spinor.

This section deals briefly with a conformally invariant fundamental spinor which is analogous to the well known conformal curvature tensor $C^{m}{}_{kls}$ (*e.g.* EISENHART (9)), and is indeed very closely related to it. From the definition (*)

$$\tfrac{1}{2}P^{\mu}{}_{\nu kl} = \Gamma^{\mu}{}_{\nu[l,k]} + \Gamma^{\alpha}{}_{\nu[l}\Gamma^{\mu}{}_{\alpha k]} \tag{3.1}$$

of the usual spin curvature tensor it follows at once that

$$\tfrac{1}{2}\,{}'P^{\mu}{}_{\nu kl} = \tfrac{1}{2}P^{\mu}{}_{\nu kl} + \Delta^{\mu}{}_{\nu[l;k]} + \Delta^{\alpha}{}_{\nu[l}\Delta^{\mu}{}_{\alpha k]}\,. \tag{3.2}$$

(*) Brackets enclosing indices act in every case on only one kind of index, *e.g.* here only on the *tensor* subscripts k and l.

Upon making use of (2.15) one is confronted with terms of the kind

$$\sigma_{k\dot{x}\nu}\sigma^{s\dot{x}\lambda}\sigma_{l\dot{\beta}\lambda}\sigma^{t\dot{\beta}\mu}q_{;s}q_{;t}\,, \tag{3.3}$$

which may be simplified by means of identities given by HARISH-CHANDRA [11]. Thus (3.3) becomes

$$\sigma_{k\dot{x}\nu}\sigma^{s\dot{x}\mu}q_{;s}q_{;l}-\sigma_{l}^{\ \dot{\alpha}\mu}\sigma_{k\dot{x}\nu}q_{;t}q^{;t}\,. \tag{3.4}$$

With this result one then has

$${}'P^{\mu}_{\ \nu kl}=P^{\mu}_{\ \nu kl}+2\sigma^{s\dot{\alpha}\mu}Q_{s[l}\sigma_{k]\dot{\alpha}\nu}\,, \tag{3.5}$$

where

$$Q_{st}=q_{;st}-q_{;s}q_{;t}+q_{st}q_{;r}q^{;r}\,. \tag{3.6}$$

From (3.5) it may be inferred that

$$({}'P^{\mu}_{\ \nu kl}-P^{\mu}_{\ \nu kl})\sigma_{r}^{\ \dot{\lambda}\nu}\sigma^{l}_{\ \dot{\lambda}\mu}=\tfrac{1}{2}g_{rk}Q+Q_{rk}\,, \tag{3.7}$$

and hence

$$({}'P^{\mu}_{\ \nu kl}-P^{\mu}_{\ \nu kl})\sigma^{k\dot{\lambda}\nu}\sigma^{l}_{\ \dot{\lambda}\mu}=3Q\,. \tag{3.8}$$

By means of the last two equations Q_{st} may be eliminated from (3.5), and one has the result that the spin tensor

$$\Gamma^{\mu}_{\ \nu kl}=P^{\mu}_{\ \nu kl}-2\sigma^{t\dot{\lambda}}_{\ \ \alpha}P^{\alpha\mu}_{\ \ t[k}\sigma_{l]\dot{\lambda}\nu}-\tfrac{1}{3}\sigma_{[k}^{\ \ \dot{\varrho}\mu}\sigma_{l]\dot{\varrho}\nu}\sigma^{s\dot{\lambda}\beta}\sigma^{t}_{\ \dot{\lambda}\alpha}P^{\alpha}_{\ \beta st} \tag{3.9}$$

is a conformal invariant. Finally it is possible to show (the details need not be reproduced here) that

$$\Gamma^{\mu}_{\ \nu kl}=\tfrac{1}{2}\sigma^{s\dot{\lambda}\mu}\sigma^{t}_{\ \dot{\lambda}\nu}C_{stkl}\,. \tag{3.10}$$

4. – The conformal behaviour of derived spinors.

To investigate the conformal behaviour of relativistic wave equations it is appropriate first to consider the behaviour of certain derived spinors of the form $p^{\dot{\alpha}\beta}\xi$, where ξ (indices suppressed) is a spinor of arbitrary valence $r+s$,

[11] HARISH-CHANDRA: *Proc. Ind. Acad. Sci.*, **23**, 152 (1946).

symmetric in its dotted and undotted indices, and

$$p^{\dot\alpha\beta}(\ldots) = \sigma^{k\dot\alpha\beta}(\ldots)_{;k}\,. \tag{4.1}$$

Since it is clearly immaterial whether a given set of indices be written as subscripts or as superscripts, ξ will be taken in the standard form

$$\xi = \xi^{\dot\mu_1\cdots\dot\mu_r\nu_1\cdots\nu_s}\,. \tag{4.2}$$

The spinor which results when $\dot\mu_t$ is replaced by $\dot\lambda$ will be denoted by $\xi^{(\dot\lambda)_t}$; and $\xi^{(\lambda)_m}$ similarly denotes the spinor which results when ν_m is replaced by λ.

a) Now let ξ have the conformal weight v. Then

$$'(p^{\dot\alpha\beta}\xi) = \sigma^{k\dot\alpha\beta}(e^{vq}\xi)_{;k} = \sigma^{k\dot\alpha\beta}e^{vq}\Big(\xi_{;k} + vq_{;k}\xi + \sum_{t=1}^{r} \Delta^{\dot\mu_t}{}_{\dot\lambda k}\xi^{(\dot\lambda)_t} + \sum_{t=1}^{s}\Delta^{\nu_t}{}_{\lambda k}\xi^{(\lambda)_t}\Big)\,.$$

Introducing (2.17) this becomes

$$'(p^{\dot\alpha\beta}\xi) = e^{vq}\Big(p^{\dot\alpha\beta}\xi + vq^{\dot\alpha\beta}\xi - \sum_{t=1}^{r} q^{\dot\mu_t\beta}\xi^{(\dot\alpha)_t} - \sum_{t=1}^{s} q^{\dot\alpha\nu_t}\xi^{(\beta)_t}\Big)\,. \tag{4.3}$$

Applying the symmetry operators s and $\dot s$ (cf. GÅRDING [12]) one then has

$$'(s\dot s p^{\dot\alpha\beta}\xi) = e^{vq}s\dot s\big(p^{\dot\alpha\beta}\xi + (v-r-s)q^{\dot\alpha\beta}\xi\big)\,. \tag{4.4}$$

Hence: *$s\dot s p^{\dot\alpha\beta}\xi$ is a conformal covariant if and only if $v = r+s$; and its conformal weight is then $r+s$.*

b) From (4.3), $(s>0)$, keeping (1.4) in mind,

$$'(p^{\dot\mu_{r+1}}{}_{\nu_s}\xi) = e^{(v-1)q}\Big(p^{\dot\mu_{r+1}}{}_{\nu_s}\xi + vq^{\dot\mu_{r+1}}{}_{\nu_s}\xi - \sum_{t=1}^{r} q^{\dot\mu_t}{}_{\nu_s}\xi^{(\dot\mu_{r+1})_t} + q^{\dot\mu_{r+1}}{}_{\nu_s}\xi\Big)\,,$$

in view of the symmetry properties of ξ. Consequently

$$'(\dot s p^{\dot\mu_{r+1}}{}_{\nu_s}\xi) = e^{(v-1)q}\,\dot s\big(p^{\dot\mu_{r+1}}{}_{\nu_s}\xi + (v-r+1)q^{\dot\mu_{r+1}}{}_{\nu_s}\xi\big)\,. \tag{4.6}$$

Hence: *$\dot s p^{\dot\mu_{r+1}}{}_{\nu_s}\xi$ is a conformal covariant if and only if $v = r-1$; and its conformal weight is then $r-2$.*

c) Proceeding exactly as under *b*) above one has also that *$sp_{\dot\mu_r}{}^{\nu_{s+1}}\xi$ is a conformal covariant if and only if $v = s-1$; and its conformal weight is then $s-2$.*

---

[12] L. GÅRDING: *Proc. Camb. Phil. Soc.*, **41**, 49 (1945).

d) Finally, from (4.3),

$$'(p_{\dot{\mu}_r \nu_s}\xi) = e^{(v-2)q}(p_{\dot{\mu}_r \nu_s}\xi + (v+2)q_{\dot{\mu}_r \nu_s}\xi)\,. \tag{4.9}$$

Hence: *$p_{\dot{\mu}_r \nu_s}\xi$ is a conformal covariant if and only if $v=-2$; and its conweight is then -4.*

5. – Linear field equations for particles of any spin and finite rest mass.

a) In galilean space-time R_4 one may take the equations for fields corresponding to particles of finite rest mass and arbitrary spin $S=\frac{1}{2}(r+s)$, $(s>0)$, in the form

$$\dot{s}p^{\dot{\mu}_{r+1}}{}_{\nu_s}\xi = \varkappa\eta\,, \tag{5.1}$$

$$sp_{\dot{\mu}_{r+1}}{}^{\nu_s}\eta = \varkappa\xi\,. \tag{5.2}$$

where $\varkappa$ is a constant, together with the subsidiary conditions

$$p_{\dot{\mu}_r \nu_s}\xi = 0\,, \qquad p_{\dot{\mu}_{r+1}\nu_{s-1}}\eta = 0\,, \tag{5.3, 4}$$

required to ensure that the field describe only particles of spin S, *i.e.* not a mixture of particles of spin $\leqslant S$. The explicit form of ξ is given by (4.1), whilst $\eta = \eta^{\dot{\mu}_1 \cdots \dot{\mu}_{r+1}\nu_1 \cdots \nu_{s-1}}$. Here the operator $p^{\dot{\alpha}\beta}$ means

$$p^{\dot{\alpha}\beta}(\ldots) = \sigma^{k\dot{\alpha}\beta}(\ldots)_{,k}\,. \tag{5.5}$$

Because of (5.3, 4) the operators s and $\dot{s}$ could be omitted from (5.1, 2) ,but it is convenient to retain them here.

Suppose now that fields are contemplated in some V_4 whose curvature tensor does not necessarily vanish. Then it will be laid down that the correct field equations are just (5.1-4) *$p^{\dot{\alpha}\beta}$ having the meaning given by* (4.2). In other words the view is taken that the equations for an R_4 are the degenerate form of the equations for a V_4 adopted here. (This seems to be generally taken for granted (*e.g.* reference ([6])), but it will be understood that the inclusion of terms containing the curvature tensors as factors would leave the equations relating to an R_4 unaffected. Such terms would however appear to be necessarily rather artificial.)

Starting, then, with an R_4 the equations (5.1-4) are certainly compatible. For spin $S>\frac{1}{2}$ their compatibility in an arbitrary V_4 is however no longer assured, as I have shown on an earlier occasion ([13]). Thus since $S>\frac{1}{2}$,

([13]) H. A. Buchdahl: *Nuovo Cimento*, **10**, 96 (1958). This paper will be referred to as A.

take $s > 1$; then the condition of consistency, corresponding to eq. A(13) for the case $S = \frac{3}{2}$, follows easily:

$$\sigma^{k\dot{\lambda}}{}_{\nu_s}\sigma^{l}{}_{\dot{\lambda}\nu_{s-1}}\xi_{;[kl]} = 0\,. \tag{5.6}$$

In terms of the spin curvature this tensor becomes

$$S^{kl}{}_{\nu_s\nu_{s-1}}\Big(\sum_{t=1}^{r} P^{\dot{\mu}_t}{}_{\dot{\alpha}kl}\xi^{(\dot{\alpha})_t} + \sum_{t=1}^{s} P^{\nu_t}{}_{\alpha kl}\xi^{(\alpha)_t}\Big) = 0\,, \tag{5.7}$$

where

$$S^{kl}{}_{\alpha\beta} = \sigma^{[k\dot{\lambda}}{}_{\alpha}\sigma^{l]}{}_{\dot{\lambda}\beta}\,. \tag{5.8}$$

(The first sum is absent if $r = 0$). Now, if the V_4 is conformal to an R_4 then it is a space of constant Riemannian curvature (9), Λ, say. This means that

$$P^{\mu}{}_{\nu kl} = -\tfrac{1}{12}\Lambda S_{kl}{}^{\mu}{}_{\nu}\,. \tag{5.9}$$

One therefore has to consider terms of the kind (i) $S^{kl}{}_{\nu_s\nu_{s-1}}S_{kl}{}^{\dot{\mu}_t}{}_{\dot{\alpha}}\xi^{(\dot{\alpha})_t}$ and (ii) $S^{kl}{}_{\nu_s\nu_{s-1}}S_{kl}{}^{\nu_t}{}_{\alpha}\xi^{(\alpha)_t}$. Now one has (14)

$$S^{kl\alpha\beta}S_{kl\dot{\mu}\dot{\nu}} = 0\,, \qquad S^{kl\alpha\beta}S_{kl\mu\nu} = 2\delta^{(\alpha}{}_{\mu}\delta^{\beta)}{}_{\nu}\,. \tag{5.10-11}$$

Hence without having to invoke the symmetry properties of ξ one concludes already that all the terms above vanish except those of the second type which have $t = s$ or $s - 1$. Omitting irrelevant numerical factors, these terms are $\delta^{\nu t}{}_{(\nu_s}\gamma_{\nu_{s-1})\alpha}\xi^{(\alpha)_t}$; and they vanish becauses of the symmetry of ξ. Thus it has been shown that *the field equations are compatible in any V_4 of constant Riemannian curvature*; that is to say, the possibility of conformal invariance of the equations is not impaired by any *a priori* incompatibility in the V_4.

b) Two alternatives now present themselves in principle, *viz.* (i) either (5.1, 2) alone are required to be conformally invariant, or, (ii) the subsidiary equations (5.3, 4) shall also be invariant.

As regards the first alternative, the subsidiary equations must then be imposed upon the field quantities *after* transformations. (It may be remarked that McLennan in his work (4) concerning conformal invariance under C_0 does not consider any subsidiary equations.) This procedure is somewhat unnatural; and the first alternative is therefore contemplated largely for heuristic reasons.

Suppose now that the conformal weights of ξ and η are a and b respectively. Then, in view of (4.6), one has in the case of (5.1)

$$a = r - 1\,, \qquad b = r - 2\,, \tag{5.12}$$

(14) E. M. Corson: *Tensors, Spinors and Relativistic Wave Equations* (London, 1953), chap. II, § 13.

where the second member of (5.12) follows from the required equality of both members of eq. (5.1). Keeping in mind that, in (5.2,) η has not $\dot{s}$ but $s-1$ undotted superscripts, one has similarly, with (4.8),

$$b = s-2\,, \qquad a = s-3\,. \tag{5.13}$$

(5.12) and (5,13) are mutually incompatible. Thus without having to draw upon the subsidiary equations at all, it follows *that the (linear) field equations associated with particles of arbitrary spin S cannot be invariant under the extended conformal group for any value of S.* (The phrase « ... cannot be invariant... » is preferred to « ... are not invariant... » since invariant equations could be made non-invariant by a different choice of conformal weights. Note also that it has been supposed above that $s > 0$, *i.e.* $S > 0$; but the non-invariance of the scalar field equations under C is known).

6. – Field equations with conform-covariant mass-scalar.

a) The « mass-scalar » $\varkappa$ was taken to be a constant in (5.1, 2). This condition may be relaxed: without as yet making any hypothesis about the detailed structure of $\varkappa$ one may simply suppose that it has a conformal weight c (cf. PAULI ([6])). Then in place of (5.12, 13) one has now

$$a = r-1\,, \qquad b+c = r-2\,, \tag{6.1}$$

$$b = s-2\,, \qquad a+c = s-3\,. \tag{6.2}$$

It follows that

$$c = -1\,, \qquad r = s-1\,, \tag{6.3}$$

and incidentally

$$a = b = s-2\,. \tag{6.4}$$

The equality of a and b might have been anticipated and might indeed have been imposed from the outset. The second member of (6.3) implies that the field equations must be reflection-invariant (FIERZ ([15])), the total number of indices and therefore $2S$ being odd. Thus *the pair of field equations* (5.12) *with conform-covariant mass-scalar can be invariant under the transformations of the extended conformal group only if they are reflection-invariant and the particles associated with them have half-odd integral spin.*

As regards the structure of $\varkappa$, one may for example take it to be a power of a suitable invariant K formed bilinearly from ξ and η. Taking into account that $\lambda_{\alpha\beta}$ must enter into it multiplicatively $r+s = 2s-1$ times, the con-

([15]) M. FIERZ: *Helv. Phys. Acta*, **12**, 3, § 5 (1938).

formal weight of K will be $2(s-2)-(2s-1)=-3$. The first member of (6.3) then requires

$$\varkappa = K^{\frac{1}{3}} . \tag{6.5}$$

This result is consistent with that obtained by McLennan [4], eq. (24).

b) The situation is greatly altered if it be required that the subsidiary equations (5.3, 4) be conformally invariant at the same time. For in accordance with (4.10) one must then have in addition

$$a = b = -2 , \tag{6.6}$$

whenever $s > 1$; but (6.6) is incompatible with (6.4). Accordingly the case $s = 1$ remains as the only possibility, the subsidiary equations then being absent. Accordingly *the entire set of field equations* (5.1-4) *cannot be conformally invariant* (*under C*), *even when the mass-scalar* $\varkappa$ *is supposed to be a conformal covariant.* In this sense, then, *the condition of extended conformal invariance distinguishes Dirac's equations* (*the mass-scalar* $\varkappa$ *kaving the conformal weight* -1)

$$p^{\dot{\mu}}{}_{\nu}\xi^{\nu} = \varkappa\eta^{\dot{\mu}} , \qquad p_{\dot{\mu}}{}^{\nu}\eta^{\dot{\mu}} = \varkappa\xi^{\nu} , \tag{6.7}$$

from the equations for all other fields associated with particles of integral or half-odd integral spin.

It may be noted that if one adopts (6.5) one is left essentially with just the equations considered by Gürsey [5] in the context of C_0^+.

RIASSUNTO (*)

Il lavoro tratta principalmente del comportamento degli spinori di valenza arbitraria e delle loro derivate prime rispetto alle trasformazioni del gruppo conforme esteso C, i cui elementi sono essenzialmente le trasformazioni della metrica secondo $'g_{kl} = \lambda g_{kl}$, dove λ è una funzione positiva arbitraria delle coordinate. I risultati ottenuti si applicano ad alcune equazioni relativistiche per campi associati a particelle di spin arbitrario S. Si dimostra che: (i) se la massa scalare $\varkappa$ che compare nelle stesse si considera conformalmente invariante, le equazioni possono essere invarianti rispetto a C per *qualsiasi* valore di S; (ii) se $\varkappa$ si considera conformalmente covariante, le equazioni possono essere invarianti rispetto a C solo se sono invarianti rispetto alla riflessione e S è semi intero e le equazioni sussidiarie sono impostate *dopo* la trasformazione, cioè la loro invarianza non è richiesta; (iii) se è richiesta anche l'invarianza conforme delle equazioni sussidiarie, le sole equazioni che possono essere invarianti rispetto a C sono le equazioni di Dirac ($S = \frac{1}{2}$) con massa scalare conformalmente covariante, mancando in tal caso le equazioni sussidiarie.

(*) *Traduzione a cura della Redazione.*

IL NUOVO CIMENTO Vol. XI, N. 4 16 Febbraio 1959

About the μ-Meson Spin from Ionization Bursts Data.

I. X. Ion, N. J. Ionescu-Pallas and C. C. Potoceanu

Institute of Atomic Physics of the Rumanian Academy - Bucarest

(ricevuto il 3 Novembre 1958)

Summary. — Accurate calculations of appearance frequencies of bursts generated by muons in a shielding layer of lead at sea level were performed. Cross sections for bremsstrahlung when the screening of the nucleus by the orbital electrons is incomplete, and Furry's distribution model revised by Christy and Kusaka in order to diminish the fluctuations, were used. Theoretical results fall in good agreement with experimental data in the range $100 \div 1200$ particles, assuming a spin $\frac{1}{2}$ for the μ-meson.

1. – Introduction.

It is well known that the hard component of the cosmic rays, generates ionization bursts in a matter shielded ionization chamber.

If measurements are carried out at sea level, and the protonic component is removed, the process is determined especially by the muons. Muon interactions with shielding matter via knock-on and bremsstrahlung processes, the first process giving a negligible contribution with respect to the last, generates electrono-photonic cascade showers.

Cross-sections of both processes are dependent on primary particle spin for energies greater than 10^{10} eV. Hence, a calculation leading to the frequency of ionization bursts, involving a number of particles $\geqslant S$ may determine (by comparison with experimental data) the value of the muon spin.

The problem was resolved under these conditions, by Christy and Kusaka [1] (*) who found spin 0 with an uncertainty implying also the possibility of spin $\frac{1}{2}$, and by Chakrabarthy [2] who found spin 1.

(*) We refer to Christy and Kusaka's work by the abbr. C.K.

[1] R. F. Christy and S. Kusaka: *Phys. Rev.*, **59**, 414 (1941).

[2] S. K. Chakrabarty: *Ind. Journ. Phys.*, **46**, 377 (1942).

The investigations continued ([3-5]), most of the results favouring the value $\frac{1}{2}$. The present work continued on the C. and K. line to see if it was possible to find agreement between theoretical results and experimental data ([7,8]).

In this connection, several sources of possible errors, arising from the uncertainty of the value of some experimental constants used in calculations were eliminated.

Finally, a discussion on C. and K.'s work and on other methods used up to now is given.

2. – Muon spectrum renormalization.

The first difficulty arising in calculations consists in the fact that a power law for the muon energy spectrum leads, according to Wilson's experimental data ([9]) to an energy dependence of the exponential coefficient (we use the differential spectrum coefficient)

$$\alpha \sim 2.9 \quad \text{for} \quad E_0 < 6 \cdot 10^{10} \text{ eV} \quad \text{and} \quad \alpha \sim 3.4 \quad \text{for} \quad 6 \cdot 10^{10} < E_0 < 2 \cdot 10^{11}.$$

On the assumption of experimental coefficient variation with energy and because of muon hemispheric isotropy, C. and K.'s expression,

$$N(E_0)\,\mathrm{d}E_0\,\mathrm{d}\Omega = \frac{0.02\,(E_c)^{1.9}\,\mathrm{d}E_0\,\mathrm{d}\Omega}{(E_0 + 1.8 \cdot 10^9 \sec\theta)^{2.9}}, \tag{2.1}$$

for the differential spectrum (used without changes by other authors) may be modified by a suitable expression for spectrum normalization at an arbitrary value of α. To find with accuracy the total muon number, the spectrum was cut-off at a given energy, which in the present case is $E_0 \sim 0.6 \cdot 10^9$ eV. Now the question arises at which energy the spectrum has to be cut-off to obtain precisely, for a given exponential coefficient α, the muon number by means of the power law.

([3]) S. Hyrokava, H. Komori and S. Ogava: *Nuovo Cimento*, **7**, 736 (1956).
([4]) A. Mitra: *Nucl. Phys.*, **3**, 262 (1957).
([5]) M. Gupta: *Nuovo Cimento*, **7**, 39 (1958).
([6]) B. Rossi: *Rev. Mod. Phys.*, **20**, 537 (1948).
([7]) M. Schein and P. S. Gill: *Rev. Mod. Phys.*, **44**, 267 (1939).
([8]) R. E. Lapp: *Phys. Rev.*, **64**, 255 (1943).
([9]) J. G. Wilson: *Nature*, **158**, 415 (1946).

Eq. (2.1) may be written:

$$N(E_0)\,\mathrm{d}E_0\,\mathrm{d}\Omega = \frac{(\alpha-1)\,I_0\mathcal{E}_0^{\alpha-1}g^{\alpha-1}(\alpha)\,\mathrm{d}E_0\,\mathrm{d}\Omega}{(E_0+\mathcal{E}_0\sec\theta)^{\alpha}}\,, \tag{2.2}$$

where I_0 is the muon intensity per unit of solid angle and per second, near the vertical, at sea level and $g(\alpha)$ the ratio $E_c/\mathcal{E}_0$, where $\mathcal{E}_0 = 1.8\cdot10^9$ eV is a spectrum constant. The value assigned to I_0, namely $I_0 = 0.88\cdot10^{-2}/\mathrm{cm}^2\,\mathrm{sr}\cdot\mathrm{s}$ [6] gives a correction of $\sim 12\,\%$ with respect to $I_0 \approx 10^{-2}/\mathrm{cm}^2\cdot\mathrm{sr}\cdot\mathrm{s}$, used by C. and K. in their calculations.

By integrating the differential spectrum (2.2) over the upper hemisphere and over all energies and with the condition to obtain C. and K.'s (who took $\alpha \sim 3$) value for the ratio between total intensity and $2\pi I_0$, where I_0 is the vertical intensity, we obtain a transcendent equation for $g(\alpha)$. For $\alpha = 3$ the total spectrum will be

$$y = 2\pi I_0\left(\frac{E_1}{E_{\min}}\right)^2\left\{2 - \frac{E_{\min}}{E_0+E_{\min}} - 2\,\frac{E_0}{E_{\min}}\ln\frac{E_0+E_{\min}}{E_0}\right\}, \tag{2.3}$$

where $E_{\min} = E_1 - E_0$; $E_1/E_0 = E_1/\mathcal{E}_0 = g(3)$. Introduction of numerical values in (2.3) gives

$$\frac{y}{2\pi I_0} = k = 0.382\,7\,\ldots\,. \tag{2.4}$$

For a given α, eq. (2.2) will be integrated first with respect to energy (the integration limits being $E_{\min}$ and ∞) and second with respect to angles. Therefore

$$y = 2\pi I_0\left(\frac{E_1}{E_{\min}}\right)^{\alpha-1} J_{\alpha-1}\left(\frac{E_0}{E_{\min}}\right), \tag{2.5}$$

with the same notations as in eq. (2.3) but for a given α, function $J_\alpha(a)$ may be defined by means of the transcendent function

$$J_\alpha(a) = \int_0^{\pi/2} \frac{\sin\theta\,\mathrm{d}\theta}{(1+(a/\cos\theta))^{\alpha}}\,. \tag{2.6}$$

Expanding the integral in a rapid convergent infinite series, we obtain the following infinite degree algebraic equation (see App. I)

$$\sum_1^{\infty}{}_{\lambda}\,\frac{x^{\lambda}}{(\alpha+\lambda)(\alpha+\lambda-1)} = k_0\,, \tag{2.7}$$

where

$$x = \frac{E_{\min}}{E_0 + E_{\min}} = 1 - \frac{1}{g(\alpha)} \qquad \text{and} \qquad k_0 = \frac{1}{\alpha - 1}\left(\frac{y}{2\pi I_0} - \frac{1}{\alpha}\right).$$

As $k_0 \ll 1$ the real positive root may be given as an expansion in powers of k_0. Finally the equation relating x to $g(\alpha)$ gives

$$g(\alpha) = 1 + \alpha\frac{\alpha+1}{\alpha-1}\left(k - \frac{1}{\alpha}\right) + \frac{2}{\alpha+2}\alpha^2\left(\frac{\alpha+1}{\alpha-1}\right)^2\left(k - \frac{1}{\alpha}\right)^2 + \tag{2.8}$$

$$+ \frac{2(\alpha+6)}{(\alpha+2)^2(\alpha+3)}\alpha^3\left(\frac{\alpha+1}{\alpha-1}\right)^3\left(k - \frac{1}{\alpha}\right)^3 + \ldots .$$

Very good approximation ($\ll 1\,‰$) is obtained taking in the whole α variation interval $2.9 \leqslant \alpha \leqslant 3.4$ the following expression for $g(\alpha)$

$$g(\alpha) \approx 1.335 + 0.870(\alpha - 3)\,. \tag{2.9}$$

3. – The integral spectrum of muons.

The second difficult task is to obtain a proper expression for the integral spectrum, which may be used in further calculations. As it is impossible to obtain a finite expression for $\alpha \neq 3$, we shall take, instead, a power series of the variable, as rapidly convergent as possible. This difficulty does not arise in C. and K.'s work, who use the following approximation

$$N(E_0)\,\mathrm{d}E_0\,\mathrm{d}\Omega \approx \frac{0.02\,(E_c)^{1.9}\,\mathrm{d}E_0\,\mathrm{d}\Omega}{E_j^{2.9}\left(1 + \dfrac{1.8\cdot 10^9 \sec\theta\varepsilon}{15\beta S}\right)^{2.9}}\,, \tag{3.1}$$

in which the energy of the muon generating the shower is replaced by $15(\beta S/\varepsilon)$, where ε is the energy transfer ratio from the muon to the electron or the photon generating the cascade, and S is the number of particles in the shower. On the assumption that $6\beta S$ (β being the energy at which the multiplication process stops) is the most probable energy of the particle (electron or photon) generating the cascade, as results from Furry's model modified by C. and K., and that the mean value of transfer ratio is $\frac{3}{4}$, we obtained for the muon initiating the process, an energy of $20\beta S$, a too great value with respect to $8\beta S$ resulting from the model and with respect to $13.3\beta S$ obtained without considering the fluctuations.

To resolve this problem, the following change of variable, whose meaning will appear later, will be made

$$E_0 = \frac{\mathcal{E}_0}{a}, \tag{3.2}$$

where E_0 is the muon energy and $\mathcal{E}_0$ the differential spectrum constant (2.2). For simple dimensional reasons, E_0 will be expressed in $15\beta S$ units: $E_0 = 15\beta S E_0'$; $E_0' = E/\varepsilon$, where E is the energy (in arbitrary units) of the photon or electron generating the cascade. Hence, $\mathcal{E}_0/a = 15\beta S(E/\varepsilon)$ and setting $\xi = 1/E$, we obtain the second important transformation

$$\varepsilon = \frac{S}{C_1} a, \tag{3.3}$$

where

$$C_1 = \frac{\mathcal{E}_0}{15\beta} = 8.57142\ldots, \tag{3.4}$$

and $\beta = 14$ MeV a more correct value than that of 13 MeV given by C. and K.

According to eq. (3.2) and eq. (3.3) the differential spectrum (2.2) will be

$$N(\alpha)\,\mathrm{d}E_0\,\mathrm{d}\Omega = \frac{(\alpha-1)I_0 a^{\alpha-1} g^{\alpha-1}(\alpha)\,(\mathrm{d}\xi/\xi)\,\mathrm{d}\Omega}{(1+(a/\cos\theta))^{\alpha}}, \tag{3.5}$$

where the sign (—) before eq. (3.5) was omitted; it will be taken into account only at the end by reversing the integration limits of the integral with respect to ξ, which gives the shower appearance frequencies. The integral spectrum will now be

$$\mathrm{d}E_0 \int_{\text{(upper hemi ph.)}} N(\alpha)\,\mathrm{d}\Omega = 2\pi I_0(\alpha-1)\,a^{\alpha-1} g^{\alpha-1}(\alpha)\,J_\alpha(a)\,\frac{\mathrm{d}\xi}{\xi}, \tag{3.6}$$

where $J_\alpha(a)$ which was defined by eq. (2.6) will not be expressed any more as a series of type (2.7) but, according to the purpose of the present work, as a rapidly convergent asymptotic series (see App. II),

$$J_\alpha(a) = 1 + \alpha a \ln a + C_\alpha a - \sum_1^\infty{}_k\, (-1)^{k-1} C_{\alpha+k}^{\alpha-1} \frac{a^{k+1}}{k}, \tag{3.7}$$

where C_α is in its turn

$$C_\alpha = \alpha(\alpha-1) \sum_1^\infty{}_k \frac{1}{(k+1)(k+\alpha)}. \tag{3.8}$$

For $\alpha = 3$, $C_\alpha = \frac{5}{2}$ and $J_3(a)$ may be written as a finite expression

$$J_3(a) = \left\{ \frac{6a^2 + 9a + 2}{2(a+1)^2} - 3a \ln\left(\frac{a+1}{a}\right) \right\}. \tag{3.9}$$

Using Stirling's formula it may be observed that series (3.7) is rapidly convergent for $0 < a < 1$ and $\alpha > 1$ and both conditions are fulfilled in this case.

4. – Cross section transformations for processes initiating the cascade.

Both for knock-on processes with atomic electrons and for muon bremsstrahlung we shall take the cross-sections given in C. and K.'s work (critical considerations on the applicability limits of these expressions will be given further).

Cross-sections for electron knock-on processes in both cases discussed above (spin 0 and spin $\frac{1}{2}$) are

a) spin 0, magnetic moment 0

$$\sigma_0^{(e)}(E_0, \varepsilon) = 2\pi \left(\frac{137}{Z}\right) \left(\frac{\mu}{m}\right)^2 \frac{mc^2}{E_0} \frac{1}{\varepsilon^2} \left(1 - \frac{\varepsilon}{\varepsilon_m}\right). \tag{4.1}$$

b) spin $\frac{1}{2}$, magnetic moment $e\hbar/2\mu c$

$$\sigma_{\frac{1}{2}}^{(e)}(E_0, \varepsilon) = 2\pi \left(\frac{137}{Z}\right) \left(\frac{\mu}{m}\right)^2 \frac{mc^2}{E_0} \frac{1}{\varepsilon^2} \left(1 - \frac{\varepsilon}{\varepsilon_m} + \frac{1}{2}\varepsilon^2\right), \tag{4.2}$$

where ε_m is the maximum energy transfer ratio from a muon (of energy E_0) to an electron (of energy E)

$$\varepsilon_m \approx \left[1 + \frac{1}{2}\left(\frac{\mu}{m}\right)^2 \frac{mc^2}{E_0}\right]^{-1}. \tag{4.3}$$

Cross sections are measured in radiation units

$$\overline{\varphi} \approx \left(\frac{e^2}{\mu c^2}\right)^2 \frac{Z^2}{137}. \tag{4.4}$$

Cross-sections for muon bremsstrahlung in the Coulomb field of a nucleus, are

a) spin 0, magnetic moment 0

$$\sigma_0^{(\gamma)}(E_0, \varepsilon) = \frac{16}{3} \frac{1-\varepsilon}{\varepsilon} \left\{ \ln \frac{2(1-\varepsilon)E_0}{(5/6)\mu c^2 Z^{\frac{1}{3}} \varepsilon} - \frac{1}{2} \right\}, \tag{4.5}$$

b) spin $\frac{1}{2}$, magnetic moment $e\hbar/2\mu c$

$$\sigma_{\frac{1}{2}}^{(\gamma)}(E_0, \varepsilon) = \frac{16}{3}\left(\frac{3}{y}\varepsilon + \frac{1-\varepsilon}{\varepsilon}\right)\left\{\ln\frac{2(1-\varepsilon)E_0}{(5/6)\mu c^2 Z^{\frac{1}{3}}\varepsilon} - \frac{1}{2}\right\}. \tag{4.6}$$

To write eq. (4.1), (4.2), (4.3), (4.5) and (4.6) in the new variables (a, ξ), changes of variables (3.2) and (3.3) will be used. We have to find first, the expression relating a_m and ε_m to get the variation limit of ε in the « a » scale. From (4.3) it follows that.

$$\varepsilon_m \approx \frac{S}{S + C_2\xi}, \tag{4.7}$$

where

$$C_2 = \frac{1}{2}\left(\frac{\mu}{m}\right)^2\left[\frac{mc^2}{15\beta}\right] = 54.679\,09\ldots. \tag{4.8}$$

In computing C_2 the precise value $\mu \approx 207\mathrm{m}_e$ has been assumed for the muon mass. Writing eq. (3.3) for the limiting values (ε_m, a_m) and using eq. (4.7) we shall find the following equation relating a_m to ξ

$$a_m = \frac{C_1\xi}{S + C_2\xi}, \tag{4.9}$$

which allows for the reciprocal conversion of these variables. In the limiting case $\xi \to \infty$

$$\lim_{\xi\to\infty} a_m(\xi) = \max(a_m) = \frac{C_1}{C_2} = 0.156\,76. \tag{4.10}$$

Using the equations relating a_m to ξ, and ε_m to ξ and taking ξ from eq. (4.7) and eq. (4.9), we shall obtain

$$\varepsilon_m = 1 - \frac{C_2}{C_1}a_m = 1 - 6.379\,3\ldots a_m, \tag{4.11}$$

which is the energy transformation. Now the cross-sections of the investigated processes may be expressed only in terms of a and a_m. The great advantage of this transformation consists in the possibility of obtaining—as will be seen further—an integrant for the expression giving the shower appearance frequency, in which the particle number S does not appear. In this connection it is opportune to notice that the relative low value obtained in (4.10) assures a rapid convergence of the series (3.7).

Before writing the cross-sections in the new variables we shall introduce some simplifying notations

$$\mathcal{S}(Z) = 2\pi \frac{137}{Z}\left(\frac{\mu}{m}\right)^2 \frac{mc^2}{\mathcal{E}_0} C_1^2, \tag{4.12}$$

$$Q(Z) = \ln \frac{2\mathcal{E}_0}{(5/6)\mu c^2 Z^{\frac{1}{3}}} = \tag{4.13}$$

$$= 2.22533\left\{1 - 0.14978\left(\frac{\delta Z_0}{Z_0}\right) + 0.07489\left(\frac{\delta Z_0}{Z_0}\right)^2 - 0.04993\left(\frac{\delta Z_0}{Z_0}\right)^3 + \ldots\right\},$$

where

$$Z_0 = 80 \qquad \text{and} \qquad \delta Z_0 = Z - Z_0 .$$

Taking into account all changes between old and new variables (that is ε, E_0, ε_m and a, ξ, a_m) respectively, we finally obtain

$$\sigma_0^{(e)}(a, \xi) = \mathcal{S}(Z)\frac{\xi^2}{S^2}\left\{\frac{1}{a} - \frac{1}{a_m}\right\}, \tag{4.14}$$

$$\sigma_{\frac{1}{2}}^{(e)}(a, \xi) = \mathcal{S}(Z)\frac{\xi^2}{S^2}\left\{\frac{1}{a} - \frac{1}{a_m} + \frac{1}{2}\left(\frac{1}{a_m} - 6.3793\right)^2 a\right\}, \tag{4.15}$$

$$\sigma_0^{(\gamma)} = \frac{16}{3}\left[\frac{a_m}{a}\,\frac{1}{1 - 6.3793\,a_m} - 1\right]\left\{\left(Q - \frac{1}{2}\right) + \ln\left[\frac{a_m}{a}\,\frac{1}{1 - 6.3793\,a_m} - 1\right]\frac{1}{a}\right\}. \tag{4.16}$$

$$\sigma_{\frac{1}{2}}^{(\gamma)} = \frac{16}{3}\left[\frac{a_m}{a}\,\frac{1}{1 - 6.3793\,a_m} - 1 + \frac{3}{4}\,\frac{a}{a_m}\,(1 - 6.3793\,a_m)\right] \cdot \tag{4.17}$$

$$\cdot\left\{\left(Q - \frac{1}{2}\right) + \ln\left[\frac{a_m}{a}\,\frac{1}{1 - 6.3793\,a_m} - 1\right]\frac{1}{a}\right\}.$$

5. – General expressions for cascade shower appearance frequencies as functions of the particle number S.

In order to find these expressions we shall perform the integral

$$N_i(S) = \bar{\varphi} N \int_0^\infty \mathrm{d}E \int_{0\ (\text{upper hemisph.})}^{\varepsilon_m} \frac{\mathrm{d}\varepsilon}{\varepsilon} \int F\left(\frac{E}{\varepsilon}, \theta\right) \sigma_i\left(\frac{E}{\varepsilon}, \varepsilon\right) P(E, S)\,\mathrm{d}\Omega , \tag{5.1}$$

where $P(E, S)$ is the probability for an electron (or a photon) of energy E of generating a cascade shower which contains more than S particles, σ_i the cross-section of the process in which an electron (or a photon) of energy E is

freed (or created) by a muon of energy E/ε, $F(E/\varepsilon, 0)$ the meson differential spectrum intensity and N the number of shielding atoms per unit of path (N does not appear in the final result). According to our transformations eq. (5.1) will be written in terms of ξ and a. Let us note

$$\mathcal{L}(Z, \alpha) = \frac{2\pi}{C_1} I_0 \overline{\varphi} N x_0 K(\alpha - 1) g^{\alpha - 1}(\alpha) = \frac{2\pi}{C_1} I_0 \overline{\varphi} N x_0 K \Xi(\alpha) , \tag{5.2}$$

where K and x_0 are used to express the probability $P(E, S)$, which in the ξ scale will take the form

$$P(\xi) = \frac{K x_0}{\sqrt{\xi}} \exp [-\xi]; \tag{5.3}$$

here $K = 13.5$ and x_0 (the shower unit for length) is given by

$$x_0 = \left[4 \frac{Z^2}{137} \left(\frac{e^2}{mc^2} \right)^2 N \ln \frac{191}{Z^{\frac{1}{3}}} \right]^{-1} . \tag{5.4}$$

The probability (5.3) results from Furry's model (for spatial distribution of particles in the shower) modified by C. and K. to diminish its somewhat great fluctuations.

Now we may write for both processes (knock-on and bremsstrahlung) the following general equation giving the frequencies $N(S)$

$$\frac{N_i(S)}{S} = \mathcal{L}(Z, \alpha) \int_0^\infty \xi^{-\frac{5}{2}} \exp [-\xi] \, d\xi \int_0^{a_m} a^{\alpha - 1} \sigma_i(a) J_\alpha(a) \, da , \tag{5.5}$$

where the subscript i denotes a definite process, $J_\alpha(a)$ is the function defined by eq. (2.6) but in the form (3.7); a_m must be replaced after integration by its expression as a function of ξ (4.9); cross-sections are those given in (4.14)–(4.17).

Cross-sections for the collision process are of the form

$$\sigma^{(e)}(\xi, a) = \mathcal{S}(Z) \frac{\xi^2}{S^2} f^{(e)}(a) , \tag{5.6}$$

and if we set

$$\mathcal{L}(Z, \alpha) \mathcal{S}(Z) = \Gamma(Z) \Xi(\alpha) , \tag{5.7}$$

shower appearance frequencies for this process will be

$$N_{(i)}^{(e)}(S) = \frac{\Gamma(Z)}{S} \Xi(\alpha) \int_0^\infty \frac{\exp [-\xi]}{\sqrt{\xi}} \cdot d\xi \int_0^{a_m} a^{\alpha - 1} f_{(i)}^{(e)}(a) J_\alpha(a) \, da , \tag{5.8}$$

where i now refers to a definite muon spin value, and the functions $\Gamma(Z)$ and $\Xi(\alpha)$ are, respectively

$$\Gamma(Z) = \pi^2 \frac{137}{Z} \frac{mc^2}{15\beta} \ln \frac{KI_0}{(191/Z^{\frac{1}{3}})} \simeq \tag{5.9}$$

$$\simeq 1.2886 \cdot 10^{-3} \left[1 - 0.91208 \left(\frac{\delta Z_0}{Z_0} \right) + 0.87585 \left(\frac{\delta Z_0}{Z_0} \right)^2 - 0.85360 \left(\frac{\delta Z_0}{Z_0} \right)^3 + \ldots \right],$$

and

$$\Xi(\alpha) = (\alpha - 1)\, g^{\alpha-1}(\alpha) \simeq \tag{5.10}$$

$$\simeq 3.5644 \{ 1 + 2.0923 (\alpha - 3) + 2.2908 (\alpha - 3)^2 + 1.7538 (\alpha - 3)^3 + \ldots \} .$$

For the other process (bremsstrahlung) we may write

$$N_{(i)}(S) = S T(Z)\, \Xi(\alpha) \int_0^\infty \xi^{-\frac{5}{2}} \exp[-\xi]\, \mathrm{d}\xi \int_0^{a_m} a^{\alpha-1} \sigma_{(i)}^{(\gamma)}(a)\, J_\gamma(a)\, \mathrm{d}a , \tag{5.11}$$

when $T(Z)$ takes the form

$$T(Z) = \frac{\pi}{2C_1} \left(\frac{m}{\mu} \right)^2 \frac{KI_0}{\ln (191/Z^{\frac{1}{3}})} \simeq \tag{5.12}$$

$$\simeq 1.2776 \cdot 10^{-7} \left\{ 1 + 0.08791 \left(\frac{\delta Z_0}{Z_0} \right) - 0.03622 \left(\frac{\delta Z_0}{Z_0} \right)^2 + 0.02225 \left(\frac{\delta Z_0}{Z_0} \right)^3 - \ldots \right\} .$$

Eq. (5.11) may be written similarly to eq. (5.8) by introducing transformed cross-sections

$$\tilde{\sigma}_{(i)} = \sigma_{(i)} \left[\frac{1}{a_m} - 6.3793 \ldots \right]^2 . \tag{5.13}$$

Thus eq. (5.11) becomes

$$N_i^{(\gamma)}(S) = C_1^2 \frac{T(Z)}{S}\, \Xi(\alpha) \int_0^\infty \frac{\exp[-\xi]}{\sqrt{\xi}}\, \mathrm{d}\xi \int_0^{a_m} a^{\alpha-1}\, \tilde{\sigma}_i(a)\, J_\alpha(a)\, \mathrm{d}a . \tag{5.14}$$

Now we must compute the functions G_i and F_i which are the integrals over a in (5.8) and (5.14).

6. – Computation of functions G_i and F_i.

Functions G_0 and $G_{\frac{1}{2}}$ are easily obtained because the series of which they consist may be integrated term by term. Thus, we find

$$G_0(a_m) = \frac{a_m^{\alpha-1}}{\alpha(\alpha-1)} \left\{ 1 + \alpha \frac{\alpha-1}{\alpha+1} a_m \ln a_m + \frac{\alpha-1}{\alpha+1} \left(C_\alpha - \frac{2\alpha+1}{\alpha+1} \right) a_m - \right. \tag{6.1}$$

$$\left. - \alpha(\alpha-1) \sum_1^\infty{}_k \frac{(-1)^{k-1}}{k}\, C_{\alpha+k}^{\alpha-1} \frac{a_m^{k+1}}{(k+a)(k+\alpha+1)} \right],$$

and

$$(6.2)\qquad G_{\frac{1}{2}}(a_m) - G_0(a_m) = \frac{1}{2}\frac{a_m^{\alpha-1}}{\alpha+1}(1-6.3793\,a_m)^2\left\{1+\alpha\frac{\alpha+1}{\alpha+2}a_m \ln a_m + \right.$$

$$\left. + \frac{\alpha+1}{\alpha+2}\left(C_\alpha - \frac{\alpha}{\alpha+2}\right)a_m - (\alpha+1)\sum_1^\infty{}_k \frac{(-1)^{k-1}}{k} C_{\alpha+k}^{\alpha-1}\frac{a_m^{k+1}}{k+\alpha+2}\right\}.$$

Functions F_i are much more intricate and may not be written as simple power series. Therefore we shall introduce 9 auxiliary functions $g_i(a_m)$, $i = 1, 2, \ldots$ in terms of which function F_i will be written,

$$(6.3)\qquad g_1(x) = 1 + (\alpha-1)x\ln x + $$

$$+ \frac{\alpha-1}{\alpha}(C_\alpha - 1)x - (\alpha-1)\sum_1^\infty{}_k (-1)^{k-1}\frac{C_{\alpha+k}^{\alpha-1}}{k(k+\alpha)}x^{k+1},$$

$$(6.4)\qquad g_2(x) = 1 + \frac{\alpha^2}{\alpha+1}x\ln x + $$

$$+ \frac{\alpha}{\alpha+1}\left(C_\alpha - \frac{\alpha}{\alpha+1}\right)x - \alpha\sum_1^\infty{}_k (-1)^{k-1}\frac{C_{\alpha+k}^{\alpha-1}}{k(k+\alpha+1)}x^{k+1},$$

$$(6.5)\qquad g_3(x) = 1 + (\alpha-1)x\ln x\frac{1+\dfrac{\alpha}{\ln(y/x)}\sigma_{\alpha-1}}{1+\dfrac{\alpha-1}{\ln(y/x)}\sigma_{\alpha-2}} +$$

$$+ \frac{\alpha-1}{\alpha}(C_\alpha-1)x\frac{1+\dfrac{\alpha}{\ln(y/x)}\left[\dfrac{C_\alpha}{C_\alpha-1}\sigma_{\alpha-1} + \dfrac{\alpha\sigma'_{\alpha-1}}{C_\alpha-1}\right]}{1+\dfrac{\alpha-1}{\ln(y/x)}\sigma_{\alpha-2}} -$$

$$- (\alpha-1)\sum_1^\infty{}_k (-1)^{k-1}\frac{C_{\alpha+k}^{\alpha-1}}{k(k+\alpha)}x^{k+1}\cdot\frac{1+\dfrac{k+\alpha}{\ln(y/x)}\sigma_{k+\alpha-1}}{1+\dfrac{\alpha-1}{\ln(y/x)}\sigma_{\alpha-2}},$$

$$(6.6)\qquad g_4(x) = 1 + \frac{\alpha^2}{\alpha+1}x\ln x\frac{1+\dfrac{\alpha+1}{\ln(y/x)}\sigma_\alpha}{1+\dfrac{\alpha}{\ln(y/x)}\sigma_{\alpha-1}} +$$

$$+ \frac{\alpha}{\alpha+1}\left(C_\alpha - \frac{\alpha}{\alpha+1}\right)x\frac{1+\dfrac{(\alpha+1)}{(C_\alpha-\alpha/(\alpha+1))\ln(y/x)}(C_\alpha\sigma_\alpha+\alpha\sigma'_\alpha)}{1+\dfrac{\alpha}{\ln(y/x)}\sigma_{\alpha-1}} -$$

$$- \alpha \sum_{1}^{\infty}{}_{k} (-1)^{k-1} \frac{C_{\alpha+k}^{\alpha-1}}{k(k+\alpha+1)} x^{k+1} \frac{1+\dfrac{k+\alpha+1}{\ln (y/x)} \sigma_{k+\alpha}}{1+\dfrac{\alpha}{\ln (y/x)} \sigma_{\alpha-1}},$$

(6.7) $$g_5(x) = 1 + (\alpha-1) x \ln x +$$

$$+ \frac{\alpha-1}{\alpha} \left(C_\alpha - \frac{\alpha-2}{\alpha-1} \right) x \frac{\ln x - \dfrac{1}{\alpha} \dfrac{C_\alpha - 2}{C_\alpha - ((\alpha-2)/(\alpha-1))}}{\ln x - \dfrac{1}{\alpha-1}} -$$

$$- (\alpha-1) \sum_{1}^{\infty}{}_{k} (-1)^{k-1} \frac{C_{\alpha+k}^{\alpha-1}}{k(k+\alpha)} x^{k+1} \frac{\ln x - \dfrac{1}{k+\alpha}}{\ln x - \dfrac{1}{\alpha-1}},$$

(6.8) $$g_6(x) = 1 + \frac{\alpha^2}{\alpha+1} x \ln x +$$

$$+ \frac{\alpha}{\alpha+1} \left(C_\alpha - \frac{\alpha-1}{\alpha+1} \right) x \frac{\ln x - \dfrac{1}{\alpha+1} \dfrac{C_\alpha - 2\,(\alpha/(\alpha+1))}{C_\alpha - ((\alpha-1)/(\alpha+1))}}{\ln x - \dfrac{1}{\alpha}} -$$

$$- \alpha \sum_{1}^{\infty}{}_{k} (-1)^{k-1} \frac{C_{\alpha+k}^{\alpha-1}}{k(k+\alpha+1)} x^{k+1} \frac{\ln x - \dfrac{1}{\alpha+k+1}}{\ln x - \dfrac{1}{\alpha}},$$

(6.9) $$g_7(x) = 1 + \alpha \frac{\alpha+1}{\alpha+2} x \ln x +$$

$$+ \frac{\alpha+1}{\alpha+2} \left(C_\alpha - \frac{\alpha}{\alpha+2} \right) x - (\alpha+1) \sum_{1}^{\infty}{}_{k} (-1)^{k-1} \frac{C_{\alpha+k}^{\alpha-1}}{k(k+\alpha+2)} x^{k+1},$$

(6.10) $$g_8(x) = 1 + \alpha \frac{\alpha+1}{\alpha+2} x \ln x \frac{1+\dfrac{\alpha+2}{\ln (y/x)} \sigma_{\alpha+1}}{1+\dfrac{\alpha+1}{\ln (y/x)} \sigma_1} +$$

$$+ \frac{\alpha+1}{\alpha+2} \left(C_\alpha - \frac{\alpha}{\alpha+2} \right) x \frac{\dfrac{\alpha+2}{(C_1 - \alpha/(\alpha+2) \ln (y/x))} (C_1 \sigma_{\alpha+1} + \alpha \sigma'_{\alpha+1})}{1+\dfrac{\alpha+1}{\ln (y/x)} \sigma_\alpha} -$$

$$- (\alpha+1) \sum_{1}^{\infty}{}_{k} (-1)^{k-1} \frac{C_{\alpha+k}^{\alpha-1}}{k(k+\alpha+2)} x^{k+1} \frac{1+\dfrac{\alpha+k+2}{\ln (y/x)} \sigma_{\alpha+k+1}}{1+\dfrac{\alpha+1}{\ln (y/x)} \sigma_\alpha},$$

$$(6.11)\quad g_9(x) = 1 + \alpha\frac{\alpha+1}{\alpha+2}\,x\ln x + \\ + \frac{\alpha+1}{\alpha+2}\left[C_\alpha - \frac{\alpha^2}{(\alpha+1)(\alpha+2)}\right] x\,\frac{\ln x + \dfrac{[2\alpha/(\alpha+2) - C_\alpha]1/(\alpha+2)}{C_\alpha - (\alpha^2/(\alpha+1)(\alpha+2))}}{\ln x - \dfrac{1}{\alpha+1}} - \\ - (\alpha+1)\sum_1^\infty{}_k\,(-1)^{k-1}\,\frac{C_{\alpha+k}^{\alpha-1}}{k(k+\alpha+2)}\,x^{k+1}\,\frac{\ln x - \dfrac{1}{k+\alpha+2}}{\ln x - \dfrac{1}{\alpha+1}},$$

where $x = a_m$, $y = 1 - 6.3793\,a_m$ and

$$(6.12)\qquad \sigma_q(y) = \sum_1^\infty{}_k\,\frac{y^k}{k(k+q+1)}.$$

The derivative of σ, stressed in the expressions giving g's is taken with respect to subscript q. (For the derivation of g_i see App. III).

Functions g_i and σ_q allow to write the functions F_0 and $F_{\frac{1}{2}}$ in a relatively simple form

$$(6.13)\qquad F_0(a_m) = \frac{16}{3}\,yx^{\alpha-2}\cdot \\ \cdot\left\{\frac{Q-\frac{1}{2}}{\alpha-1}\,g_1(x) - \left[\frac{\ln(y/x)}{\alpha-1} + \sigma_{\alpha+2}\right] g_3(x) - 2\,\frac{(\ln x - 1/(\alpha-1))}{\alpha-1}\,g_5(x)\right\} - \\ - \frac{16}{3}\,y^2x^{\alpha-2}\left\{\frac{Q-\frac{1}{2}}{\alpha}\,g_2(x) - \left[\frac{\ln(y/x)}{\alpha} + \sigma_{\alpha-1}\right] g_4(x) - 2\,\frac{\ln\alpha - (1/\alpha)}{\alpha}\,g_6(x)\right\},$$

$$(6.14)\qquad F_{\frac{1}{2}}(a_m) - F_0(a_m) = \\ = 4y^3x^{\alpha-2}\left\{\frac{Q-\frac{1}{2}}{\alpha+1}\,g_7(x) - \left[\frac{\ln(y/x)}{\alpha+1} + \sigma_\alpha\right] g_8(x) - 2\,\frac{\ln x - 1/(\alpha+1)}{\alpha+1}\,g_9(x)\right\}.$$

7. – Numerical data.

Expressions obtained in Sect. 6 for the functions G and F have been derived very clearly—without any approximation—and are therefore, the most precise solutions of the problem discussed above.

Now, the following integrals have to be performed,

$$\int_0^\infty \frac{\exp[-\xi]}{\sqrt{\xi}}\,G(a_m)\,\mathrm{d}\xi \qquad \text{and} \qquad \int_0^\infty \frac{\exp[-\xi]}{\sqrt{\xi}}\,F(a_m)\,\mathrm{d}\xi\,.$$

As the integrand of both integrals do not contain explicitly the particle number S, functions G and F are quite general, this was of course, the main reason determining us to perform all transformations from Sect. 2 and 3. Function G_0, $G_{\frac{1}{2}}$ and F_0, $F_{\frac{1}{2}}$ were tabulated after previous tabulation of functions f_i and g_i. All numerical calculations were performed for $\alpha = 3$ and $Z = 82$ (Pb).

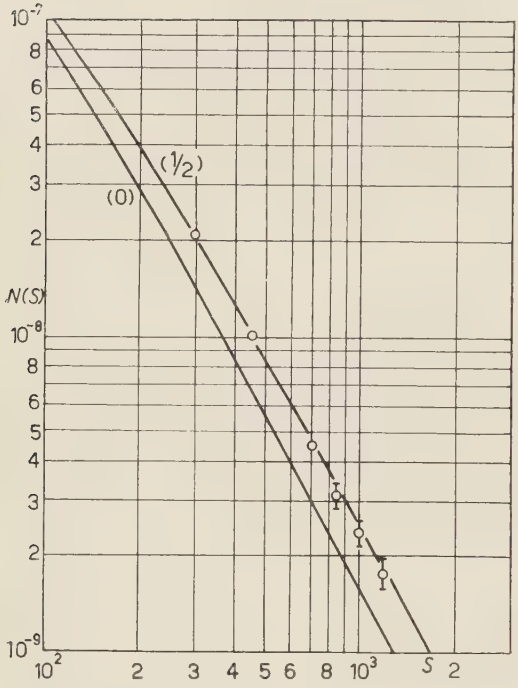

Fig. 1. – Plot of burst frequency against minimum burst size given in terms of the number of particles S of the burst. The circles indicate the experimental points of ([7]) and ([8]).

After plotting G and F to a scale allowing for great precision, we made the conversion from the hyperbolic scale a_m to the linear scale ξ, using transformation (4.9) which was also tabulated. Graphical calculations were performed up to $\xi = 5$; for the remaining interval, adequate tail corrections were made. Frequencies of the two processes (knock-on and bremsstrahlung) generating the cascade are given in the table below, for both values (0 and $\frac{1}{2}$) of the muon spin.

A comparison between total frequencies and Lapp's experimental data is given in Fig. 1. For showers containing no more than 1 200 particles, a good agreement was found. Comparison with Schein and Gill's experimental data is also satisfactory.

TABLE I. – *The values of* $N(S)$.

S	$N_0^{(e)}(S)$	$N_{\frac{1}{2}}^{(e)}(S)$	$N_0^{(\gamma)}(S)$	$N_{\frac{1}{2}}^{(\gamma)}(S)$
75	$2.532 \cdot 10^{-8}$	$3.105 \cdot 10^{-8}$	$1.083 \cdot 10^{-7}$	$1.316 \cdot 10^{-7}$
150	$5.713 \cdot 10^{-9}$	$8.286 \cdot 10^{-9}$	$4.039 \cdot 10^{-8}$	$5.003 \cdot 10^{-8}$
300	$1.136 \cdot 10^{-9}$	$1.664 \cdot 10^{-9}$	$1.259 \cdot 10^{-8}$	$1.852 \cdot 10^{-8}$
600	$1.963 \cdot 10^{-10}$	$2.999 \cdot 10^{-10}$	$3.883 \cdot 10^{-9}$	$5.990 \cdot 10^{-9}$
1 200	$2.900 \cdot 10^{-11}$	$4.807 \cdot 10^{-11}$	$1.102 \cdot 10^{-9}$	$1.714 \cdot 10^{-9}$

8. – Concluding remarks.

In the present work some sources of errors were removed by introducing in our calculations the precise values for the muon mass, the vertical intensity I_0 and the critical energy β. Errors arising from some approximative calculation methods were also eliminated. C. and K. made the approximation mentioned in (3.1) and took $\varepsilon = \bar{\varepsilon} = \frac{3}{4}$ without discussing the errors introduced in this manner. In more recent works ([4,5]), the saddle-point method giving an error 20% is used (*).

A cross-section determined with incomplete shielding has been used for the bremsstrahlung, because its applicability limit is given by

$$E_0 \ll \left(\frac{\mu}{m}\right)^2 \frac{137}{Z^{\frac{1}{3}}} mc^2 \approx 6.78 \cdot 10^{11} .$$

Measurements carried out with the muon spectrum at sea level and theoretical calculations ([9]) show a variation of α with energy

$$\begin{aligned} &\text{in the range} \quad (8 \cdot 10^9 - 5.3 \cdot 10^{10}) \text{ eV} \qquad \alpha = 2.8 , \\ &\text{in the range} \quad (5.3 \cdot 10^{10} - \quad 10^{12}) \text{ eV} \qquad \alpha = 3.2 \div 3.3 . \end{aligned}$$

As the variation of α with energy is not known, spectrum normalization was performed according to Sect. 2. For $S > 1200$ a value of parameter > 3 is—as results from an estimated calculus—a possible explanation for the data in this domain.

For particle distribution in the shower, we have used Furry's model modified by C. and K., which gives good approximations in the range of $(10^{10} \div 10^{11})$ eV, that is for $S \approx (10^7 \div 10^8)$ particles. Therefore, it may be considered that our results are in agreement with experimental data up to $S = 1200$ particles.

Appendix I

Muon spectrum normalization.

Integration with respect to angles over the upper hemisphere and with respect to energies from $E_{\min}$ to ∞ gives

$$(1) \qquad \frac{y}{2\pi I_0} = \left(1 + \frac{E_0}{E_{\min}}\right)^{\alpha-1} J_{\alpha-1}\left(\frac{E_0}{E_{\min}}\right) = k .$$

(*) This method applies successfully only when the integrand vanishes rapidly to infinity (*e.g.* like e^{-x}) and the maximum peak is sufficiently far from the origin. For the integrals present in our work (7.1) the second condition is not fulfilled.

Noting $E_0/E_{\min} = N$; $N \gg 1$ we have according to definition

$$(2) \qquad k = (N+1)^{\alpha-1}\int_0^1 \frac{\mathrm{d}x}{(1+N/x)^{\alpha-1}} = N(N+1)^{\alpha-1}\int_N^\infty \frac{\mathrm{d}\eta}{\eta^2(1+\eta)^{\alpha-1}} =$$

$$= N(N+1)^{\alpha-1}\sum_1^\infty{}_\lambda\, \lambda \int_N^\infty \frac{\mathrm{d}\eta}{(1+\eta)^{\alpha+\lambda}} = N\sum_1^\infty{}_\lambda \frac{\lambda}{\alpha+\lambda-1}\cdot\frac{1}{(N+1)^\lambda}$$

If we set

$$\frac{1}{N+1} = x \qquad \text{and} \qquad k_0 = \frac{1}{\alpha-1}\left(k-\frac{1}{\alpha}\right),$$

and take into account the identity

$$(3) \qquad \sum_1^\infty{}_\lambda \frac{\lambda}{\alpha+\lambda-1}\,x^\lambda \equiv \frac{1}{\alpha} + (\alpha-1)\sum_1^\infty{}_\lambda \frac{x^\lambda}{(\alpha+\lambda)(\alpha+\lambda-1)},$$

the problem is reduced to finding the real positive root of

$$\sum_1^\infty{}_\lambda \frac{x^\lambda}{(\alpha+\lambda)(\alpha+\lambda-1)} = k_0\,.$$

If $x = \sum_1^\infty{}_j K_j k_0^j$ by identification we find

$$(5) \qquad \frac{E_{\min}}{E_0+E_{\min}} = \left(1-\frac{1}{g(\alpha)}\right) = \alpha\,\frac{\alpha+1}{\alpha-1}\left(k-\frac{1}{\alpha}\right) - \frac{\alpha^3}{(\alpha+2)}\left(\frac{\alpha+1}{\alpha-1}\right)^2\left(k-\frac{1}{\alpha}\right)^2 +$$

$$+ \frac{\alpha^4}{(\alpha+2)^2(\alpha+3)}\left(\frac{\alpha+1}{\alpha-1}\right)^3(\alpha^2+3\alpha-2)\left(k-\frac{1}{\alpha}\right)^3 - \ldots,$$

hence

$$(6) \qquad g(\alpha) = 1 + \alpha\,\frac{\alpha+1}{\alpha-1}\left(k-\frac{1}{\alpha}\right) + \frac{2}{\alpha+2}\,\alpha^2\left(\frac{\alpha+1}{\alpha-1}\right)^2\left(k-\frac{1}{\alpha}\right)^2 +$$

$$+ \frac{2(\alpha+6)\alpha^3}{(\alpha+2)^2(\alpha+3)}\left[\frac{\alpha+1}{\alpha-1}\right]^3\left(k-\frac{1}{\alpha}\right)^3$$

Appendix II

Asymptotic expansion of $J_\alpha(a)$.

By definition

$$(1) \qquad J_\alpha(a) = \int_0^{\pi/2} \frac{\sin\theta\,\mathrm{d}\theta}{(1+(a/\cos\theta))^\alpha} = \int_0^1 \frac{\mathrm{d}x}{(1+a/x)^\alpha}\,.$$

If we set $x/a = \xi$, $1/a = N$, then

$$(2) \qquad J_\alpha\left(\frac{1}{N}\right) = \frac{1}{N}\int_0^N \left(1+\frac{1}{\xi}\right)^{-\alpha} \mathrm{d}\xi = 1 - \alpha\frac{\ln N}{N} + \frac{C_\alpha}{N} - \sum_1^\infty{}_k \frac{(-1)^{k-1}}{k}\frac{C_{\alpha+k}^{k+1}}{N^{k+1}}.$$

The integration constant C_α is defined so that (2) be an asymptotic series

$$(3) \qquad C_\alpha = \lim_{N\to\infty}\left\{\int_0^N \left(1-\frac{1}{\xi}\right)^{-\alpha}\mathrm{d}\xi - N + \alpha\ln N\right\} =$$

$$= \int_1^\infty \left\{\left(1-\frac{1}{\zeta}\right)^\alpha - 1 + \frac{\alpha}{\zeta}\right\}\mathrm{d}\zeta = \alpha(\alpha-1)\sum_1^\infty{}_k \frac{1}{(k+1)(k+\alpha)}.$$

Expanding eq. (3) in series, after some straightforward transformations we find around the point $\alpha = 3$; $\alpha - 3 = \varepsilon$

$$(4) \qquad C_\alpha = \frac{5}{2} + \left\{\frac{\pi^2}{2} - \left(3+\frac{1}{4}\right)\right\}\varepsilon + \sum_1^\infty{}_\lambda \frac{\lambda}{\lambda+3}\,\frac{(\varepsilon/(\lambda+3))^2}{1+[\varepsilon/(\lambda+3)]},$$

or using Riemann's function $\zeta(p) = \sum_1^\infty{}_k 1/k^p$

$$(5) \qquad C_\alpha = \frac{5}{2} + \left\{\frac{\pi^2}{2} - \left(3+\frac{1}{4}\right)\right\}\varepsilon + \sum_1^\infty{}_k (-1)^{k-1}\cdot$$

$$\cdot\left\{\zeta(k+1) - 3\zeta(k+2) + 2 + \frac{1}{2^{k+2}}\right\}\varepsilon^{k+1}.$$

Appendix III

About the derivation of the functions $g_k(a_m)$.

Functions g_1, g_2, g_5, g_6, g_7, g_9 are obtained performing a direct integration of expressions arising from functions F_0, $F_{\frac{1}{2}}$.

Functions g_3, g_4, g_8 — that are similar — may be expressed by means of transcendent functions $Y_p(x)$ and $L_p(x)$

$$(1) \qquad Y_\nu(a_m) = \int_0^{a_m} x^p \ln\left[\frac{a_m}{1 - 6.3793\,a_m} - x\right]\mathrm{d}x,$$

$$(2) \qquad L_\nu = \frac{\partial}{\partial p}\,Y_p(a_m).$$

For $g_3(a_m)$, for example, we obtain

$$(3) \qquad g_3(a_m) = 1 + \alpha \frac{L_{\alpha-1}(a_m)}{Y_{\alpha-2}(a_m)} + C_\alpha \frac{Y_{\alpha-1}(a_m)}{Y_{\alpha-2}(a_m)} - \sum_1^\infty{}_k \frac{(-1)^{k-1}}{k} C_{\alpha+k}^{\alpha-1} \frac{Y_{\alpha+k-1}(a_m)}{Y_{\alpha-2}(a_m)} .$$

After some transformations of the integrand in eq. (1), we find for $Y_p(x)$:

$$(4) \qquad Y_p(x) = -x^{p+1} \left\{ \frac{\ln((1/x) - 6.3793)}{p+1} + \sum_1^\infty{}_k \frac{(1 - 6.3793x)^k}{k(k+p+1)} \right\} .$$

Introducing in eq. (3) the eqs. (1), (2) and (4), this takes, after some simple algebraic transformations, the form used in calculations.

RIASSUNTO (*)

Si sono eseguiti accurati calcoli delle frequenze dei burst generati dai muoni in uno strato schermante di piombo a livello del mare. Per diminuire le fluttuazioni si sono usati le sezioni d'urto per la bremsstrahlung nel caso di schermatura incompleta del nucleo da parte degli elettroni orbitali e il modello di Furry modificato da Christy e Kusaka. I risultati teorici risultano in buon accordo coi dati sperimentali nell'ambito di (100÷1200) particelle assumendo pel mesone μ lo spin $\frac{1}{2}$.

(*) *Traduzione a cura della Redazione.*

IL NUOVO CIMENTO Vol. XI, N. 4 16 Febbraio 1959

Investigations of Bremsstrahlung of Electrons in the Energy Interval $(10^{11} \div 10^{12})$ eV.

J. Benisz, Z. Chyliński and W. Wolter

Institute of Nuclear Research - Cracow

(ricevuto il 7 Novembre 1958)

Summary. — Four high energy ($\sim 10^{12}$ eV) electron-photon cascades have been investigated at the first stage of their development. The number and the energy of the electron pairs of the first generation, produced on the first radiation length were estimated and compared with the theoretical values calculated on the basis of the theory of Bethe and Heitler. On the other hand, the same was calculated according to the theories of Landau, Pomerančuk and Ter-Mikaelyan which take into account the influence of the medium on the bremsstrahlung of electrons of very high energy. The experimental results are in better agreement with the predictions of Landau, Pomerančuk and Ter-Mikaelyan than with that of Bethe and Heitler. This fact confirms the results obtained earlier in our laboratory and given in a previous paper [1].

1. – Introduction.

Up to the present time there were very few experiments investigating the problem of the influence of a dense medium on the probability of emission of bremsstrahlung photons by electrons of very high energies. The point in question is an effect first predicted by Landau [2], Pomerančuk and Ter-Mikaelyan [3,4] and followed up in papers by Migdal [5-7]. According to

[1] M. Mięsowicz, O. Stanisz and W. Wolter: *Nuovo Cimento*, **5**, 513 (1957).
[2] L. D. Landau and I. A. Pomerančuk: *Dokl. Akad. Nauk SSSR*, **92**, 535, 735 (1953).
[3] M. L. Ter-Mikaelyan: *Žu. Éksper. Teor. Fiz.*, **25**, 289, 296 (1953).
[4] M. L. Ter-Mikaelyan: *Dokl. Akad. Nauk SSSR*, **94**, 1033 (1954).
[5] A. B. Migdal: *Dokl. Akad. Nauk. SSSR*, **96**, 48 (1954).
[6] A. B. Migdal: *Dokl. Akad. Nauk SSSR*, **105**, 77 (1955).
[7] A. B. Migdal: *Žu. Éksper. Teor. Fiz.*, **32**, 633 (1957).

the theories developed by these authors we ought to expect that for very high energies ($\gtrsim 10^{12}$ eV in nuclear emulsions) the spectrum of bremsstrahlung photons is strongly cut down for low energy photons as compared with the Bethe and Heitler spectrum.

LANDAU, POMERANČUK and TER-MIKAELYAN have called in question the validity of the Bethe and Heitler formulas for very high electron energies and for photons for which $W/E \ll 1$, where W denotes the energy of the emitted photon and E the energy of the radiating electron. According to the LANDAU, POMERANČUK and TER-MIKAELYAN theory which will be further denoted by L-P-T the reason for this is as follows. If W/E is sufficiently small, the change of the momentum of an electron in consequence of an emission of a photon is so small that the uncertainty of the localization of the event due to Heisenberg's principle is much greater than the distances between the scattering centres. If so, in Landau's opinion, the effects due to the particular centres can not be treated additively as in BETHE and HEITLER's (B-H) [8] calculations. If this uncertainty range is large enough, the L-P-T theory predicts that multiple Coulomb scattering of the electron on the distance can destroy the coherence between electron and photon waves. It is thus expected that the bremsstrahlung cross-section at high energy will decrease below the B-H value. The polarization of the medium leads also to an analogous « decoherence » effect. The quantitative estimations of these phenomena were made firstly yb LANDAU and POMERANČUK (multiple scattering effect) and TER-MIKAELYAN (polarization effect). More rigorous calculations based on a quantum theoretical treatment were given by MIGDAL.

The existence of the effect mentioned above was reported in a previous paper from our laboratory (MIĘSOWICZ *et al.* [1]). To study the quantitative agreement of the observed effect with the theory, more events of very high energy electron-photon cascades were needed, in order to increase the statistical significance of the obtained results.

The aim of this paper is to present an analysis performed on four electromagnetic cascades with primary energies $\sim 10^{12}$ eV. The results obtained, were compared with the theoretical predictions of the B-H and L-P-T theories.

Just before sending our work to print we received a paper by VARFOLOMEEV *et al.* [9] [*] in which the discrepancy between the observed development of electron-photon cascades and the development predicted by cascade theory, has been also interpreted on the basis of the L-P-T theory.

[8] W. HEITLER: *The Quantum Theory of Radiation* (Oxford, 1954).

[9] A. A. VARFOLOMEEV, R. I. GERASIMOVA, I. I. GUREVIČ, L. A. MAKARINA, A. C. ROMANTSEVA, I. A. SVETLOBOV and S. A. ČUEVA: *Proc. of the International Conference on High Energy Physics at CERN* (Geneve, 1958), Appendix I, p. 297.

[*] We are much indebted to Professor GUREVIČ for sending us the preprint before publication.

2. – Experimental method.

The present analysis concerns four electron-photon cascades. Three of them (cascade *A*, *B*, *C* in Table I) have been generated in a nucleon-nucleon interaction of the type $0-14\alpha$ and energy $3.3\cdot10^{14}$ eV/nucleon (Ciok *et al.* [10]). The fourth isolated cascade (cascade *D* in Table I) was described in the paper of Mięsowicz *et al.* [1]. The energy of the primary photon of cascade *D* was found to be $(7.0^{+3.4}_{-2.6})\cdot10^{11}$ eV.

Since cascades *A*, *B*, *C* originate from decays of π^0 generated in the same nuclear interaction, the mutual radial distances between them are small. In consequence, electron tracks belonging to the different cascades are crossing each other at greater depths than about one radiation length from the point of origin of each primary pair. Therefore there was no possibility of evaluating the energy of each cascade separately. For this reason we have evaluated the mean energy of each cascade under the assumption that there is energy equipartition between primary photons and electrons of the primary pairs. This mean energy has been evaluated from the longitudinal development of the cascade taking into account the correction for lateral distribution according to Pinkau [11]. From the number of electrons with energies greater than $1\cdot10^9$ eV and $4\cdot10^8$ eV within two different radii (the values of energies have been received from scattering measurements) at the depth 2.76 rad lengths from the point of interaction we have obtained for the mean energy of the cascade the values $(1.1^{+0.4}_{-0.4})\cdot10^{12}$ eV, $(1.3^{+0.8}_{-0.5})\cdot10^{12}$ eV respectively. In these calculations we used the cascade tables of Jánossy [12] as well as Jánossy's [13] standard deviation. In the sequel we have accepted the value $1.2\cdot10^{12}$ eV for the mean energy of each cascade.

The mean energy of a π^0 meson (assuming the equipartition of energy between the two photons) equal to $2.4\cdot10^{12}$ eV is in good agreement with the energy values of two charged mesons which are contained within the same angle as the cascades. Their energies obtained from the secondary interactions are equal to $1\cdot10^{12}$ eV and $2\cdot10^{12}$ eV respectively.

Now we investigated the energy spectrum of pairs of the first generation only, generated on a given length from the point of origin of the cascade, and not the energy spectrum of all secondary electrons at a given depth as in cascade theory. By first generation pairs we understand pairs produced by the con-

---

([10]) P. Ciok, M. Danysz, J. Gierula, A. Jurak, M. Mięsowicz, J. Pernegr, J. Vrana and W. Wolter: *Nuovo Cimento*, **6**, 1409 (1957).

([11]) K. Pinkau: *Nuovo Cimento*, **3**, 1285 (1956).

([12]) L. Jánossy and H. Messel: *Proc. Roy. Irish Acad.*, A **54**, 217 (1951).

([13]) L. Jánossy: *Acta Phys. Hung.*, **2**, 289 (1952).

TABLE I.

Pair	Distance from the point of origin of the primary pair (rad. lenghts)	Obtained from the scattering measurements			Obtained from the angle of divergence	Remarks
		E_1 (eV)	E_2 (eV)	$W = E_1 + E_2$		
			Cascade A			
1	0	—	—	—	—	Primary pair (*) $E_1+E_2=1.2\cdot10^{12}$ eV
2	0.26	$7.7\cdot10^8$	$1.2\cdot10^9$	$2.0\cdot10^9$	—	First generation
3	0.42	$1.3\cdot10^8$	$6.6\cdot10^8$	$7.9\cdot10^8$	—	The order of generation is unknown
4	0.50	$> 2.4\cdot10^9$	$> 2.5\cdot10^9$	$> 4.9\cdot10^9$	—	First generation
5	0.64	—	—	—	$> 1\cdot10^9$	First generation
6	0.81	$(3.0^{+2.5}_{-0.9})\cdot10^8$	$(3.5^{+4.0}_{-1.2})\cdot10^8$	$(6.5^{+6.5}_{-2.1})\cdot10^8$	—	The order of generation is unknown
7	0.92	—	—	—	$> 4.6\cdot10^9$	First generation
8	0.96	—	—	—	$> 3.5\cdot10^9$	First generation
			Cascade B			
1	0	—	—	—	—	Primary pair (*) $E_1+E_2=1.2\cdot10^{12}$ eV
2	0.02	$> 1.0\cdot10^{10}$	$(7.8^{+10.7}_{-2.7})\cdot10^8$	$> 1.0\cdot10^{10}$	$> 1\cdot10^{10}$	First generation
3	0.18	$> 3.8\cdot10^9$	$> 3.4\cdot10^9$	$> 7.2\cdot10^9$	$> 1\cdot10^{10}$	First generation
4	0.52	$> 3.5\cdot10^9$	—	$> 3.6\cdot10^9$	$> 1\cdot10^9$	First generation
5	0.93	—	—	—	$> 1\cdot10^{10}$	First generation
6	0.94	—	—	—	$> 7\cdot10^9$	First generation
			Cascade C			
1	0	—	—	—	—	Primary pair (*) $E_1+E_2=1.2\cdot10^{12}$ eV
2	0.27	$(1.1^{+0.6}_{-0.3})\cdot10^8$	$(1.3^{+2.6}_{-0.5})\cdot10^9$	$(1.4^{+2.7}_{-0.5})\cdot10^9$	$> 5\cdot10^8$ $< 1\cdot10^9$	First generation
3	0.57	$> 3.2\cdot10^9$	$> 4.8\cdot10^9$	$> 8.0\cdot10^9$	$> 1\cdot10^{10}$	First generation
4	0.57	$(1.3^{+0.5}_{-0.3})\cdot10^8$	$(3.0^{+3.6}_{-2.0})\cdot10^8$	$(4.3^{+4.1}_{-2.3})\cdot10^8$	$< 1\cdot10^8$	First generation
5	0.89	$(2.2^{+2.5}_{-0.7})\cdot10^8$	$(2.7^{+2.2}_{-0.8})\cdot10^8$	$(4.9^{+4.7}_{+1.5})\cdot10^8$	—	The order of generation is unknown
			Cascade D			
1	0	—	—	—	—	Primary pair (*) $E_1+E_2=7.0\cdot10^{11}$ eV
2	0.32	$2.0\cdot10^8$	$1.0\cdot10^8$	$3.0\cdot10^8$	—	First generation
3	0.57	$1.3\cdot10^8$	$1.0\cdot10^7$	$1.4\cdot10^8$	—	First generation
4	0.60	$6.0\cdot10^8$	$\geqslant 7.0\cdot10^8$	$\geqslant 1.3\cdot10^9$	—	First generation
5	0.82	$1.3\cdot10^8$	$8.0\cdot10^7$	$2.1\cdot10^8$	—	First generation
6	0.96	$\geqslant 1.0\cdot10^9$	$7.5\cdot10^8$	$\geqslant 1.8\cdot10^9$	—	First generation

(*) $E_1+E_2=2E_0$ according to the assumption of equipartition of the energy.

version processes of bremsstrahlung photons emitted by electrons of the primary pair.

We succeeded in evaluating the energy of almost all electron pairs of first generation for each cascade separately. It is obvious that the distance from the point of origin of the primary pair up to the end point where the scanning for electron pairs is stopped, ought to be as long as possible (in our case about one radiation length from the point of origin of each primary pair).

The restriction to electron pairs of the first generation only, was imposed by the conditions of our measurements. As it was mentioned above, the small radial distances between the separate cascades A, B, C do not allow to correlate with the particular cascade any electron pair generated at a rather great distance from the tracks of the primary electron pair. On the other hand, it is known that all the electron pairs of the first generation, in consequence of great energy of the primary electrons, must originate in close proximity of the parent track as apparent tridents. Since the losing of such pairs is rather improbable, we avoid in this way the scanning bias.

In our opinion, investigation performed on electron pairs of the first generation is more sensitive for detecting the L-P-T effect than the investigation of the development of the whole cascade. The L-P-T effect is rather reduced by the degradation of energy, whereas in our procedure such a degradation does not take place.

We have used two criteria, energy and geometry criteria, whether a pair is a first generation one. Such a procedure was successful in all cases except in the case of three electron pairs where there was no possibility to establish the order of generation, *i.e.* in which successive generation each pair was produced. The energy measurements have been performed by scattering, especially the differential one. In cases in which the application of scattering was not possible, we have based on the data derived from the measurements of the angle of divergence.

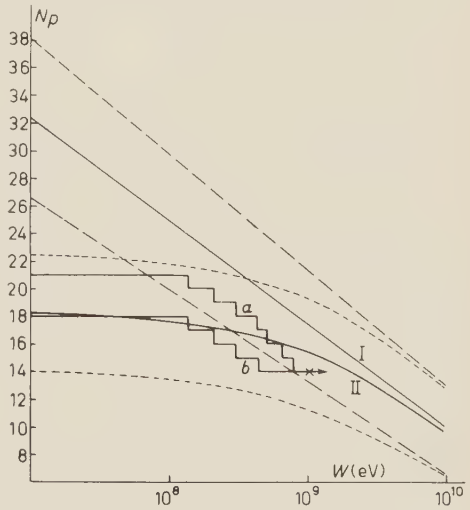

Fig. 1. – Integral energy spectrum of electron pairs of the first generation created in the first radiation length. N_p: number of pairs of energy greater than the given value W. a, b: experimental histograms. I, II: Bethe, Heitler and Landau, Pomerančuk, Ter-Mikaelyan curves respectively (primary electron energy $5 \cdot 10^{11}$ eV). Curves I and II are given with their standard deviations.

In Table I there are given the results of our measurements performed on four cascades. The energy spectrum of electron pairs of the first generation created on the first radiation length has been done on the basis of the data given in Table I (Fig. 1). The histograms represent the experimental spectrum taking into account the uncertainty of the order of generation of the three electron pairs (histograms *a* and *b*). For energies greater than about 10^9 eV (see the point with an arrow on Fig. 1) the shapes of the histograms are unknown because of the impossibility of evaluating the upper limit of such high energies. Curves I and II represent the B-H and L-P-T spectra respectively for the primary electron energy equal to $5 \cdot 10^{11}$ eV at the depth of one radiation length. This energy value corresponds to the mean energy of eight primary electrons of four cascades under consideration (six primary electrons each of energy of $6 \cdot 10^{11}$ eV and two primary electrons each of energy of $3.5 \cdot 10^{11}$ eV). The dashed curves represent the Poisson deviation from the theoretical curves of B-H and L-P-T.

3. – Discussion on experimental procedure.

We have calculated the average number of electron pairs of first generation with energy greater than W, created by the primary electron of initial energy E_0 on the length t, where t is the distance from the beginning of the electron trajectory. The calculations were made, first on the basis of the B-H formulas and then also performed by means of the L-P-T formulas.

Fig. 2 shows the integral energy spectrum of electron pairs of the first generation obtained from these two theories. Theoretical curves I and II of Fig. 1 have been obtained in the same way as the curves of Fig. 2.

We have taken into account the energy loss of the primary electron resulting from radiation. The energy losses from ionization (about $2 \cdot 10^7$ eV on one radiation length) are in our case negligible in comparison with the energy of about 10^{12} eV.

In our problem we must take into consideration the cross-sections of the following processes which are decisive in forming the energy spectrum of electron pairs.

1) Pair production by photons,

2) Compton effect,

3) Photonuclear reactions,

4) Production of tridents.

Processes 1), 2) and 3) are competitive. From the geometry of the experiment, *i.e.* from the fact that the number of pairs is observed on the first radiation length follows that the reduction of the number of pairs caused by 2 and 3 is negligible. The number of pairs of energy $W \sim 10^7$ eV is diminished by about (2 ÷ 3 %). The number of pairs of energy $W \gtrsim 10^8$ eV practically rests unchanged, because in this energy range the cross-sections of processes 2) and 3) are very small in comparison with the cross-section of 1.

The increasing of the mean free path for pair production with the decreasing energy of photons ($\sim 10^7$ eV) results in the same direction. Although this effect and the effects 2) and 3) act in the same direction as the modification of L-P-T, nevertheless they are much smaller than this modification. We have estimated that the whole cumulative influence amounts to only some per cent and so, is negligible in comparison with the L-P-T modification.

So we see that the number of electron pairs of first generation is a sensitive detector of the character of the bremsstrahlung spectrum and quite insensitive to competitive effects, in comparison with the process of pair production.

The number of pairs is of course increased by the trident production, however, this last one does not favour the production of pairs of small energies. Accepting for $E_0 = 5 \cdot 10^{11}$ eV the mean free path for trident production about 3.5 radiation lengths, we obtain a contribution of about 6 % of the whole number of pairs produced by the first process. Finally we see that the effects 2), 3) and 4) are of no importance in our problem.

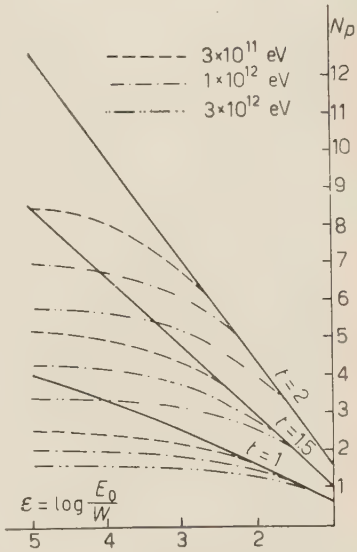

Fig. 2. – Integral energy spectrum of electron pairs of the first generation. N_p: number of pairs of energy greater than that corresponding to the value ε. Full curves: Bethe-Heitler curves for three different depths (1.0, 1.5, 2.0 radiation lengths). Dashed and dotted dashed curves: Landau, Pomerančuk, Ter-Mikaelyan curves for the depths 1.0, 1.5, 2.0 radiation lengths and the primary electron energy $E_0 = 3 \cdot 10^{11}$ eV, $1 \cdot 10^{12}$ eV and $3 \cdot 10^{12}$ eV.

On Fig. 2, representing the results of both theories (B-H and L-P-T), it is interesting to remark that in the B-H energy spectrum we have the dependence of the number of pairs on E_0/W only, while in the analogous curves of L-P-T there is a dependence on both E_0 and W.

Although there is a possibility of large errors in estimating E_0, the primary energy of the electron, it is important to stress that the change of E_0 even by one order of magnitude, does not change the character of the L-P-T spectrum. From Fig. 2 we see also that the L-P-T spectrum curves have a plateau be-

ginning from a certain ε, which feature is not shown by the B-H spectrum curve. This is the main consequence of the L-P-T theory which just expresses the lack of small energy pairs.

4. – Conclusions.

1) The experimental energy spectrum of the electron pairs of the first generation, produced in the first radiation length, shows a statistically significant deviation from the Bethe and Heitler energy spectrum curve.

2) There is rather a good agreement between the experimental results and the curve which represents the energy spectrum of Landau, Pomerančuk and Ter-Mikaelyan.

3) The method of investigation of electron pairs of the first generation only, is in the author's opinion a sensitive tool in detecting the difference between the energy spectrum of Bethe and Heitler and that of Landau, Pomerančuk and Ter-Mikaelyan, since in cascade development there is a degradation of energy of the emitting electron.

* * *

We wish to express our gratitude to Professor M. MIĘSOWICZ for suggesting these investigations, his permanent interest in our work, and many valuable ideas and hints during the progress of this work.

RIASSUNTO (*)

Si sono esaminate quattro cascate elettrofotoniche di alta energia ($\sim 10^{12}$ eV) nel primo stadio del loro sviluppo. Il numero e l'energia delle coppie di elettroni della prima generazione prodotte nella prima lunghezza di radiazione sono stati stimati e confrontati coi valori teorici calcolati sulla base della teoria di Bethe e Heitler. Le stesse grandezze sono state anche calcolate in base alle teorie di Landau, Pomerančuk e Ter-Mikaelyan che tengono conto dell'influenza del mezzo sulla bremsstrahlung di elettroni di altissima energia. I risultati sperimentali sono in miglior accordo colle previsioni di Landau, Pomerančuk e Ter-Mikaelyan che con quelle di Bethe e Heitler, confermando i risultati ottenuti nel nostro laboratorio e comunicati in un precedente lavoro [1].

(*) *Traduzione a cura della Redazione.*

IL NUOVO CIMENTO Vol. XI, N. 4 16 Febbraio 1959

Rayleigh Scattering of Polarized Photons.

D. Brini, E. Fuschini, D. S. R. Murty (*) and P. Veronesi

Istituto di Fisica dell'Università - Bologna
Istituto Nazionale di Fisica Nucleare - Sezione di Bologna

(ricevuto il 22 Novembre 1958)

Summary. — We discuss two criteria for comparing in a decisive manner the theoretical predictions on the Rayleigh scattering deduced by Franz and by Brown and Mayers. The first deals with the study of the Rayleigh scattering of the polarized photons, the second considers the polarization effects due to the Rayleigh scattering of an unpolarized radiation. In the elastic scattering of polarized photons an asymmetry ratio R can be defined as $(\mathrm{d}\sigma_0/\mathrm{d}\Omega+\xi_{\parallel}\,\mathrm{d}_1\sigma/\mathrm{d}\Omega)/(\mathrm{d}\sigma_0/\mathrm{d}\Omega+\xi_{\perp}\,\mathrm{d}\sigma_1/\mathrm{d}\Omega)$, where the numerator and the denominator represent the Rayleigh cross-section for the same angle of scattering in two orthogonal planes. The quantities $\xi_{\parallel}$ and $\xi_{\perp}$ are the degrees of polarization of the incident beam referred to the previous planes, while $\mathrm{d}\sigma_0/\mathrm{d}\Omega$ is the cross-section for the unpolarized photons and $\mathrm{d}\sigma_1/\mathrm{d}\Omega$ is the term sensitive to polarization. The value of R was determined by using a beam of photons of energy $1.28\,\mathrm{mc}^2$ scattered on a target of Hg at angles of scattering $\theta_1=65°$, $\theta_2=90°$ and $\theta_3=110°$. The experimental results are in closer agreement with the calculations of Brown and Mayers. The polarized beam was obtained by means of a Compton scattering at an angle of 50° of the unpolarized beam coming from a ^{60}Co source.

1. – Introduction.

It is known that in all the experiments performed in order to put in evidence the Delbrück scattering, the knowledge of the contribution of the Rayleigh scattering has a fundamental importance.

(*) On leave from the Physics Department, Osmania University, Hyderabad (India).

In fact it is possible, in principle, to deduce the cross-section of the Delbrück effect by subtracting the THOMSON and RAYLEIGH contributions from the values of the differential cross-section of the elastic scattering. While the THOMSON contribution can be easily calculated, some uncertainty exists for the Rayleigh effect. The theory of the latter effect due to FRANZ [1] was the only one available until a few years back, and this is based on an atom model and on a simplifying hypothesis which could not be considered completely satisfying to describe the phenomenon. In recent years more precise calculations were made by BRENNER, BROWN and WOODWARD [2] and by BROWN and MAYERS [3,4] for different energies of photons but only for the scattering on the K-shell electrons of Hg.

Though the calculations of these authors offer a greater confidence of exactness, however, an experimental test is necessary which permits a direct confirmation of the validity of the theory proposed by them in comparison with that of FRANZ [5-8]. A comparison of the theories made by means of the measurement of the absolute value of the differential cross-section of the Rayleigh scattering results quite unprecise as shown by the different results of the various authors. The reason for the imprecision lies in the difficulties of evaluation of the corrections for the counter efficiency, the absorption of the scattered radiation in the target, and the evaluation of the number of scattering centers, etc.

Two criteria exist which permit a comparison of the two theories with experiment which eliminate to a large extent the inconveniences cited above. The first criterion consists in the study of the Rayleigh scattering of polarized photons and the second criterion in the experimental verification of the polarization effects produced by the Rayleigh scattering.

The first method was used by us in a previous work as well as in the present measurements [9]. The second method was successfully used by SOOD [10] in a very recent experiment and by SOOD and KNAPP [11] in the study of the resonance nuclear scattering.

[1] W. FRANZ: *Zeits. Phys.*, **98**, 314 (1936).
[2] S. BRENNER, G. E. BROWN and J. B. WOODWARD: *Proc. Roy. Soc.*, A **227**, 59 (1954).
[3] G. E. BROWN and D. F. MAYERS: *Proc. Roy. Soc.*, A **234**, 387 (1956).
[4] G. E. BROWN and D. F. MAYERS: *Proc. Roy. Soc.*, A **242**, 89 (1957).
[5] P. KESSLER and P. EBERHARD: *Compt. Rend.*, **245**, 1599 (1957).
[6] M. FEIX, P. KESSLER and P. NICOURD: *Compt. Rend.*, **246**, 3226 (1958).
[7] N. CINDRO and K. ILAKOVAC: *Nucl. Phys.*, **5**, 647 (1958).
[8] K. G. STANDING and J. V. JOVANOVICH: *Nature*, **182**, 521 (1958).
[9] D. BRINI, E. FUSCHINI, L. PELI and P. VERONESI: *Nuovo Cimento*, **7**, 877 (1958).
[10] B. S. SOOD: *Proc. Roy. Soc.*, A **247**, 575 (1958).
[11] V. KNAPP and B. S. SOOD: *Proc. Roy. Soc.*, A **247**, 369 (1958).

LOVAS ([12]) has recently suggested the same criterion to separate the different components of the elastically scattered radiation, particularly the Delbrück effect.

In the following two sections we examine in some detail the two criteria and report the results of some numerical calculations made following both theories and using the formalism of the Stokes parameters ([13]).

2. – Elastic scattering of polarized photons.

By means of a convenient Compton scattering of an unpolarized radiation a partially polarized photon beam is obtained a (*). This beam after a suitable collimation is sent on to a Hg target where the elastic interaction takes place. For a fixed angle of elastic scattering the ratio between the intensity of the scattered radiation in the plane of Compton scattering and the intensity scattered in the orthogonal plane, is expressed by the relation

$$R = \frac{\mathrm{d}\sigma_0/\mathrm{d}\Omega + \xi_{\parallel}(\mathrm{d}\sigma_1/\mathrm{d}\Omega)}{\mathrm{d}\sigma_0/\mathrm{d}\Omega + \xi_{\perp}(\mathrm{d}\sigma_1/\mathrm{d}\Omega)}, \tag{1}$$

where: $\mathrm{d}\sigma_0/\mathrm{d}\Omega$ is the differential cross-section of Rayleigh scattering for unpolarized photons;

$\mathrm{d}\sigma_1/\mathrm{d}\Omega$ is the term of the cross-section sensitive to polarization and ξ is the degree of polarization of the incident beam defined as the second Stokes parameter of the Compton scattered beam, making the total intensity equal to unity.

Substituting in (1) the explicit expressions of $\mathrm{d}\sigma_0/\mathrm{d}\Omega$ and $\mathrm{d}\sigma_1/\mathrm{d}\Omega$ deduced from the two theories of Franz and of Brown and Mayers one can obtain the corresponding values of R. These values of R can be compared with those obtained from the experiment. In Fig. 1 are plotted the ratios which can be deduced from the two above mentioned theories for the energies of 0.32 mc^2, 0.64 mc^2, 1.28 mc^2 and 2.56 mc^2. The solid curve represents the behaviour

---

([12]) I. LOVAS: *Nucl. Phys.*, **8**, 155 (1958).

([13]) U. FANO: *Journ. Opt. Soc. Am.*, **39**, 859 (1949).

(*) It is clear that the Compton scattering is not the only polarizing scattering. All the elastic scatterings give, as we shall see, polarization effects. Here we have considered only that Compton component whose cross-section is high.

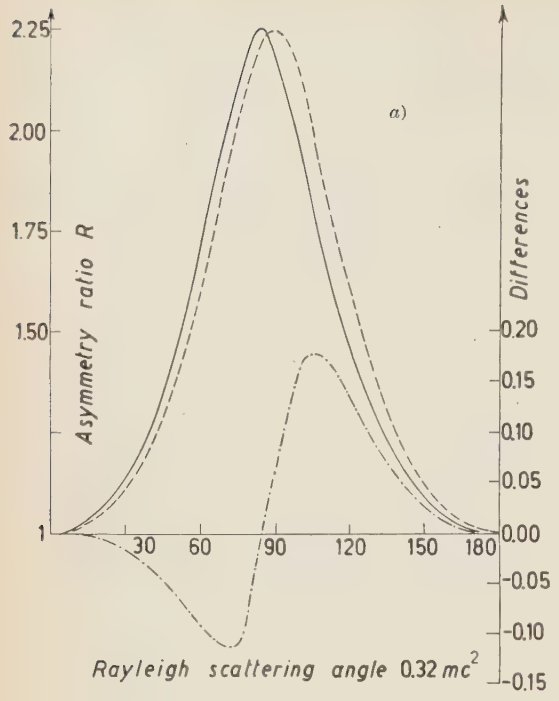

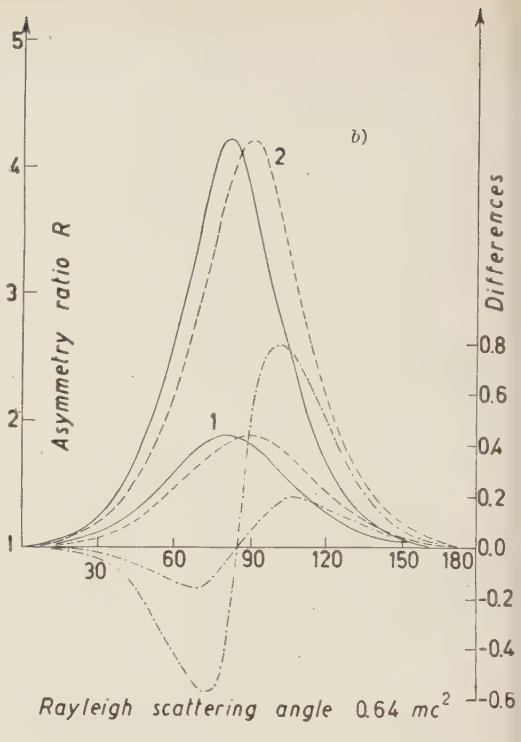

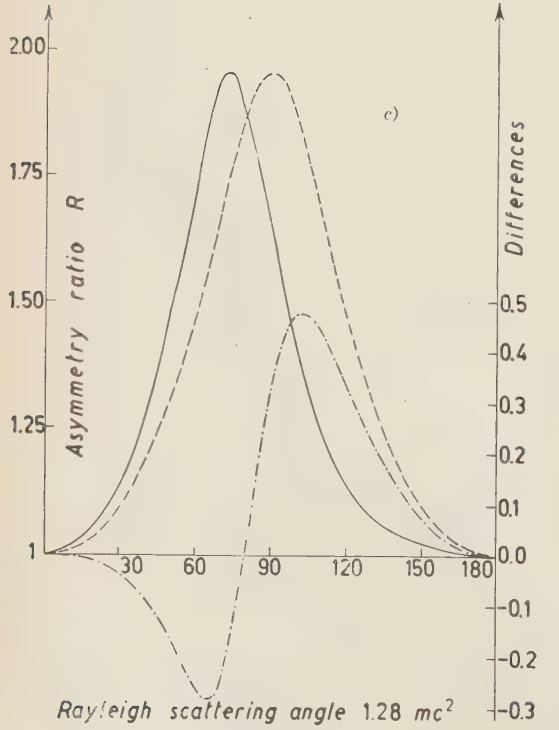

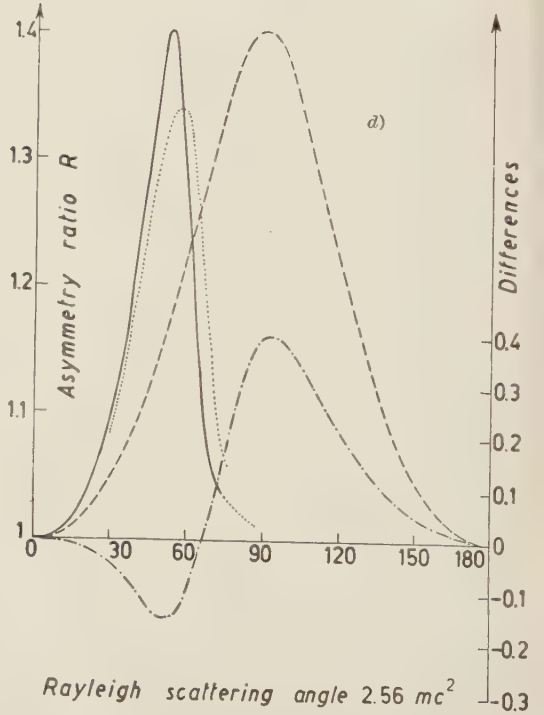

Fig. 1. Asymmetry ratio in Rayleigh scattering of polarized photons. Solid line: Brown and Mayers theory. Dashed line: Franz theory. Dashed-dotted line: differences between the values of the asymmetry ratios deduced from the two theories. (See Table 1).

of R deduced from Brown' and Mayers theory, the dashed curve the behaviour of R from Franz' theory and the dotted-dashed curve gives the difference between the ratios.

TABLE I. – *Data referring to the curves of Fig. 1.*

Energy	Source	Compton scattering angle	Polarization degree
0.32 mc^2	^{51}Cr 0.320 MeV	123°	— 0.384
0.64 mc^2	^{137}Cs 0.666 MeV	77°	— 0.615
	^{60}Co 1.17 MeV, 1.33 MeV	100°	— 0.307
1.28 mc^2	^{60}Co 1.17 MeV, 1.33 MeV	50°	— 0.322
2.56 mc^2	^{24}Na 2.75 MeV	38°	— 0.167

In the case of the energy of 2.56 mc^2 we take into account the contribution of the Thomson effect. The dotted line represents the resulting asymmetry ratio.

3. – Polarization effects in the elastic scattering.

We shall confine our consideration briefly to Thomson and Rayleigh scattering. We wish to deduce the expression for the degree of polarization of the scattered radiations as a function of the scattering angle.

3·1. *Thomson scattering.* – Let us consider an unpolarized beam represented by the parameters

$$\begin{pmatrix} 1 \\ 0 \\ 0 \\ 0 \end{pmatrix}. \tag{2}$$

The operator which, applied to the Stokes parameters of a generic γ-ray beam, permits to deduce the relations which describe the Thomson scattering is given by the matrix (*)

$$T = \frac{1}{2} r_0^2 \begin{pmatrix} 1+\cos^2\theta & -\sin^2\theta & 0 & 0 \\ -\sin^2\theta & 1+\cos^2\theta & 0 & 0 \\ 0 & 0 & 2\cos\theta & 0 \\ 0 & 0 & 0 & 2\cos\theta \end{pmatrix}, \tag{3}$$

(*) The matrix T can be deduced in this classical case, in a very simple way. We omit here the calculations which lead to its determination.

where r_0 is the classical radius of the electron and θ the scattering angle. The Stokes parameters of the scattered beam are then expressed by

$$T\begin{pmatrix}1\\0\\0\\0\end{pmatrix}=\frac{1}{2}R_0^2\begin{pmatrix}1+\cos^2\theta\\-\sin^2\theta\\0\\0\end{pmatrix}, \tag{4}$$

where we put $R_0^2=Z^2e^2/Ac^2$ instead of r_0^2 since this is the equivalent expression for the nucleus.

From (4) it can be seen that the scattered beam is partially linearly polarized in the plane of scattering with a degree of polarization ξ given by

$$\xi=-\frac{\sin^2\theta}{1+\cos^2\theta}. \tag{5}$$

ξ is independent of the energy of the photons, of the scattering material and is symmetric around 90°.

3·2. *Rayleigh scattering.* – Theory of Franz: We recall the expression for the Rayleigh scattering cross-section for a wave linearly and totally polarized deduced from the Franz theory,

$$\frac{\mathrm{d}\sigma}{\mathrm{d}\Omega}=A^2r_0^2\sin^2\Theta,$$

where A is the form factor and Θ is the angle between the direction of vibration of the incident wave and the direction of the scattering wave.

The theory of Franz for the polarization states of the scattered beam, leads to the same result found for the Thomson scattering; the matrix T in this case results identical to (3) multiplied by the form factor. Consequently the expression of ξ is still given by (5).

Theory of Brown and Mayers: The deduction of the matrix T for the Rayleigh scattering based on Brown and Mayers' theory and valid only for the K shell electrons (calculated specifically for Hg) was made by Böbel and Passatore [14]. It results in the following form:

$$T=r_0^2\begin{pmatrix}AA^*+BB^* & 2(R)AB^* & 0 & 0\\ 2(R)AB^* & AA^*+AB^* & 0 & 0\\ 0 & 0 & AA^*-BB^* & 2(I)A^*B\\ 0 & 0 & 2(I)AB^* & AA^*-BB^*\end{pmatrix}, \tag{6}$$

[14] G. Böbel and G. Passatore: private communication.

where

$$A = M(1', 1) + M(2', 2) \quad \text{and} \quad B = M(1', 2) + M(2', 1) .$$

$M(1', 1)$, $M(2', 2)$, $M(1', 2)$ and $M(2', 1)$ are the complex quantities calculated by BROWN and MAYERS in their work (*). Bearing in mind (6), the scattered beam is represented by the parameters

$$(7) \qquad T \begin{pmatrix} 1 \\ 0 \\ 0 \\ 0 \end{pmatrix} = r_0^2 \begin{pmatrix} AA^* + BB^* \\ -2(R)AB^* \\ 0 \\ 0 \end{pmatrix} .$$

Remembering the definition of the degree of polarization we can deduce in this case

$$(8) \qquad \xi = -\frac{2(R)AB^*}{AA^* + BB^*} .$$

The behaviour of $-\xi$ for the various energies and for both theories is shown in Fig. 2. The curve for 2.56 mc^2 energy does not take

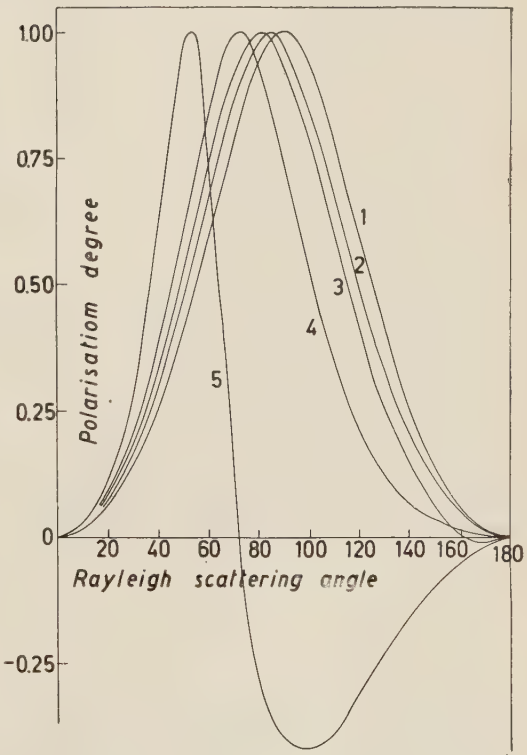

Fig. 2. – Polarization degree of the Rayleigh scattered radiation as a function of the scattering angle: 1) Franz' theory; 2) Brown and Mayers' theory for the energy of 0.32 mc^2; 3) Brown and Mayers theory for the energy of 0.64 mc^2; 4) Brown and Mayers theory for the energy of 1.28 mc^2; 5) Brown and Mayers theory for the energy of 2.56 mc^2.

(*) These authors do not report for the energy $h_\nu = 1.28\ mc^2$ the imaginary parts of the scattering amplitudes. The data which permitted us to calculate these imaginary parts were kindly supplied by the authors in a private communication. In the Appendix we shall report the scattering amplitudes completed with the imaginary parts.

into account the interference contribution due to Thomson scattering, which is not negligible at this energy. The change in the sign of the polarization degree at large angles has not any particular significance. It results only as a consequence of the approximation with which the numerical calculations of the quantities M were evaluated.

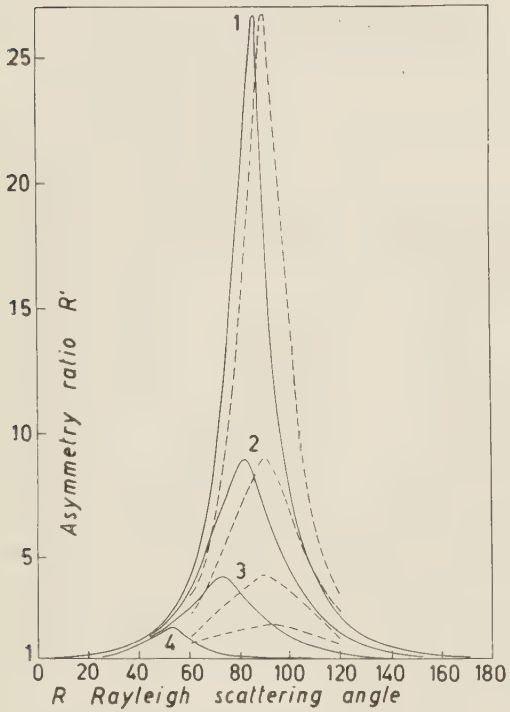

Fig. 3. – Asymmetry ratio R'. Dashed line: Franz' theory. Solid line: Brown and Mayers' theory: 1) 0.32 mc² Compton scattering angle $\theta_c=90°$; 2) 0.64 mc² Compton scattering angle $\theta_c=90°$; 3) 1.28 mc² Compton scattering angle $\theta_c=80°$; 4) 2.56 mc² Compton scattering angle $\theta_c=70°$.

The Fig. 2 shows evidently the different behaviour of the polarization effects deduced from one or the other of the theories. An experimental verification of this fact represents a check very decisive in respect of the two theories.

A Compton scattering of the radiation already polarized in the elastic scattering can be utilized for this purpose. Also in this case an asymmetry ratio R' can be conveniently determined and it results

$$(9) \qquad R' = \frac{\mathrm{d}\sigma_0/\mathrm{d}\Omega + \xi_{\parallel}(\mathrm{d}\sigma_1/\mathrm{d}\Omega)}{\mathrm{d}\sigma_0/\mathrm{d}\Omega + \xi_{\perp}(\mathrm{d}\sigma_1/\mathrm{d}\Omega)},$$

where this time the quantities $\mathrm{d}\sigma_0/\mathrm{d}\Omega$ and $\mathrm{d}\sigma_1/\mathrm{d}\Omega$ correspond to Compton scattering and are deducible from Fano's matrix ([13]). Choosing for each of the four energies considered the Compton scattering angle for which R' results maximum, it is possible to calculate its behaviour as a function of ξ, that is, as a function of the angle of the polarizing elastic scattering. Fig. 3 shows the behaviour of R': one sees that at low energies the difference between the theory of Franz and that of Brown and Mayers is less significant than at high energies. In the case of 2.56 mc² we have considered the interference with the Thomson effect.

4. – The experiment.

In the previous paper we reported the results of a measurement of R defined by (1) for an energy $h\nu = 0.64\ mc^2$. In the present paper we report the results of a measurement performed at the energy $h\nu = 1.28\ mc^2$.

By means of a Compton scattering at 50° of a collimated beam of photons from a ^{60}Co source a partially polarized beam of mean energy $1.28\ mc^2$ is obtained. The polarization degree averaged over the energies of 1.17 MeV and 1.33 MeV of the incident photons with the criterion already mentioned ([9]) results to have the absolute value

$$\xi = 0.322\ .$$

In Fig. 4 is shown the spectrum of the Compton scattered radiation after a second collimation along with a spectrum of ^{137}Cs. Observing that the counter resolution is 10% at half-maximum, the dispersion in energy of the polarized beam is 20% since our radiation has an energy of $(1.28 \pm 0.013)\ mc^2$.

The polarized beam is directed to a Hg target on which the investigated Rayleigh scattering takes place. The cross-section of the process may be given in the form

$$\frac{d\sigma}{d\Omega} = \frac{d\sigma_0}{d\Omega} + \xi \frac{d\sigma_1}{d\Omega}\ .$$

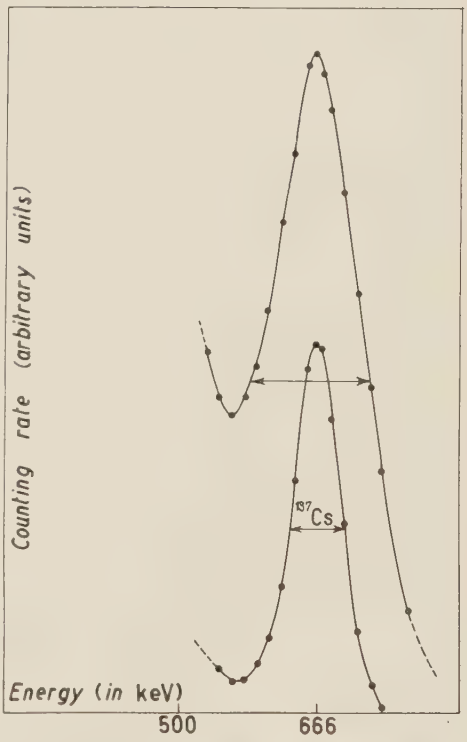

Fig. 4. – Photoelectric peak of the polarized beam and of a ^{237}Cs source.

We have calculated the values of $d\sigma_0/d\Omega$ and $d\sigma_1/d\Omega$ from both theories. In Fig. 5 is shown their behaviour as a function of the scattering angle and in units of r_0^2. In this connection one must observe that comparison between the two theories is valid only for sufficiently large angles to which correspond great transfers of momentum.

From the so calculated cross-section values and taking into account the polarization degree it is possible to evaluate from (1) the asymmetry ratio

as a function of the scattering angle. The behaviour of such asymmetry ratio for the theory of Franz as well as for that of Brown and Mayers is shown in Fig. 1.

The asymmetry ratio was measured at angles of 65°, 90° and 110° with a disposition similar to that used in our previous work and by utilizing the same criterion for the selection of the investigated events from the spurious ones (Fig. 6).

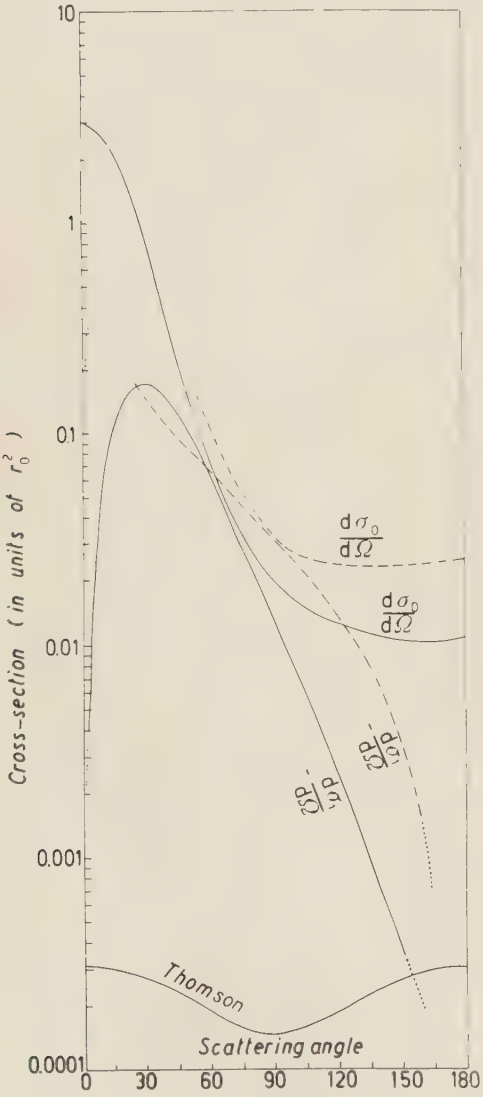

Fig. 5. – Rayleigh and Thomson scattering cross-sections. Solid curve: Brown and Mayers' theory. Dashed curve: Franz' theory.

The reason for choosing these angles is that at these values the asymmetry ratio is very significant.

In a manner similar to that followed in the previous work we evaluated the influence of the geometry due to the finite dimensions of the scatterers and detectors. The calculations made to this purpose show that for the angles of 65° and 110° the geometry does not considerably alter the results obtained for the point-like scatterers and detectors, while at 90° the influence of geometry is appreciable.

The eventual asymmetry due to geometry was measured by sending on to the target of Hg an unpolarized beam of photons. The measurements were made in two different ways, once by using a very intense source of ^{60}Co and another time by using a small source of ^{137}Cs; the results obtained have been averaged.

In Table II is given a summary of the results.

As can be seen the results are in closer agreement with the theory of Brown and Mayers.

In all our evaluations we have disregarded the contribution of the L shell to Rayleigh scattering; although little is known about it, it is generally considered to be very

TABLE II.

Angle	R_{theor}		$R_{corrected}$		$R_{measured}$	$R_{geometrical}$	$R_{effective}$
	F	B.M.	F	B.M.			
65°	1.575	1.836	1.580	1.855	1.831 ± 0.077	0.980 ± 0.012	1.868 ± 0.082
90°	1.955	1.650	1.880	1.520	1.602 ± 0.198 1.370 ± 0.120	1.115 ± 0.016 0.966 ± 0.005	1.423 ± 0.104
110°	1.685	1.250	1.660	1.234	1.337 ± 0.211	1.032 ± 0.007	1.295 ± 0.205

small especially at large angles. Similarly we have not taken into account the small percentage of Thomson scattering whose presence, however, acts in favour of Franz' theory.

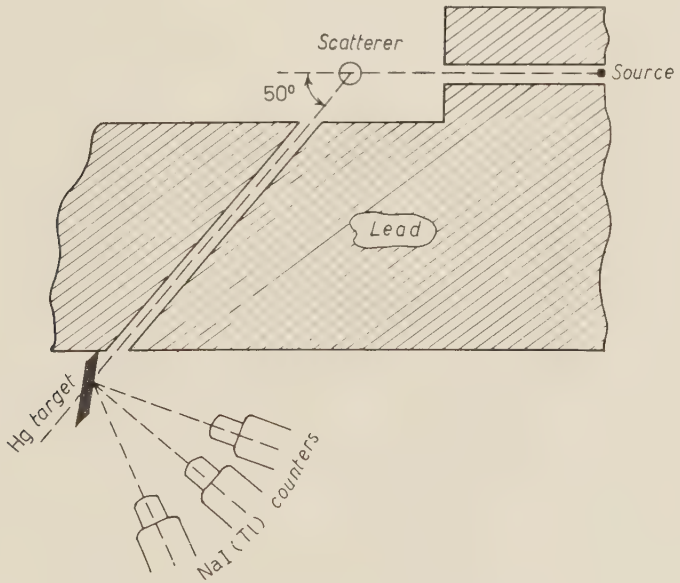

Fig. 6. – Experimental arrangement.

An evaluation of its contribution on our experimental results brings about an yet greater confirmation of the agreement with the theory of Brown and Mayers.

* * *

We are grateful to Mr. G. BUSACCHI and to Mr. R. VOLTA for their continued help in maintaining the electronic equipment.

One of us (D.S.R.M.) wishes to express his grateful thanks to Professor G. PUPPI, Director of the Institute for a fellowship and for the hospitality.

APPENDIX

We report in the following Table the scattering amplitudes on Hg for the energy 1.28 mc^2. They include the imaginary parts which were not reported in the work of Brown and Mayers.

TABLE III.

Angle	$A = M(1', 1) + M(2', 2)$	$B = M(1', 2) + M(2', 1)$
0	$1.7454 - i\,0.1062$	$-0.0000 + i\,0.0000$
10	$1.6159 - i\,0.0980$	$-0.0158 + i\,0.0032$
20	$1.2967 - i\,0.0777$	$-0.0531 + i\,0.0109$
30	$0.9316 - i\,0.0546$	$-0.0914 + i\,0.0187$
40	$0.6251 - i\,0.0357$	$-0.1182 + i\,0.0239$
50	$0.4042 - i\,0.0229$	$-0.1319 + i\,0.0258$
60	$0.2540 - i\,0.0149$	$-0.1374 + i\,0.0254$
70	$0.1568 - i\,0.0101$	$-0.1373 + i\,0.0237$
80	$0.0960 - i\,0.0074$	$-0.1335 + i\,0.0212$
90	$0.0580 - i\,0.0059$	$-0.1280 + i\,0.0184$
100	$0.0346 - i\,0.0046$	$-0.1223 + i\,0.0159$
110	$0.0204 - i\,0.0035$	$-0.1170 + i\,0.0137$
120	$0.0117 - i\,0.0027$	$-0.1123 + i\,0.0119$
130	$0.0060 - i\,0.0020$	$-0.1082 + i\,0.0105$
140	$0.0034 - i\,0.0014$	$-0.1040 + i\,0.0093$
150	$0.0021 - i\,0.0007$	$-0.1017 + i\,0.0084$
160	$0.0010 - i\,0.0002$	$-0.1013 + i\,0.0078$
170	$0.0002 - i\,0.0000$	$-0.1022 + i\,0.0076$
180	$0.0000 - i\,0.0000$	$-0.1029 + i\,0.0075$

RIASSUNTO

Si discutono due criteri per confrontare in modo decisivo le previsioni teoriche dello scattering Rayleigh effettuate da Franz e da Brown e Mayers. Il primo consiste nello studiare lo scattering Rayleigh di fotoni polarizzati, il secondo nel considerare gli effetti di polarizzazione dovuti allo scattering Rayleigh di una radiazione non polarizzata. Nello scattering di fotoni polarizzati si può definire un rapporto di asimmetria $R = (\mathrm{d}\sigma_0/\mathrm{d}\Omega + \xi_{\parallel}\mathrm{d}\sigma_1/\mathrm{d}\Omega)/(\mathrm{d}\sigma_0/\mathrm{d}\Omega + \xi_{\perp}\mathrm{d}\sigma_1/\mathrm{d}\Omega)$, dove il numeratore ed il denominatore rappresentano la sezione d'urto Rayleigh, per uno stesso angolo di scattering in due piani ortogonali. Le grandezze $\xi_{\parallel}$ e $\xi_{\perp}$ sono i gradi di polarizzazione del fascio incidente riferiti ai due piani suddetti, mentre $\mathrm{d}\sigma_0/\mathrm{d}\Omega$ è la sezione d'urto per fotoni non polarizzati e $\mathrm{d}\sigma_1/\mathrm{d}\Omega$ il termine sensibile alla polarizzazione. È stata eseguita una misura di R nello scattering Rayleigh elastico usando un fascio di fotoni di energia 1.28 mc^2, scatterati su Hg con angoli di scattering $\theta_1 = 65°$, $\theta_2 = 90°$ e $\theta = 110°$. I risultati sperimentali sono in ottimo accordo con i calcoli di Brown e Mayers. Il fascio polarizzato era ottenuto mediante uno scattering Compton ad un angolo di circa 50° di un fascio emesso da una sorgente di ^{60}Co.

IL NUOVO CIMENTO Vol. XI, N. 4 16 Febbraio 1959

A Note on the Trident Process.

P. K. Aditya (*) (**)

Physics Honours School, Panjab University - Chandigarh

(ricevuto il 2 Dicembre 1958)

Summary. — The mean free path for direct pair production by high energy electrons has been found for electrons of mean energy 20 GeV and 80 GeV. Electrons were obtained from high energy electromagnetic cascades recorded in nuclear emulsion stacks. Pair energies have been determined by using a modified relation for the pair opening angle. The cascade theory has been used to find the correction for spurious tridents. The trident mean free path values obtained at mean energy 20 GeV and 80 GeV are 10.4 ± 1.2 and 7.7 ± 1.9 respectively, measured in terms of the cascade unit. The results are in agreement with the theoretical predictions.

In recent years, some observations on the abnormal development of cascade showers (1) and the presence of a large number of tridents in them and along cores of high energy disintegrations (2) had raised doubt on the validity of the quantum electrodynamic theory. We have carried out an investigation in this field and in this note describe our method of approach and the results obtained thereof. A detailed survey (3) of all the data known to us reveals

(*) Formerly known as Prem Kumar.

(**) At present at the Institute for Theoretical Physics, University of Copenhagen.

(1) M. Schein, D. M. Haskin and R. G. Glasser: *Phys. Rev.*, **95**, 171 (1954); A. Debenedetti, C. M. Garelli, L. Tallone and M. Vigone: *Nuovo Cimento*, **2**, 220 (1955); **3**, 226 (1956); **4**, 1151 (1956); G. Wataghin: *Proc. Rochester Conference* (Feb. 1955); L. Barbanti-Silva, C. Bonacini, C. De Pietri, R. Perilli-Fedeli and A. Roveri: *Nuovo Cimento*, **3**, 1465 (1956).

(2) P. S. Freier and J. E. Naugle: *Phys. Rev.*, **92**, 1086 (1953); M. Koshiba and M. F. Kaplon: *Phys. Rev.*, **97**, 193 (1955); E. Lohrmann: *Nuovo, Cimento* **3**, 820 (1956).

(3) To be published separately.

that the observed discrepancies arose due to limitations of the experimental approach.

Two parameters entering into the determination of the trident mean free path are *a*) the energy estimation of the parent electrons and *b*) the elimination of spurious tridents. The following has been our method of approach.

a) *Energy estimation*: Since multiple Coulomb scattering measurements have a limited reliability (up to about 5 GeV for the normally available 500 μm cell size and 0.1 μm noise level), we resorted to the use of pair opening angle versus photon energy relation, taking into account the fact that, for high energy pairs of which the separation is not measurable in the first few mm from origin, the contribution due to multiple Coulomb scattering may not *a priori* be neglected (4). Assuming equipartition of energy between the two electrons we have combined the relative scattering contribution to the true opening, using the most probable value given by Borsellino's relation (5). Since the separation due to scattering varies as the $\frac{3}{2}$ power of the distance from origin, it predominates over the true opening for all distances beyond 250 μm, at which the two contributions are equal. A few typical energies, plotted in Fig. 1,

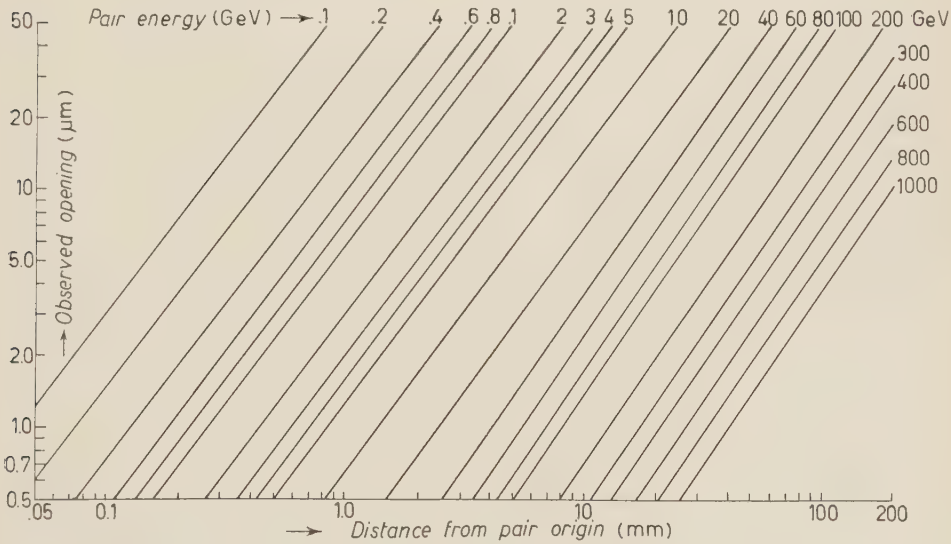

Fig. 1. – Variation of pair separation with distance from pair origin, for pairs of various energies.

(4) In two brief communications (14), the energy estimation was done on these lines, when our attention was drawn to similar arguments already published independently by E. Lohrmann (*Nuovo Cimento*, **2**, 1029 (1955)). We shall therefore not enter into details.

(5) A. Borsellino: *Phys. Rev.*, **89**, 1023 (1953).

show the curves between pair opening and distance from origin. One then needs to find pair separation at regular intervals, the interval depending upon pair energy and available length. In general up to ten such readings give a good estimate of the energy. For most part of the energy range we are interested in at present, the reliability of the method has been checked by comparing the energy spectrum of secondary electrons with that theoretically predicted ([6]). Our results are shown in Fig. 2. The availability of a few

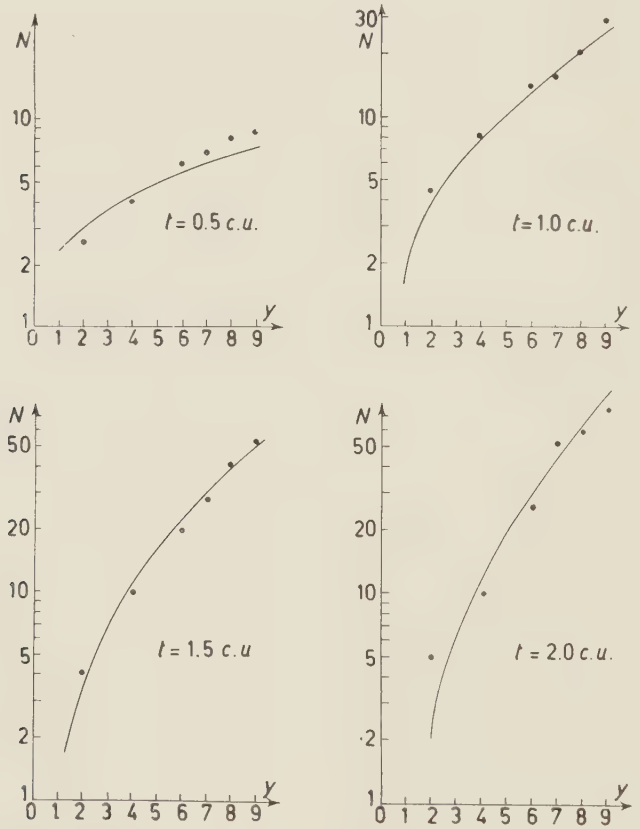

Fig. 2. – Mean number N, of secondary electrons of energy greater than E_m, against y, where $y=\ln(E_0/E_m)$, E_0 being the energy of a primary electron. Points beyond $y=7$ are derived from cascades of primary energy greater than 100 GeV.

alternate methods in the high energy region have enabled us to extend the comparison to energies even of the primary order. For six cascades of which

([6]) H. J. Bhabha and S. K. Chakrabarty: *Phys. Rev.*, **74**, 1352 (1948). We are thankful to Professor Chakrabarty for the communicated advice and some of his later calculations.

the energy could be found by three or more methods, the comparative statement is given in Table I. For the longitudinal development we have employed the calculations of BHABHA and CHAKRABARTY and CHAKRABARTY [6]. Each of the cascades was followed for more than 2.5 cascade units (one c.u. = 2.9 cm of nuclear emulsion). In order to compensate for the detection inefficiency of low energy pairs (since there is no such effect in case of tridents), an appropriate

TABLE I. – *Energy of the primary pairs* (GeV), *obtained by various methods.*

Shower designation	Longitudinal development	Lateral development	Decrease of ionization	Present method
K_1	1200	1000	800 ± 100	> 600
K_2	300	300	250 ± 50	$200 \div 300$
N_2	600	—	500 ± 80	$500 \div 600$
N_3	300	300	250 ± 50	—
N_7	250	—	250 ± 50	$250 \div 300$
N_{10}	100	—	100 ± 30	$80 \div 100$
S_3	150	—	100 ± 30	$100 \div 150$

cut-off for the minimum acceptable energy was applied, *e.g.*, at $y = \ln (E_0/E_m) = 7$ for primary energies around 100 GeV. The lateral development of three showers which were geometrically favorable was plotted and the energy estimated after the method of PINKAU [7]. The energy estimate of six pairs was also obtained from the decrease in ionization near the pair origin [8], by comparing the experimental value of the distance at which the ionization tended asymptotically to the value for two independent electrons, with that expected theoretically. The energy values obtained by us compare reasonably well also with those obtained from relative scattering, as was indicated by LOHRMANN [9], who found, using our curves, an energy of 70 to 75 GeV for some of the pairs, for which he had obtained a value of $50^{+\frac{15}{10}}$ GeV by scattering. In regard to Table I, it may be mentioned that the present method may not give a representative energy value for any individual pair, but since it is our aim to find the average energy of electrons classified into a group, the individual uncertainty does not matter, especially since the error would decrease with the increase of statistics.

b) *Correction for spurious tridents*: Theoretically it is possible to com-

[7] K. PINKAU: *Nuovo Cimento*, **3**, 1285 (1956).

[8] D. H. PERKINS: *Phil. Mag.*, **46**, 1146 (1955); G. YEKUTIELI: *Nuovo Cimento*, **5**, 1381 (1957).

[9] E. LOHRMANN: private communication (June 1956). Thanks are due Dr. LOHRMANN for the measurements and useful comments.

pute the fraction F of bremsstrahlung pairs (B.P.), which would materialize within the least resolvable distance (0.2 μm in projection and 0.4 μm in dip) from an electron track and give rise to a spurious trident (S.T.). Results of such a calculation made by KING *et al.* [10] and by KAPLON *et al.* [15], indicate that, for energies ~ 100 GeV, more than 70% of the observed tridents are spurious. According to Kaplon's procedure that has been widely used, number of S.T. $= F/(1-F)$ times observed B.P., that appear resolved from electron tracks. GREISEN [11] has however suggested the advantage of finding the correction not from the observed number of resolved B.P., but entirely from the electromagnetic theory, *i.e.*, compute the bremsstrahlung spectrum and expected number of both resolvable and unresolvable pairs. This method, though it accepts the measurement of energy and computation of F, is less sensitive to errors, because F would enter linearly rather than as $F/(1-F)$. We have obtained our experimental material from two stacks of stripped emulsions exposed in the stratosphere over India [12]. Out of a large number of scanned showers, in all 20 cascades of favorable geometry were selected for detailed investigation. Plots of showers at various stages were made for each cascade. In Fig. 3, the observed development is

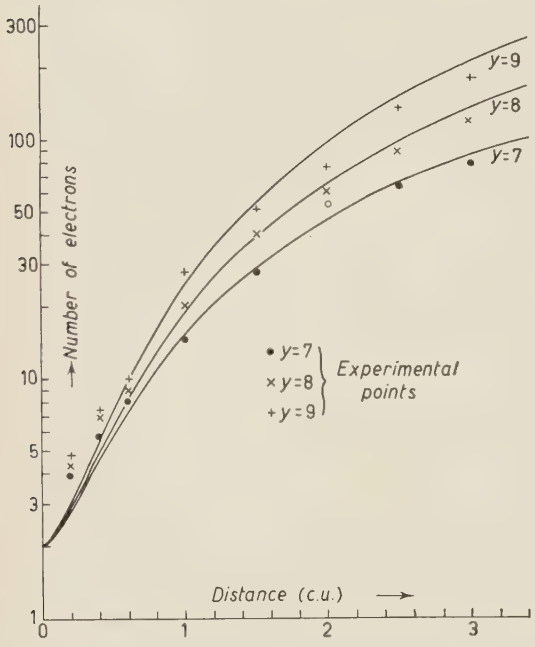

Fig. 3. - Mean number of electrons observed at various distances along the shower axis against distance in cascade units. Theoretically predicted curves are included for values of y from 7 to 9. $y = \ln(E_0/E_m)$, E_0 being the energy of a primary electron, and E_m the minimum acceptable energy for a secondary electron. Points for $y=8$ and 9 are derived from cascades of primary energy greater than 100 GeV.

[10] M. M. BLOCK and D. T. KING: *Phys. Rev.*, **95**, 171 (1954); **96**, 1627 (1954).

[11] K. GREISEN: private communication (August 1956). We are grateful to Professor GREISEN for his excellent suggestions.

[12] D. LAL, YASH PAL and B. PETERS: *Proc. Ind. Acad. Sci.*, **38**, 277 (1953); R. R. DANIEL, G. FRIEDMAN, D. LAL, YASH PAL and B. PETERS: *Proc. Ind. Acad. Sci.*, A **40**, 151 (1954). We are indebted to Professor PETERS for the loan of a stack and for the facilities of his laboratory where part of this work was done.

plotted over that predicted theoretically ([6]). But for a small though apparent deviation ([13]) within the first 0.5 c.u., the agreement appears to be good. We have not observed any case depicting abnormal behaviour. In fact, what we observed was a slightly too small number of resolved pairs and a large number of tridents, but the correct total.

In earlier brief communications ([14]) using the present method of energy estimation, we had corrected for S.T. according to KAPLON *et al.* ([15]). Using an along-the-track following procedure, a total of 125 pairs and 49 tridents (including spurious and genuine) were observed along 3.83 metre of emulsion length. The electron track was separated into two energy groups of $(1 \div 10)$ GeV and $(10 \div 100)$ GeV, obtaining the mean free path values $(6.1\ ^{+2.6}_{-1.4})$ c.u., and $(4.0^{+1.4}_{-0.8})$ c.u., respectively. (A cascade unit was there taken equal to 3.0 cm of emulsion).

In view of the above approach to the correction for S.T., it appeared useful to reconsider our previous data as well as to include some more cascades From the facsimile drawing of 20 showers an electron track length of 70 c.u. was accumulated for an average energy of 20 GeV. In this length 68 possible tridents were observed. Using an appropriate factor F, the proportion of B.P. which would appear as tridents was calculated at 61.3, leaving an excess of 6.7 tridents as genuine.

Reconsideration by KING *et al.* ([10]) of the theoretical cross-section for trident processes calculated by BHABHA ([16]), has shown it to be in agreement with that of RACAH ([17]). Accordingly, the mean free path for an average energy of 20 GeV is 35 cm, such that in 70 c.u. one expects 5.8 true tridents. This number is in fair agreement with our experimental value of 6.7, which gives $\lambda_T = (10.4 \pm 1.2)$ c.u. at 20 GeV

With a view to find the cross-section at still higher energies, we considered separately the primary pairs up to a distance of 0.5 c.u. from the origin. Such a cut-off has a further advantage, since the number of tridents increases linearly with t, while the correction goes as t^2. 16 possible tridents were observed along 18.5 c.u., of average energy 60 GeV. The calculated number of S.T., equal to 13.6, left an excess of 2.4 true tridents, leading to a mean free path of (7.7 ± 1.9) c.u., as compared to 8.9 c.u. expected theoretically. Since the small statistics does not allow stress to be laid on this result, our value of 20 GeV

([13]) It may be possible to account for part of this deviation on the basis of a genuine trident contribution likely to be present while the electrons have not lost their primary energy.

([14]) P. KUMAR: *Proc. Ind. Sci. Cong.*, III-3 (n. 18, 1955; n. 61, 1956); *Proc. Cosmic Ray Symposium* (Bombay, March 1957, unpublished).

([15]) M. KOSHIBA and M. F. KAPLON: *Phys. Rev.*, **100**, 327 (1956).

([16]) H. J. BHABHA: *Proc. Roy. Soc.*, A **152**, 559 (1935).

([17]) G. RACAH: *Nuovo Cimento*, **14**, 93 (1937).

suggests in general that the theoretical cross-section is not in error and that the observed discrepancies arise as a consequence of the methods applied.

* * *

It is a pleasure to thank Professor B. M. ANAND for his keen interest during the course of the work and for granting leave of absence the Tata Institute of Fundamental Research, Bombay. Financial assistance of the Government of India, Department of Atomic Energy, is gratefully acknowledged.

RIASSUNTO (*)

È stato trovato il cammino libero medio per la produzione di coppie di elettroni di media energia (20 GeV e 80 GeV) da parte di elettroni di alta energia. Gli elettroni sono stati ottenuti da cascate elettromagnetiche di alta energia registrati in pacchi di emulsioni nucleari. L'energia delle coppie è stata determinata servendosi di una relazione per l'angolo d'apertura della coppia modificata. La teoria della cascata è stata utilizzata per trovare la correzione pei tridenti spuri. I valori dei cammini liberi medi dei tridenti ottenuti alle medie energie di 20 GeV e 80 GeV espressi in unità di cascata sono rispettivamente 10.4 ± 1.2 e 7.7 ± 1.9. I risultati si accordano colle previsioni teoriche.

(*) *Traduzione a cura della Redazione.*

IL NUOVO CIMENTO Vol. XI, N. 4 16 Febbraio 1959

The Asymptotic Condition for Simple Scattering Systems (*).

J. M. Jauch (**) and I. I. Zinnes

CERN, Theoretical Studies Division - Geneva
Department of Physics, University of Oklahoma - Norman, Okla.

(ricevuto il 2 Dicembre 1958)

Summary. — Necessary and sufficient conditions are given for an interaction operator of a simple scattering system to admit a scattering operator. The result is applied to the study of radial scalar potentials.

1. – Introduction.

A scattering system is characterized by a certain limiting property of the state vectors in the remote past and the distant future. In a previous publication (1) we have formulated this property in terms of the unitary operators $U_t = \exp[-iH_0t]$ and $V_t = \exp[-iHt]$ which describe the time development of the free particles and the total system respectively. In these expressions H_0 represents the kinetic energy of the free particles and H the total energy of the system.

The asymptotic condition as we have used it is that the strong limits (**)

$$\Omega_{\mp} = \lim_{t \to \pm\infty} V_t^* U_t \tag{1}$$

exist for all f in the underlying Hilbert space $\mathcal{H}$ formed by the totality of state vectors of the system.

(*) Supported in part by the National Science Foundation.

(**) On leave of absence from State University of Iowa, Iowa City, U.S.A.

(1) J. M. Jauch: *Helv. Phys. Acta*, **31**, 127 (1958).

(**) Strong limits means that the numbers $\|(\Omega_{\mp} - V_t^* U_t)f\|$ tend to zero for all f and $t \to \pm\infty$ respectively.

It is easy to show with simple counter-examples that condition (I) implies certain restrictions on the interaction operator. One of the simplest of such examples is obtained for instance by setting $H = cI + H_0$. In this case $V_t^* U_t = \exp[ict] \cdot I$, and this operator cannot converge for any f as $t \to \pm \infty$

The object of this paper is to obtain necessary and sufficient conditions on the interaction operator which are equivalent to the asymptotic condition (I) and to apply them to the study of radial scalar potentials in wave mechanical scattering theory.

Roughly speaking condition (I) means that the motion of any state vector associated with a scattering system approaches in the distant past and the remote future the free motion. This can also be expressed by saying that a state vector in the interaction picture $\varphi(t)$ which is orthogonal to the bound states of H must approach a constant state vector for $t \to \pm \infty$. Now this state vector satisfies the Schrödinger equation in the interaction picture

$$i\dot{\varphi}(t) = V(t)\varphi(t)\,, \tag{1.1}$$

where

$$V(t) \equiv U_t^* V U_t \tag{1.2}$$

is the interaction operator in the interaction picture. One might therefore be led to believe that such a condition on the interaction operator is that $V(t) \to 0$ in some sense, as $t \to \pm \infty$.

However, even if this limit were made precise it would certainly not be enough to guarantee the existence of the scattering operator as may be seen from the following simple example: Let the Hilbert space be one-dimensional so that the state vectors are just complex numbers. Consider $V(t) = 1/t$ so that (1.1) becomes

$$i\dot{\varphi}(t) = \frac{1}{t}\,\varphi(t)\,,$$

with the solution $\varphi(t) = A \exp[-i \ln t]$. In this case $V(t) \to 0$ for $t \to \pm \infty$ but $\varphi(t)$ has no limit for $t \to \pm \infty$.

In this paper we shall give the necessary and sufficient conditions on the potential for the validity of property (I) in two equivalent forms.

2. – The interaction operator.

We shall assume that we are given a total Hamiltonian H and the corresponding unitary group $V_t = \exp[-iHt]$. If we are dealing with a simple

scattering system we also have an expression for the free Hamiltonian H_0 and the corresponding group $U_t = \exp[-iH_0t]$. We shall now define precisely what we mean by the interaction operator V.

The obvious procedure of setting $V = H - H_0$ is in need of elaboration because of the following circumstance. The operators H and H_0 are, in all physical systems of interest, unbounded operators, which are only definable in everywhere dense linear manifolds D_H and D_{H_0} respectively. The difference $H - H_0$ is therefore only defined on the intersection $D_H \cap D_{H_0}$ of these two manifolds. We shall always agree to define two operators as equal if they have the same domain of definition and if on this domain they have the same value. It is quite possible that the intersection of two dense linear manifolds is empty. In this case the interaction operator is undetermined.

Even in the physically more important case in which the intersection of the two domains is also everywhere dense it is still possible that the operator $H - H_0$ admits an extension. If this extension is to be continuous it is also unique and there is a maximal continuous extension. If $H - H_0$ is uniformly bounded on its domain the maximal extension is to all of $\mathcal{H}$. In the contrary case it is a dense linear manifold. In either case the maximal extension leads to a uniquely determined closed, self-adjoint but not necessarily bounded linear operator which we shall denote by V and for which we write

$$V \supseteq H - H_0 . \tag{2.1}$$

For the discussion of scattering systems the existence and uniqueness of the interaction operator is not enough. In order to formulate necessary and sufficient conditions on V for the existence of the scattering operator it is necessary to have what we shall call *admissible* interaction operators.

We define an admissible interaction operator as one which has the property: There exists a dense linear manifold D_V' on which V and H_0 are defined and which is invariant under the group U_t.

That this is a restriction can easily be verified with examples. We shall not give such examples here, since they have hardly any physical significance. It follows from this definition that $D_V' \subseteq D_H \cap D_{H_0}$.

From now on we shall only consider simple scattering systems with admissible interaction operators. It is obvious that a bounded interaction operator is always admissible with $D_V' = D_H$, $D_V' = D_H \cap D_{H_0} \equiv D_{H_0}$. Such operators already occur for a large group of physically interesting systems. But such important ones as the Yukawa potential and the Coulomb potential are not in this class. It is for this reason that it is necessary to admit unbonded interaction operators in the general theory of scattering and to replace boundedness of V by the weaker condition of admissibility.

3. – The asymptotic property of the transformation operator.

In this section we shall relate condition (I) to an asymptotic property of the transformation operator $V_t = \exp[-iHt]$. We recall that condition (I) ensures the existence of a bounded operator [1]

$$\Omega = \lim_{t\to\infty} V_t^* U_t$$

defined on all of $\mathcal{H}$ with the upper bound $\|\Omega\| = 1$. We shall prove the following

THEOREM 1: *Let U_t and V_t be two continuous unitary representations of the group of real numbers $(-\infty < t < +\infty)$ in the Hilbert space $\mathcal{H}$. The necessary and sufficient condition that the strong operator limit*

$$\Omega = \lim_{t\to\infty} V_t^* U_t \tag{3.1}$$

exists, on all of $\mathcal{H}$ is that the strong limit

$$\lim_{t\to\infty} U_t^* V_\tau U_t = U_\tau \tag{3.2}$$

exists on all of $\mathcal{H}$, for all τ uniformly in $\tau \geqslant 0$.

Proof: We shall first show that (3.2) is necessary. According to the assumption (3.1) there exists for every $f\in\mathcal{H}$ and any $\varepsilon > 0$ a T such that

$$\|(V_t^* U_t - V_{t'}^* U_{t'})f\| < \varepsilon \qquad \text{for all } t, t' > T. \tag{3.3}$$

By using the unitary property of V_t and U_t, we can transform the left-hand side with the help of the identity

$$\|(V_t^* U_t - V_{t'}^* U_{t'})f\| = \|(U_t^* V_\tau U_t - U_\tau)f\|\,, \tag{3.4}$$

where $\tau = t' - t$. Therefore for any fixed τ the right-hand side of (3.4) is $< \varepsilon$ for all t such that $t > T - \tau$ and $t > T$. This proves the existence of the limit (3.2) for all τ. Furthermore the convergence is uniform in $\tau \geqslant 0$, since $t > T$ implies that $t' = t + \tau > T$, so that by (3.3),

$$\|(U_t^* V_\tau U_t - U_\tau)f\| < \varepsilon \qquad \text{for } t > T,\ \tau \geqslant 0,$$

independently of τ *q.e.d.*

In order to prove the sufficiency of (3.2) we use the identity (3.4) in reverse.

By assumption the right-hand side of (3.4) is $< \varepsilon$ for fixed f and for all $\tau > 0$ and $t > T$. Hence the left side is $< \varepsilon$ for $t > T$, $t' = t + \tau \geqslant t$. Since it is unchanged upon interchanging t with t', this is also true for $t' > T$, $t = t' + \tau \geqslant t'$, that is for all t, $t' > T$. The set of vectors $f_t = V_t^* U_t f$ for arbitrary f satisfy the Cauchy condition and since $\mathcal{H}$ is complete there exists a uniquely defined limit

$$g = \lim_{t \to \infty} f_t .$$

Thus the operator $V_t^* U_t$ strongly converges with $t \to \infty$ to

$$\Omega = \lim_{t \to \infty} V_t^* U_t$$

on all of $\mathcal{H}$. *q.e.d.*

We remark incidentally that uniform convergence of $U_t^* V_\tau U_t$ to U_τ for $t \to \infty$ on the half-line $\tau \geqslant 0$ implies uniform convergence on any half-line $\tau \geqslant \tau_0$, with τ_0 arbitrary.

In order to show this we may assume $\tau_0 < 0$, since there is nothing to prove if $\tau_0 \geqslant 0$.

The easily verified identity

$$\| (U_t^* V_\tau U_t - U_\tau) f \| = \| (U_{t+\tau}^* V_{-\tau} U_{t+\tau} - U_{-\tau}) f \|$$

shows that

$$\| (U_t^* V_\tau U_t - U_\tau) f \| < \varepsilon \quad \text{for } t > T \text{ uniformly in } \tau \geqslant 0$$

implies

$$\| (U_t^* V_\tau U_t - U_\tau) f \| < \varepsilon \quad \text{for } t \geqslant T + |\tau_0|, \text{ uniformly in } \tau \geqslant \tau_0$$

and this proves the statement.

We also remark that Theorem 1 has its counterpart for the limit $t \to -\infty$ with the domain of uniform convergence $\tau \leqslant 0$. The proof is an obvious modification of the preceding proof and will be omitted.

4. – The asymptotic property of the interaction operator.

In this Section we shall formulate necessary and sufficient conditions for an admissible interaction operator which are equivalent to the asymptotic condition I.

We begin with a few preliminary considerations:

Let $f \in D_H$ and $g \in D_{H_0}$ then the expression

$$\Phi_t(f, g) \equiv H V_t f, U_t g) - (V_t f, H_0 U_t g) \tag{4.1}$$

is, for every fixed pair f and g, a continuous function of t for $-\infty < t < +\infty$.

We verify that for instance the first expression on the right is continuous in t. The continuity of the second term may be verified in a similar manner.

Continuity means, for every $\varepsilon > 0$, we can determine a δ such that

$$|(HV_{t+\tau}f, U_{t+\tau}g) - (HV_tf, U_tg)| < \varepsilon \qquad \text{for } |\tau| < \delta. \tag{4.2}$$

We have for the left-hand side

$$\begin{aligned} &|(HV_{t+\tau}f\,, U_{t+\tau}g) - (HV_tf, U_tg)| \leqslant \\ &\quad \leqslant |(H(V_{t+\tau} - V_t)f,\ U_{t+\tau}g)| + |(HV_tf,\ (U_{t+\tau} - U_t)g)| \leqslant \\ &\quad \leqslant \|H(V_{t+\tau} - V_t)f\|\ \|g\| + \|HV_tf\|\ \|(U_{t+\tau} - U_t)g\|\,. \end{aligned}$$

Since H commutes with V_t and $f \in D_H$ we can write for the first term

$$\|(V_{t+\tau} - V_t)Hf\|, \qquad \|g\| < \frac{\varepsilon}{2}, \qquad \text{for all } |\tau| < \delta_1,$$

because V_t is strongly continuous in t.

For the second term we have

$$\|V_tHf\|, \qquad \|(U_{t+\tau} - U_t)g\| < \frac{\varepsilon}{2}, \qquad \text{for all } |\tau| < \delta_2,$$

since U_t is strongly continuous in t.

Consequently we have verified (4.2) for $\delta = \mathrm{Min}\{\delta_1, \delta_2\}$.

Since $\Phi_t(f, g)$ is a continuous function of t it can be integrated on any interval of the real t-line. We define

$$\Psi_{t_2,t_1}(f, g) \equiv \int_{t_1}^{t_2} \Phi_t(f, g)\,\mathrm{d}t, \qquad f \in D_H,\ g \in D_{H_0}. \tag{4.3}$$

We shall now show, that the integral on the right of (4.3) can be evaluated, with the result

$$\Psi_{t_2t_1}(f, g) = -\,i(f,\ (W_{t_2} - W_{t_1})g)$$

and

$$W_t = V_t^*\,U_t\,.$$

To this end we use the fact that for every $f \in D_H$ the strong limit

$$\lim_{\tau \to 0} \frac{V_{t+\tau} - V_t}{\tau} - f = -\,iHV_t\,f, \tag{4.4}$$

exists (2), and of course a corresponding property for $g \in D_{H_0}$.

This means that for such f and g we can write (4.1) as

$$\Phi_t(f, g) = -i \frac{\mathrm{d}}{\mathrm{d}t} (V_t f, U_t g) - i\left(V_t f, \frac{\mathrm{d}}{\mathrm{d}t} U_t g\right).$$

Because of the continuity of the scalar product this can be reduced to

$$\Phi_t(f, g) = -i \frac{\mathrm{d}}{\mathrm{d}t} (V_t f, U_t g) = -i \frac{\mathrm{d}}{\mathrm{d}t} (f, W_t g),$$

consequently

$$\int_{t_1}^{t_2} \mathrm{d}t \, \Phi_t(f, g) = -i \int_{t_1}^{t_2} \mathrm{d}t \frac{\mathrm{d}}{\mathrm{d}t} (f, W_t g) = -i(f, (W_{t_2} - W_{t_1}) g).$$

We summarize the result up to this point with the

Lemma 1: For every pair of elements $f \in D_H$ and $g \in D_{H_0}$ we have

$$i \int_{t_1}^{t_2} [(HV_t f, U_t g) - (V_t f, H_0 U_t g)] \, \mathrm{d}t = (f, (W_{t_2} - W_{t_1}) g), \tag{4.5}$$

with

$$W_t = V_t^* U_t.$$

The left-hand side of (4.5) is only defined for $f \in D_H$ and $g \in D_{H_0}$ but the result of the integration shows that it represents a bounded bilinear functional in two dense domains for f and g and can therefore be extended continuously and uniquely to all of $\mathcal{H}$. Thus even though the *integrand* has only meaning for f and g in these domains the *integral* has a more general meaning after continuous extension.

If we are dealing with an admissible interaction operator, the left-hand side of (4.5) can be further transformed as follows. We assume that $g \in D_V' \subseteq D_{H_0}$ so that the norms of $H_0 U_t g$, $V U_t g$ and $H U_t g$ are all finite. We can then write

$$(HV_t f, U_t g) = (V_t f, HU_t g) = (f, V_t^* H U_t g).$$

---

(2) See for instance F. Riesz and B. Sz.-Nagy: *Functional Analysis*, esp. p. 384.

We obtain then

Lemma 2: If the interaction operator V is admissible, we have

$$(f, (W_{t_2} - W_{t_1})g) = i\int_{t_1}^{t_2} \mathrm{d}t (f, V_t^* V U_t g), \quad \text{for all } f \in D_H,\ g \in D_V' \tag{4.6}$$

Since D_V' is dense in $\mathcal{H}$ we can uniquely again extend the meaning of the integral to a bilinear functional in all of $\mathcal{H}$. Such a functional always determines a bounded linear operator which we consider the definition of

$$i\int_{t_1}^{t_2} \mathrm{d}t\ V_t^* V U_t = X_{t_2 t_1}.$$

It has the property

$$(f, X_{t_2 t_1} g) = i\int_{t_1}^{t_2} \mathrm{d}t (f, V_t^* V U_t g), \quad \text{for all } f \in D_H,\ g \in D_V'.$$

With this definition of the operator $X_{t_2 t_1}$ we have from (4.6) the following operator relation

$$W_{t_2} - W_{t_1} = i\int_{t_1}^{t_2} V_t^* V U_t \mathrm{d}t. \tag{4.7}$$

We are now prepared for the proof of

Theorem 2: *Let H, H_0 and V be the total Hamiltonian, the free Hamiltonian and the admissible interaction operator of a quantum mechanical system. The necessary and sufficient condition that property* I *holds is that the operator*

$$X_{t_2 t_1} = \int_{t_1}^{t_2} V_t^* V U_t \mathrm{d}t, \tag{4.8}$$

converges strongly to a bounded operator for $t_2 \to +\infty$, $t_1 \to -\infty$.

Proof: The convergence property of the operator $X_{t_1 t_2}$ may also be stated as follows: For every $f \in \mathcal{H}$ and every $\varepsilon > 0$, there exists a T such that

$$\|X_{t_2 t_1} f\| < \varepsilon \quad \text{for all } t_2 > T,\ t_1 > T, \tag{4.9}$$

$$\text{or all } t_2 < -T,\ t_1 < -T.$$

In this form we shall prove the equivalence with I. Let us first assume I. The for every f, $W_t f$ satisfies the Cauchy condition for $t \to \pm \infty$. Therefore, given $\varepsilon > 0$, there exists a T such that

$$\begin{aligned} \| W_{t_2} f - W_{t_1} f \| = \| X_{t_2 t_1} f \| \qquad & \text{for all } t_2 > T,\ t_1 > T, \\ < \varepsilon \qquad & \text{for all } t_2 < -T,\ t_1 < -T. \end{aligned}$$

Let us next assume (4.9). It follows from (4.7) that the elements $W_t f$ satisfy a Cauchy condition for $t \to \pm \infty$. Since $\mathcal{H}$ is complete they converge strongly to a limit $f_{\mp}$

$$\lim_{t \to \pm \infty} W_t f = f_{\mp} .$$

This is the assertion of I. Thus the theorem is proved.

In conclusion of this section we mention a few consequences of Eq. (4.7). Since the limits $t_1 \to -\infty$, $t_2 \to +\infty$ exist if we are dealing with a scattering system, we can put

$$\Omega_- - \Omega_+ = i \int_{-\infty}^{+\infty} V_t^* V U_t \, \mathrm{d}t . \tag{4.10}$$

We multiply this from the left with Ω^* and use the relations (*)

$$\Omega_-^* \Omega_- = I , \qquad \Omega_-^* V_t = U_t \Omega_-^* , \qquad S = \Omega_-^* \Omega_+ ,$$

and we obtain

$$I - S = i \int_{-\infty}^{+\infty} U_t^* \Omega_-^* V U_t \, \mathrm{d}t . \tag{4.11}$$

In a similar way one obtains

$$I - S = - i \int_{-\infty}^{-\infty} U_t^* V \Omega_+ U_t \, \mathrm{d}t . \tag{4.12}$$

There are corresponding formulae for the operator $S' = \Omega_+ \Omega_-^*$

$$E_N - S' = i \int_{-\infty}^{+\infty} V_t^* V \Omega_-^* V_t \, \mathrm{d}t , \tag{4.13}$$

$$E_N - S' = - i \int_{-\infty}^{+\infty} V_t^* \Omega_+ V V_t \, \mathrm{d}t . \tag{4.14}$$

(*) For the proof of these relations, see ref. (1).

In the last two expressions E_y is the projection operator for the subspace of the continuum states.

The expressions (4.11) and (4.12) are a useful starting point for a study of the convergence of perturbation theory. One obtains for instance the « first Born approximation » of scattering theory from (4.11) by setting $\Omega_- = I$.

5. – The asymptotic condition for a radial potential.

In this section we shall study the implications of the asymptotic condition for a radial potential $V(r)$. The Hilbert space is realized by L^2-functions $\psi(\boldsymbol{x})$ over the three-dimensional Euclidean space. The total Hamiltonian is assumed to be of the form

$$H = \frac{p^2}{2m} + V, \tag{5.1}$$

where

$$(V\psi)(\boldsymbol{x}) = V(r)\psi(\boldsymbol{x}) \tag{5.2}$$

and the operator p^2 has the usual meaning

$$(p^2\psi)(\boldsymbol{x}) = -\nabla^2(\boldsymbol{x}) .$$

The first question to be investigated is under what condition the interaction operator is admissible in the sense defined in Section 2. The answer is contained in the

THEOREM 3: *If there exists an R and two positive numbers M_1 and M_2 such that*

$$\int_0^R r^2 V^2(r)\,\mathrm{d}r < M_1 , \qquad \int_R^\infty \exp[-r^2]\, V^2(r)\,\mathrm{d}r < M^2 , \tag{5.3}$$

then V is an admissible interaction operator.

It is satisfactory that the conditions (5.3) of this theorem include the important cases of the Coulomb and the Yukawa potential. But the case $V(r) = 1/r^{\frac{3}{2}}$ is excluded by the first of the conditions (5.3). Since these conditions are only sufficient it is not clear whether this case represents a real anomaly or not.

Before we prove this theorem we mention that the conditions (5.3) imply that for any pair R_1 and R_2 such that $0 < R_1 < R_2 < \infty$ and for any bounded

integrable function $\Phi(r)$ in $[R_1, R_2]$ we have

$$\int_{R_1}^{R_2} \Phi(r)\, V^2(r)\, \mathrm{d}r < \infty\,. \tag{5.4}$$

We shall omit the easy proof of this statement.

Proof of Theorem 3: In order to prove Theorem 3 we must show that there exists a dense linear manifold D_V' on which V and H_0 are defined and which is invariant under $U_t = \exp[-iH_0 t]$.

In order to do this we utilize the displacement theorem of WIENER [3] which may be stated as follows:

Let $K_1(x)$ belong to L^2 and be such that its Fourier transform does not vanish except possibly on a set of measure zero, then if $K_2(x)$ belongs to L^2 and $\varepsilon > 0$, there exists an integer N together with a set of real numbers Λ_n and complex numbers A_n such that

$$\int_{-\infty}^{+\infty} |K_2(x) - \sum_{n=1}^{N} A_n K_1(x - \Lambda_n)|^2\, \mathrm{d}x < \varepsilon\,.$$

What this theorem says in brief is that there exist suitable generating functions K_1, which when displaced and superposed can approximate in the norm any function in L^2 to any desired accuracy.

It is clear that the set of functions

$$\sum_{n=1}^{N} A_n K_1(x - \Lambda_n) = F(x)$$

with all finite N and arbitrary Λ_n are a linear manifold $\mathcal{L}$. The theorem says that, if $K_1(x)$ satisfies the conditions of the theorem, then this linear manifold is dense in $\mathcal{H}$.

As stated above, the theorem refers to functions on the line. By considering the closed linear manifolds formed by products of functions on the line it is possible to extend Wiener's theorem to L^2-functions defined on a space of three or more dimensions.

We shall not stop to carry this through here.

For the functions which generate the linear manifold we choose the Fourier

---

[3] N. WIENER: *The Fourier Integral*, (Cambridge, 1933).

transforms of

$$\varphi_{\boldsymbol{k}_0}(\boldsymbol{k}) = \exp\left[-a^2(\boldsymbol{k}-\boldsymbol{k}_0)^2\right] \tag{5.5}$$

for fixed real $a > 0$.

This function of $\boldsymbol{k}$ vanishes nowhere and its norm is

$$\|\varphi_{\boldsymbol{k}_0}\|^2 = \int \exp\left[-2a^2(\boldsymbol{k}-\boldsymbol{k}_0)^2\right] \mathrm{d}^3k = \left(\frac{\pi}{2a^2}\right)^{\frac{3}{2}} < \infty . \tag{5.6}$$

Hence it satisfies the conditions of Wiener's theorem.

Furthermore we have

$$(H_0\varphi_{\boldsymbol{k}_0})(\boldsymbol{k}) = \frac{1}{2m}\,\boldsymbol{k}^2 \exp\left[-a^2(\boldsymbol{k}-\boldsymbol{k}_0)^2\right],$$

and therefore

$$\|H_0\varphi_{\boldsymbol{k}_0}\|^2 = \frac{1}{4m^2}\int \boldsymbol{k}^4 \exp\left[-2a^2(\boldsymbol{k}-\boldsymbol{k}_0)^2\right] \mathrm{d}^3k < \infty , \qquad \text{for all } \boldsymbol{k}_0 .$$

Thus $\varphi_{\boldsymbol{k}_0} \in D_{H_0}$ for all $\boldsymbol{k}_0$ and therefore

$$\mathcal{L} \in D_{H_0} . \tag{5.7}$$

For the Fourier transform of $U_t\varphi_{\boldsymbol{k}_0}$ we have

$$(U_t\varphi_{\boldsymbol{k}_0})(\boldsymbol{x}) = \frac{1}{(2\pi)^{\frac{3}{2}}}\int \mathrm{d}^3k \exp\left[-a^2(\boldsymbol{k}-\boldsymbol{k}_0)^2\right] - \frac{it}{2m}\,\boldsymbol{k}^2 + i\boldsymbol{k}\cdot\boldsymbol{x} .$$

This can be evaluated in closed form with the result

$$(U_t\varphi_{\boldsymbol{k}_0})(\boldsymbol{x}) = \frac{1}{\left[2\left(a^2 + (it/2m)\right)\right]^{\frac{3}{2}}} \exp\left[-i\boldsymbol{k}_0\cdot\left(\frac{t}{2m}\,\boldsymbol{k} - \boldsymbol{x}\right) - \frac{\left((t/2m)\,\boldsymbol{k}_0 - \frac{1}{2}\boldsymbol{x}\right)^2}{a^2 + (it/2m)}\right]. \tag{5.8}$$

From this we obtain

$$\|VU_t\varphi_{\boldsymbol{k}_0}\|^2 = \frac{1}{8\alpha^3}\int V^2(r) \exp\left[-\frac{2a^2}{\alpha^2}\left(\frac{1}{2}\,\boldsymbol{x} - \frac{t}{2m}\,\boldsymbol{k}_0\right)^2\right] \mathrm{d}^3x , \tag{5.9}$$

with

$$\alpha^2 = a^4 + \left(\frac{t}{2m}\right)^2 .$$

When we carry out the angle integration in (5.9) we find

$$\|VU_t\varphi_{k_0}\|^2 = \frac{\pi}{2\alpha r_0 a^2}\int_0^\infty \exp\left[-\frac{a^2}{2\alpha^2}(r^2+r_0^2)\right]\sinh\left(\frac{rr_0a^2}{\alpha^2}\right) rV^2\,\mathrm{d}r\,, \tag{5.10}$$

with

$$r_0 = \frac{t}{m}k_0\,.$$

By changing to the dimensionless variable

$$\frac{ar}{\alpha} = \varrho\,,$$

and defining

$$F(\varrho) = V\left(\frac{\alpha\varrho}{a}\right), \qquad \varrho_0 = \frac{a}{\alpha}r_0\,,$$

we obtain finally

$$\|VU_t\varphi_{k_0}\|^2 = \frac{\pi}{2\varrho_0 a^3}\exp\left[-\frac{1}{2}\varrho_0^2\right]\int_0^\infty \exp\left[-\frac{1}{2}\varrho^2\right]\sinh(\varrho\varrho_0)\,\varrho F^2(\varrho)\,\mathrm{d}\varrho\,.$$

In order to finish the proof of Theorem 3, we need to show that the integral is finite for all $V(r)$ which satisfy the conditions (5.3).

We choose an arbitrary $\varrho_1 > 0$ and C_1 such that

$$\frac{\sinh\varrho\varrho_0}{\varrho\varrho_0} < C_1\,. \qquad \text{for all } \varrho < \varrho_1.$$

On account of the first of conditions (5.3) it follows that

$$\int_0^{\varrho_1}\exp\left[-\frac{1}{2}\varrho^2\right]\sinh(\varrho\varrho_0)\,\varrho F^2(\varrho)\,\mathrm{d}\varrho < C_1\varrho_0\int_0^{\varrho_1}\varrho^2F^2(\varrho)\,\mathrm{d}\varrho < \infty\,.$$

Then, because of the inequality

$$\exp[-\tfrac{1}{2}\varrho^2]\sinh\varrho\varrho_0 \leqslant \exp[\tfrac{1}{2}\varrho_0^2]\left(\exp[-\tfrac{1}{2}(\varrho-\varrho_0)^2] + \exp[-\tfrac{1}{2}(\varrho+\varrho_0)^2]\right)$$

and the second of conditions (5.3) we can choose a ϱ_2 and a number C_2 such

that

$$\int_{\varrho_2}^{\infty} \exp\left[-\frac{1}{2}\varrho^2\right] \sinh(\varrho\varrho_0)\,\varrho F^2(\varrho)\,\mathrm{d}\varrho < C_2 \int_{\varrho_2}^{\infty} \exp[-\varrho^2]\,\varrho F^2(\varrho)\,\mathrm{d}\varrho < \infty .$$

Finally the integral from ϱ_1 to ϱ_2 is always finite. Thus the result:

$$\|V U_t \varphi_{\boldsymbol{k}_0}\|^2 < \infty \qquad \text{for all } \boldsymbol{k}_0 \text{ and all } t.$$

We have now established that every function of the form $U_t\varphi_{\boldsymbol{k}_0}$ with with arbitrary $\boldsymbol{k}_0$ and t is in D_{H_0} as well as in D_V. This is also true for every finite linear combination of such functions. By Wiener's theorem such linear combinations generate the dense linear manifold $\mathfrak{L}$. Therefore we have with $\mathfrak{L} = D_V'$ obtained a linear manifold which satisfies all the conditions stated in Theorem 3.

This completes the proof of Theorem 3.

We shall now further specialize the potential to be of the form $V(r) = 1/r^\beta$ with $1 < \beta < \frac{3}{2}$ For these values of β conditions (5.3) are satisfied.

Since

$$\left\| \int_{t_1}^{t_2} V_t V U_t \varphi_{\boldsymbol{k}_0}\,\mathrm{d}t \right\| \leqslant \int_{t_1}^{t_2} \| V U_t \varphi_{\boldsymbol{k}_0} \|\,\mathrm{d}t \leqslant$$

$$\leqslant \int_{t_1}^{t_2} \mathrm{d}t\, \frac{\sqrt{\pi}}{\sqrt{2}\varrho_0^{\frac{1}{2}}} \frac{a^{\beta-\frac{3}{2}}}{\alpha^\beta} \left\{ \left| \int_0^{\infty} \exp\left[-\frac{1}{2}\varrho^2\right] \sinh(\varrho\varrho_0)^{1-2\beta}\,\mathrm{d}\varrho \right| \right\}^{\frac{1}{2}},$$

and $\varrho_0 = (a/\alpha) r_0 \to 2ak_0$ with $t \to \infty$, and $1 < \beta < \frac{3}{2}$, the integral remains uniformly bounded for $t \to \infty$, and

$$\left\| \int_{t_1}^{t_2} V_t^* V U_t \varphi_{\boldsymbol{k}_0}\,\mathrm{d}t \right\| \leqslant \text{const} \int_{t_1}^{t_2} \frac{1}{t^\beta}\,\mathrm{d}t = \text{const}\left(\frac{1}{t_1^{\beta-1}} - \frac{1}{t^{\beta-1}} \right).$$

Thus the asymptotic condition is satisfied for such potentials.

This example shows that it is possible to weaken the sufficient condition on $V(r)$ which was previously obtained by Cook [4]. His condition is

$$\int_0^{\infty} V^2(r) r^2\,\mathrm{d}r < \infty ,$$

and it excludes the cases: $1 < \beta < \frac{3}{2}$.

---

[4] J. M. Cook: *Journ. Math. and Phys.*, **26**, 82 (1957).

It is regrettable on the other hand that the Coulomb potential ($\beta = 1$) cannot be shown to admit a scattering operator with the methods employed.

RIASSUNTO (*)

Si danno le condizioni necessarie e sufficienti perchè un operatore d'interazione di un sistema semplice di scattering ammetta un operatore di scattering. Si applica il risultato allo studio di potenziali radiali scalari.

(*) *Traduzione a cura della Redazione.*

IL NUOVO CIMENTO Vol. XI, N. 4 16 Febbraio 1959

Weak and Electromagnetic Interactions.

Abdus Salam

Imperial College - London

J. C. Ward

University of Miami - Miami, Flo. (*)

(ricevuto il 3 Dicembre 1958)

Summary. — The postulate of a « local connection » in a [3] charge space leads to the introduction of three spin one fields. One of these can be identified with the electro-magnetic field and the other two can be shown to mediate all known weak interactions, thus unifying these interactions with electro-magnetism. The theory takes account of the fact that weak interactions violate parity and strangeness conservation while electromagnetic interactions do not do so.

---

1. – D'Espagnat, Prentki and Salam (1) have recently advanced the hypothesis that a three-dimensional [3] charge space Q exists and that all elementary particles correspond to its scalar or vector representations.

These authors show that possibly weak interactions exhibit full rotational symmetry in Q space. Electro-magnetic and strong interactions violate the full symmetry; however these interactions are invariant for rotations around one particular axis in this space (the « charge-axis ») so that Q_z is always conserved.

In this paper we wish to make a fresh approach with the idea of a [3] charge space. Following some ideas first advanced by Schwinger (2), we show

---

(*) Visiting Professor at the University of Maryland, present address, Free University, of Brussels.

(1) B. d'Espagnat, J. Prentki and A. Salam: *Nucl. Phys.*, **5**, 447 (1958). This paper will here by referred to as ESP. Similar ideas have been suggested by G. Takeda: to be published. In ESP the Q space is designated as M space.

(2) J. Schwinger: *Ann. of Phys.*, **2**, 407 (1957).

that parity-conserving weak and electromagnetic interactions taken together form a unit which exhibits full rotational symmetry in Q space. This full symmetry is broken on the one hand by parity-violating weak interactions (γ_5-invariance) and on the other hand by strong interactions. We go further in respect of the rotational invariance of electro-magnetic and (parity conserving) weak interactions in Q space; we wish to make the hypothesis that the orientation of all three charge axes can be chosen arbitrarily at all space time points.

Just as it is necessary to introduce the electro magnetic field if it is assumed that the orientation of axes in the conventional [2] ([3]) space spanned by fields Φ and Φ^* (or alternatively by the fields Φ_1 and Φ_2, where $\Phi = \Phi_1 + i\Phi_2$) is arbitrary at all space time points, our « three-dimensional gauge invariance » makes it necessary to introduce in Q space a triplet of fields consisting of two charged vector bose fields in addition to the electro-magnetic field ([4]). It will be shown that the form of the interaction of the charged fields is such that they can mediate weak interactions.

2. – Let us first consider the problem of the generalized gauge transformation ([5]). Let $\boldsymbol{\psi}$ represent a vector in charge-space, ($\boldsymbol{\psi} = \psi_1, \psi_2, \psi_3$ where, ψ_1, ψ_2, ψ_3 are 3 Fermi fields), which transforms as

$$\boldsymbol{\psi}' = S\boldsymbol{\psi} \,. \tag{1}$$

If S is a function of x, y, z, t it is necessary for invariance, that all derivatives of ψ appear in the combination

$$(\partial_\mu - i\varepsilon B_\mu)\psi \,, \tag{2}$$

where B_μ are 3×3 matrices, and transform as

$$B'_\mu = S^{-1} B_\mu S + \frac{i}{\varepsilon} S^{-1} \frac{\partial S}{\partial x_\mu} \,.$$

([3]) A priori, it is more attractive to associate charge with a [3] group structure, rather than with a [2] structure as in conventional theory. This is because infinitesimal matrices describing rotations in three dimensions possess three eigenvalues $\pm 1, 0$ (rather than just ± 1), so that the same formulation can give charge values of *all* charged and neutral particles. We are indebted for this remark to Prof. M. Fierz.

([4]) This was first done by Schwinger (ref. ([1])). The difference between our work and Schwinger's is that here the charged Bose fields arise naturally from the 3-dimensional charge-gauge and there is little arbitrariness in writing down the interaction Lagrangian.

([5]) Mathematically the work in this Section in completely analogous with that of Yang and Mills (*Phys. Rev.*, **96**, 191 (1954)); and R. Shaw (Cambridge dissertation, unpublished (1954)).

Yang and Mills were considering the possibility of a generalized gauge transformation in three-dimensional isotopic rather than charge-space.

If Q_i are the set of three rotation matrices in Q space, one may write

$$B_\mu = \boldsymbol{A}_\mu(x)\cdot\boldsymbol{Q}$$

and define

$$\boldsymbol{f}_{\mu\nu} = \boldsymbol{e}_{\mu\nu} - \boldsymbol{S}_{\mu\nu}\,, \tag{3}$$

where

$$\boldsymbol{e}_{\mu\nu} = \frac{\partial \boldsymbol{A}_\mu}{\partial x_\nu} - \frac{\partial \boldsymbol{A}_\nu}{\partial x_\mu}\,, \tag{4}$$

$$\boldsymbol{S}_{\mu\nu} = \varepsilon(\boldsymbol{A}_\mu \times \boldsymbol{A}_\nu)\,. \tag{5}$$

Here $\times$ is the symbol for vector-product.

It is easy to verify that

$$F_{\mu\nu} = \boldsymbol{f}_{\mu\nu}\cdot\boldsymbol{Q}$$

transforms as

$$F'_{\mu\nu} = S^{-1}F_{\mu\nu}S\,. \tag{6}$$

The $\boldsymbol{A}$ field (or alternatively $\boldsymbol{f}_{\mu\nu}$ field) has arisen as a direct consequence of our demand that S depends on x, y, z, t.

A charge-gauge invariant Lagrangian for $\boldsymbol{A}$ field is

$$-\tfrac{1}{4}\boldsymbol{f}_{\mu\nu}\boldsymbol{f}_{\mu\nu}\,. \tag{7}$$

The $S_{\mu\nu}$ terms are necessary for the invariance. Analogously to ref. ([5]), the total lagrangian density is

$$-\tfrac{1}{4}\boldsymbol{f}_{\mu\nu}\boldsymbol{f}_{\mu\nu} - \overline{\boldsymbol{\psi}}\gamma(\gamma - i\varepsilon\boldsymbol{Q}\boldsymbol{A})\boldsymbol{\psi} - m\overline{\boldsymbol{\psi}}\boldsymbol{\psi}\,. \tag{8}$$

Notice that

$$\boldsymbol{J} = \overline{\boldsymbol{\psi}}\boldsymbol{Q}\boldsymbol{\psi} = -i(\overline{\boldsymbol{\psi}}\times\boldsymbol{\psi})$$

so that the interaction term in (8) is

$$\boldsymbol{J}\cdot\boldsymbol{A} = \varepsilon\,\overline{\boldsymbol{\psi}}_\Lambda\gamma_\mu\boldsymbol{\psi}\cdot\boldsymbol{A}\,.$$

It is easy to verify that the subsidiary condition

$$\frac{\partial \boldsymbol{A}_\mu}{\partial x_\mu} = 0\,, \tag{9}$$

is compatible with the equations of motion derived from the Lagrangian; also that the « current »

$$\mathcal{J}_\mu = \boldsymbol{J}_\mu + \varepsilon \boldsymbol{A}_\nu \times \boldsymbol{f}_{\mu\nu} \tag{10}$$

satisfies the equation of continuity

$$\frac{\partial \mathcal{J}_\mu}{\partial x_\mu} = 0 \,. \tag{11}$$

Thus

$$\boldsymbol{Q} = \int \mathcal{J}_4 \mathrm{d}^3 x \,,$$

is independent of time.

One can verify that components of $\boldsymbol{A}$ field carry charge $+\varepsilon$, 0, $-\varepsilon$. Picking out an arbitrary charge axis and defining

$$A^\pm = \frac{1}{\sqrt{2}} (A_1 \mp i A_2) \,, \qquad A^0 = A_3 \,, \tag{12}$$

and similarly for $\psi^\pm$, ψ^0 we note that

$$\frac{1}{2} (f^1_{\mu\nu} f^1_{\mu\nu} + f^2_{\mu\nu} f^2_{\mu\nu}) = (e^+_{\mu\nu} - S^+_{\mu\nu})(e^-_{\mu\nu} - S^-_{\mu\nu}) =$$

$$= \left[\left(\frac{\partial}{\partial x_\nu} - i\varepsilon A^0_\nu\right) A^+_\mu - \left(\frac{\partial}{\partial x_\mu} - i\varepsilon A^0_\mu\right) A^+_\nu\right] \left[\left(\frac{\partial}{\partial x_\nu} + i\varepsilon A^0_\nu\right) A^-_\mu - \left(\frac{\partial}{\partial x_\mu} + i\varepsilon A^0_\mu\right) A^-_\nu\right],$$

while

$$-\tfrac{1}{4} f^3_{\mu\nu} f^3_{\mu\nu} = -\tfrac{1}{4} e^0_{\mu\nu} e^0_{\mu\nu} + \tfrac{1}{2} S^0_{\mu\nu} e^0_{\mu\nu} - \tfrac{1}{4} S^0_{\mu\nu} S^0_{\mu\nu} \,.$$

Identifying A^0_μ and $e^0_{\mu\nu}$ with the electro-magnetic field, the lagrangian $-\frac{1}{4} \boldsymbol{f}_{\mu\nu} \boldsymbol{f}_{\mu\nu}$ is a sum of terms which represent

1) the free Maxwell Lagrangian $(-\frac{1}{4} e^0_{\mu\nu} e^0_{\mu\nu})$;

2) the terms: $-\frac{1}{2}(\partial^+_\nu A^+_\mu - \partial^+_\mu A^+_\nu)(\partial^-_\nu A^-_\mu - \partial^-_\mu A^-_\nu)$,

where

$$\partial^\pm = \left(\frac{\partial}{\partial x} \mp i\varepsilon A^0\right).$$

These terms describe the conventional electro-magnetic interaction of charged fields A^+, A^-.

3) Terms $-\frac{1}{4}S^0_{\mu\nu}S^0_{\mu\nu} = \frac{1}{4}\varepsilon^2((A^+_\mu A^-_\nu - A^-_\mu A^+_\nu)^2$ which are in a sense « mass » terms for the charged fields A^+, A^-.

4) A term $\frac{1}{2}S^0_{\mu\nu}e^0_{\mu\nu} = -(i/2)(A^+_\mu A^-_\nu - A^+_\nu A^-_\mu)e^0_{\mu\nu}$.

This term would represent a (Pauli) anomalous magnetic moment for A^+, A^- fields, if these fields had mass.

The A field by itself is then a most remarkable field. One of its components can be identified with the Maxwell field, the other two represent charged particles, carrying « anomalous magnetic moment » while in place of the conventional mass term $-\mu^2 A^+A^-$, there is a more complicated (quartic) term

$$\frac{\varepsilon^2}{2}\left[(A^+_\mu A^-_\mu)^2 - (A^+_\mu)^2(A^-_\mu)^2\right].$$

Even in the presence of interactions with other particles the supplementary condition has the transparent form

$$\frac{\partial \boldsymbol{A}_\mu}{\partial x_\mu} = 0\,.$$

The theory is renormalizable; it is perhaps the only theory of charged vector mesons which can be renormalized. Finally note that

$$-\overline{\boldsymbol{\Psi}}\times\boldsymbol{\Psi}\cdot\boldsymbol{A} = (\overline{\psi}^+\psi^+ - \overline{\psi}^-\psi^-)A^0 + (\overline{\psi}_0\psi^- - \overline{\psi}^+\psi_0)A^+ + \text{h. c.}$$

3. – Let us assume that $L_1 = (e^+, \nu, e^-)$ form a vector in charge-space. With

$$e^\pm = \frac{1}{\sqrt{2}}(\psi_1 \mp i\psi_2)\,, \qquad \psi_3 = \nu\,,$$

(where the three ψ are Majorana fields), the derivative term in the free Lagrangian is

$$\overline{\boldsymbol{\Psi}}\gamma\partial\boldsymbol{\Psi}\,,$$

which leads to an interaction with $\boldsymbol{A}$ field of the type $\overline{\boldsymbol{\Psi}}\times\boldsymbol{\Psi}\cdot\boldsymbol{A}$. Writing this in full

$$[\overline{e}^+\gamma_\mu\nu - \overline{\nu}\gamma_\mu e^-]A^+_\mu + \text{h. c.} + [\overline{e}^+\gamma_\mu e^+ - \overline{e}^-\gamma_\mu e^-]A^0_\mu\,. \tag{14}$$

The last term represents electromagnetic interaction while the first two

terms could give the weak interactions of (e, ν) pair. However so far there is nothing in the theory to pick out any one axis in charge-space.

We wish now to do precisely this, by requiring that the neutrino Lagrangian remain invariant for

$$\nu \to \gamma_5 \nu \,. \tag{15}$$

in so far as the neutrino mass must be zero. One result of this is that the first term in L_{int} reads

$$\tfrac{1}{2}[\bar{e}^{+}\gamma_\mu(1+\gamma_5)\nu - \bar{\nu}\gamma_\mu(1+\gamma_5)e^{-}]A_\mu^{+} \,.$$

Thus the neutrino-gauge, conflicting as it does with the [3] charge-gauge, picks an axis in charge-space, and (incidentally) leads to parity violation of interactions of the A_μ^{+}, A_μ^{-} fields. The possibility of gauging the neutrino ($\nu \to \gamma_5\nu$) arises from the fact that neutrino has zero mass while the electron does not. In a sense then the existence of mass is incompatible with full rotational symmetry in [3] charge-space; the fact that all known charged particles have mass is the expression of the fact that one particular axis is preferentially chosen in [3] charge-space.

One can consider a second lepton vector $L_2 = (\mu^{+}, \nu', \mu^{-})$, where ν′ is gauged as $\nu' \to -\gamma_5\nu'$ (*). The interaction Lagrangian for L_2 fields is $-\varepsilon \overline{\boldsymbol{L}}_2 \times \boldsymbol{L}_2 \cdot \boldsymbol{A}$. Through the intermediacy of the A^{+}, A^{-} fields, one then has a possibility of $\mu \to e + \nu + \nu'$, all helicities given by our interaction Lagrangian being precisely the ones which are observed.

The major problem that remains is the problem of the mass of $A^{\pm}$ fields. Before the introduction of the parity violating term in (14), there was nothing in the theory to differentiate $A^{\pm}$ from A^{0}. The charged A fields would (in spite of the term

$$-\frac{\varepsilon^2}{2}\left[(A_\mu^{+}A_\mu^{-})^2 - (A_\mu^{+})^2(A_\mu^{-})^2\right]\Big),$$

acquire no self-mass from its interactions (**). The parity violating terms give the possibility that self-mass for A^{+}, A^{-} no longer vanishes. Also the charge-renormalization for A^{+}, A^{-} interactions is different than for the A^{0} interactions.

(*) In a sense ν and ν′ are twin neutrinos.

(**) This has actually been checked to the lowest order by S. Kamefuchi. We are indebted for a private communication. He has also checked that an effective mass will appear for the $A^{\pm}$ fields if parity-violating terms are added.

We propose to come back to this problem in a subsequent paper. Here we simply note that if $\varepsilon^2/4\pi = 1/137$, A^+, A^- fields would need to have an effective mass $\approx\sqrt{\varepsilon^2/g}$, *i.e.* about $30\,m_p$. Note that a (quadratic) self-mass is $\alpha\varepsilon^2\Lambda^2$, where Λ is the cut-off mass. Thus $\varepsilon^2\Lambda^2 \approx \varepsilon^2/g$ gives $\Lambda \approx 350\,m_p$. This does not appear too excessive a value for the cut-off.

4. – Baryons and mesons.

For π and K mesons, define the charge space vectors $\boldsymbol{\pi}$ and $\boldsymbol{K}$ composed from (π^+, π^0, π^+) and $(\mathrm{K}^+, \mathrm{K}_1^0, \mathrm{K}^-)$ particles. (More precisely $\boldsymbol{\pi} = (\pi_1, \pi_2, \pi_3)$

$$\pi^0 = \pi^3, \quad \pi^\pm = \frac{1}{\sqrt{2}}(\pi^1 \mp i\pi^2), \qquad K_1^0 = \frac{1}{\sqrt{2}}(K^0 + \overline{K^0}).$$

The interaction with the A field is

$$-\varepsilon(\partial\boldsymbol{\pi}\times\boldsymbol{\pi}\cdot\boldsymbol{A}) - \varepsilon^2[\boldsymbol{A}^2\boldsymbol{\pi}^2 - (\boldsymbol{A}\cdot\boldsymbol{\pi})^2]$$

and similarly for the K mesons.

For baryons, we make the fundamental assumption that all bare baryon masses are equal. Defining

$$Y_1 = \frac{1}{\sqrt{2}}(\Lambda^0 + \Sigma), \qquad Y_2 = \frac{1}{\sqrt{2}}(\Lambda^0 - \Sigma^0),$$

we write two baryon vectors

$$\boldsymbol{B}_1 = \frac{1}{\sqrt{2}}\begin{pmatrix} p + \Sigma^- \\ i(p - \Sigma^-) \\ n + Y_1 \end{pmatrix}, \qquad \boldsymbol{B}_2 = \frac{1}{\sqrt{2}}\begin{pmatrix} \Sigma^+ + \Xi^- \\ i(\Sigma^+ - \Xi^-) \\ Y_2 + \Xi^0 \end{pmatrix}.$$

The free baryon Lagrangian can be written as

$$[\overline{\boldsymbol{B}}_1 D\boldsymbol{B}_1 + \overline{\boldsymbol{B}}_2 D\boldsymbol{B}_2 + \overline{B}_{s1} DB_{s1} + \overline{B}_{s2} DB_{s2}] + \\ + [\overline{\boldsymbol{B}}_1^c D\boldsymbol{B}_1^c + \overline{\boldsymbol{B}}_2^c D\boldsymbol{B}_2^c + \overline{B}_{s1}^c DB_{s1}^c + \overline{B}_{s2}^c DB_{s2}^c].$$

Here

$$B_{1s} = \frac{1}{\sqrt{2}}[n - Y_1], \qquad B_{2s} = \frac{1}{\sqrt{2}}[Y_2 - \Xi^0],$$

D is the Dirac operator and $\boldsymbol{B}^c$ is the charge-conjugate vector. (Using Majorana representation of Dirac matrices if $\psi = \psi_1 + i\psi_2$ the charge conjugate spinor is $\psi^c = \psi_1 - i\psi_2$).

We note here an essential difference from the case of leptons. Each one

of our vectors $\boldsymbol{B}_1$, $\boldsymbol{B}_2$, etc., contains complex fields as components. For leptons ($\boldsymbol{L}_1$, $\boldsymbol{L}_2$) as well as for π and K mesons, the corresponding charge-space vectors were real. The reason why $\boldsymbol{B}_1$, $\boldsymbol{B}_2$ are complex lies in baryon-conservation. Thus one can adopt two completely different attitudes for baryons; one can consider that there are essentially four independent charge-space vectors $\boldsymbol{B}_1$, $\boldsymbol{B}_2$, $\boldsymbol{B}_1^c$ and $\boldsymbol{B}_2^c$ and baryon-conservation demands that $\boldsymbol{B}_1$, $\boldsymbol{B}_2$ (for example) should occur symmetrically. Alternatively one may split each of the vectors $\boldsymbol{B}_1$, $\boldsymbol{B}_2$ into real and imaginary parts and work with the resulting four vectors. It is crucial that there are four baryons which are charged (P,Σ^-), (Σ^+, Ξ^-). One could never arrive at the ideas of charge-space vectors before the discovery of new particles.

A charge space rotation will produce the interaction Lagrangian.

$$\varepsilon[\overline{\boldsymbol{B}}_1\boldsymbol{B}_1\cdot\boldsymbol{A}+\overline{\boldsymbol{B}}_2\boldsymbol{B}_2\cdot\boldsymbol{A}]-\varepsilon[\overline{\boldsymbol{B}}_1^c\boldsymbol{B}_1^c+\overline{\boldsymbol{B}}_2^c\boldsymbol{B}_2^c]\cdot\boldsymbol{A}\,. \tag{12}$$

The Lagrangian combines formally electro-magnetic interactions, as well as interaction terms which could be responsible (through A^+, A^- fields) for β decays as well as for hyperon decays. However at this stage only parity conserving weak decays are included.

On the other hand we know from our work with leptons, that the postulated γ_5-invariance of neutrino interactions picks out a direction in charge-space and also symmetrizes the weak lepton interactions for parity-conserving and parity-violating terms. It thus appears that neutrino γ_5-invariant Lagrangian is also γ_5-symmetrized in the sense used earlier by SALAM (*).

A term in a Lagrangian is « γ_5-symmetrized » if the trasnformation $\psi\to\gamma_5\psi$, $m\to -m$ are made *independently* for all fields concerned (**) and the result summed. Since the lepton and A field interaction Lagrangian happens to be « γ_5-symmetrized » in the above generalized sense, it seems necessary to « γ_5-symmetrize » the baryon-Lagrangian as well. Thus

$$p,\ Y_1,\ \Sigma^-\to\gamma_5(p,\ Y_1,\ \Sigma)\,. \tag{13}$$

A priori (Σ^+, Y_2, Ξ^-) could transform as $+\gamma_5$ or $-\gamma_5$ but Y_1 and Y_2 are related and thus it appears likely that (Σ^+, Y_2, Ξ^-) $\to\gamma_5(\Sigma^+,\ Y,\ \Sigma^-)$. After this symmetrization the electro-magnetic interaction remains unchanged, (*e.g.* $\overline{p}\gamma_\mu p\to\frac{1}{2}(\overline{p}\gamma_\mu p-\overline{p}\gamma_5\gamma_\mu\gamma_5 p)=\overline{p}\gamma_\mu p$, while $\overline{p}\gamma_\mu n\to\frac{1}{2}(\overline{p}(1-\gamma_5)n)$.

(*) A. SALAM: *Phys. Rev.* Letters (to be published). « γ_5-symmetrization » is not synonymous with « γ_5-invariance » of a Lagrangian though these may be equivalent in some special cases.

(**) If spin zero Bose fields are present $\varphi\to-\varphi$ simultaneously with $\psi\to\gamma_5\psi$. All currently accepted strong and weak Lagrangians appear to be γ_5-symmetrized.

It is now necessary to introduce strong interactions of baryons and mesons and to insure that these conserve charge in the conventional sense. This is an important point, for we do not wish to use the vector combinations $\boldsymbol{B}_1$ and $\boldsymbol{B}_2$ (and singlets B_{s1}, B_{s2}) etc., for writing strong interactions. If we did so, and if strong interactions were rotation invariant in the [3] Q space, there would be no distinction between these interactions and weak and e.m. interactions so far as conventional strangeness, isotopic-spin etc., are concerned. In other words it is necessary to state some criterion which guarantees that even if strong interactions are not rotation-invariant in charge-space these conserve charge in the conventional sense.

Such a criterion is easily stated. Among the $\boldsymbol{A}$ fields, γ_5 symmetry has picked out the component A^0. The divergence of the current $\mathcal{J}_\mu^{(1)}$ vanishes.

Here $\mathcal{J}_\mu^{(0)}$ equals the third component of

$$\varepsilon(\overline{\boldsymbol{L}}_1\boldsymbol{L}_1+\overline{\boldsymbol{L}}_1\boldsymbol{L}_2+\overline{\boldsymbol{B}}_1\boldsymbol{B}_1+\overline{\boldsymbol{B}}_2\boldsymbol{B}_2-\overline{\boldsymbol{B}}_1^c\overline{\boldsymbol{B}}_1^c-\overline{\boldsymbol{B}}_2^cB_2)+$$

$$+\text{terms from } \pi,\ \mathrm{K} \text{ and } A \text{ fields}.\quad (\text{See Equ. (10)}).$$

Thus charge operator

$$Q=\int\mathcal{J}_4^0\mathrm{d}^3x\,,$$

can be defined in the usual manner. If we now demand that the hamiltonian for all strong interactions H_s must commute with Q (and must satisfy baryon conservation) charge in the conventional sense is conserved even if H_5 is not rotation-invariant in Q-space. Thus the usual isotopic rotation invariant Lagrangian with 8 different coupling constants

$$g_1\overline{N}N\pi+g_2\overline{\Lambda}\Sigma\pi+g_3\overline{\Sigma}\Sigma\pi+\ldots\ g_5\overline{N}K\Lambda+g_6\overline{N}K\Sigma+\ldots$$

is fully acceptable. The mass degeneracy of baryons in the free Lagrangian will be removed by these strong interactions.

5. – The simple interaction Lagrangian written symbolically as

$$(\overline{\boldsymbol{L}}\boldsymbol{L}+\overline{\boldsymbol{B}}\boldsymbol{B}+\boldsymbol{\pi}\boldsymbol{\pi}+\boldsymbol{K}\boldsymbol{K}+\boldsymbol{A}\boldsymbol{A})\cdot\boldsymbol{A}$$

combines electro-magnetic interactions, as well as weak interactions. For weak interactions γ_5-symmetrization gives parity-violating terms while electromagnetic interaction terms still conserve parity. The weak interactions appropriately violate strangeness conservation while electromagnetic interactions do not.

There are also a number of conservation (eq. (10)) laws for the weak inter-

action currents. These are similar to the conservation laws previously discovered by GELL-MANN (*) and ZELDOVICH and GERŠTEJN.

The idea that weak interactions and electromagnetic interactions should be combined, originating as it did with SCHWINGER (2), has been often discussed privately, as has also the possibility that the resulting A-fields should be associated with a Yang-Mills type of gauge transformation. In this connection we are unable to disentangle the extent to which we are indebted to others. Particularly we would like to mention Dr. S. L. GLASHOW who has expressed similar ideas to us privately and a recent preprint (H. MAYER, Dubno) where a future paper on this subject is promised.

* * *

The work of one of the authors (J.C.W.) was supported by the U.S. Air Force through the Office of the Scientific Research of the Air Research and Development Command.

(*) M. GELL-MANN: *Phys. Rev.*, to be published. S. S. GERŠTEJN and ZELDOVICH: *Žurn. Èksper. Teor. Fiz.*, **29**, 698, (1958).

RIASSUNTO (*)

Il postulato di una « connessione locale » in un [3] spazio della carica conduce all'introduzione di tre campi di spin uno. Uno di questi può identificarsi col campo elettromagnetico e si può dimostrare che gli altri due sono il veicolo di tutte le interazioni deboli note, unificando così tali interazioni coll'elettromagnetismo. La teoria tien conto del fatto che, a differenza delle interazioni elettromagnetiche, le interazioni deboli violano la conservazione della parità e della stranezza.

(*) *Traduzione a cura della Redazione.*

IL NUOVO CIMENTO Vol. XI, N. 4 16 Febbraio 1959

Nuclear Matrix Elements for Some 1st-Forbidden Unique β Transitions.

B. Oquidam and B. Jancovici

Laboratoire de Physique, Ecole Normale Supérieure - Paris

(ricevuto il 6 Dicembre 1958)

Résumé. — On étudie dans le cadre du modèle des couches les éléments de matrice nucléaires pour les transitions β interdites du premier ordre uniques, autour du nombre de masse $A=40$. L'analyse des résultats expérimentaux permet d'obtenir des éléments de matrice expérimentaux. Puis on calcule ces éléments de matrice, d'abord avec le modèle simple dans lequel les moments angulaires du groupe des protons et du groupe des neutrons sont séparément de bons nombres quantiques; ensuite avec un modèle plus compliqué. Les résultats du deuxième modèle sont en assez bon accord avec l'expérience en ce qui concerne les valeurs relatives des éléments de matrice; un écart systématique est obtenu pour les valeurs absolues. L'étude de transitions γ analogues permet d'attribuer l'écart, au moins pour sa plus grande part, à des effets de structure nucléaire.

1. – Introduction.

It has been established by the work of I. Talmi and his collaborators [1-3] that the shell model with j-j coupling is quantitatively able to account in a very precise way for the energies of the nuclei, at least in certain regions of the mass number. This for a long time unsuspected agreement could be obtained by avoiding the introduction of poorly known numerical values for the radial wave functions or the two-body forces; the energy matrix elements for

(1) R. Thieberger and I. Talmi: *Phys. Rev.*, **102**, 589 (1956).
(2) I. Talmi and R. Thieberger: *Phys. Rev.*, **103**, 718 (1956).
(3) S. Goldstein and I. Talmi: *Phys. Rev.*, **105**, 995 (1957).

simple configurations were instead treated as free parameters, and the energies for more complicated configurations then followed.

Other properties than energies are not expected to be in such as good an agreement with experiment, since the energy is exceptionally favoured by its stationary character. For instance, the nuclear matrix elements for allowed β transitions (4) show marked deviations from the *j-j* coupling shell model values. These deviations however are strongly reduced if some configuration mixing is introduced (5).

In the present paper, we study the nuclear matrix elements for 1st-forbidden unique β transitions in the mass number region around $A = 40$. The $d_{\frac{3}{2}}$ shell closes at N or $Z = 20$, and is followed by the $f_{\frac{7}{2}}$ shell. These β^- radioactive nuclei with a proton number $Z < 20$ and a neutron number $N > 20$ undergo transitions in which a $f_{\frac{7}{2}}$ neutron turns into a $d_{\frac{3}{2}}$ proton. All these transitions (with the exception of the ^{40}K decay) occur with a spin change of 2 units and with a change of parity: they are unique 1st-forbidden (6).

We shall first determine the experimental values of the nuclear matrix elements, through an analysis of the experimental information. We shall then proceed to the calculation of these matrix elements with simple wave functions, and also with more refined wave functions. These results will be discussed. The relation with some γ matrix elements will also be studied.

2. – Experimental β nuclear matrix elements.

In the notation of (6), the nuclear matrix element for a 1st-forbidden unique transition is:

$$|M|^2 = \sum |\mathcal{Y}_{2m}(\boldsymbol{\sigma})|^2 , \tag{1}$$

where the summation is on m and on the spin states of the final nucleus. $\mathcal{Y}_{2m}$ is a second-order tensor, bilinear in $\boldsymbol{\sigma}$ and $\boldsymbol{r}$, defined by:

$$\mathcal{Y}_{lm}(\boldsymbol{\sigma}) = \frac{1}{l}\boldsymbol{\sigma}\cdot\mathbf{grad}\,\mathcal{Y}_{lm}(\boldsymbol{r}), \tag{2}$$

where $\mathcal{Y}_{lm}(\boldsymbol{r})$ is the usual solid spherical harmonic.

(4) W. C. Grayson Jr. and L. W. Nordheim: *Phys. Rev.*, **102**, 1093 (1956).

(5) R. J. Blin-Stoyle and C. A. Caine: *Phys. Rev.*, **105**, 1810 (1957).

(6) For a review of the theory of forbidden β decay, see *e.g.* E. Konopinski, in *Beta- and Gamma-Ray Spectroscopy*, edited by K. Siegbahn (Amsterdam, 1955), p. 292. We here follow the notations of this paper.

This matrix element is related to the comparative half-life $f_1 t$ by:

$$f_1 t = \frac{2\pi^3 \ln 2/g^2}{(32\pi/15)\,|M|^2}, \tag{3}$$

where g is the Gamow-Teller coupling constant. We adopt the value which results from the most recent measurements of the half-lives of ^{14}O (7) and of the neutron (8) which yield $2\pi^3 \ln 2/g^2 = 4366$ s, when M in (3) is expressed in units of electron Compton wave length $\hbar/mc$. f_1 is defined by DAVIDSON (9),

TABLE I.

		log ft	log $f_1 t$	$10^6 \lvert M \rvert^2_{exp} = 651/f_1 t \cdot 10^6$	Simple wave functions		Detailed wave functions	
					ϱ	$10^6 \lvert M \rvert^2_{SP.eff}$	ϱ	$10^6 \lvert M \rvert^2_{SP.eff}$
(*a*, *b*)	$^{37}S \rightarrow {}^{37}Cl$	7.23	7.93	7.7	1	7.7	1	7.7
(*c*, 19)	$^{38}Cl \rightarrow {}^{38}A$	7.42	8.19	4.20	4/5	5.2	0.80	5.2
(*d*)	$^{39}Cl \rightarrow {}^{39}A$	7.8	8.3	3.26	1/4	13.0	0.9	3.6
(*e*, *f*)	$^{39}A \rightarrow {}^{39}K$	9.91	9.01	0.64	1/2	1.3	0.11	5.8
(*g*)	$^{41}A \rightarrow {}^{41}K$	8.34	8.50	2.15	3/8	5.7	3/8(*)	5.7 (*)
(*h*, 19)	$^{42}K \rightarrow {}^{42}Ca$	7.95	8.42	2.48	6/5	2.1	0.66	3.8
(*i*)	$^{43}K \rightarrow {}^{43}Ca$	8.70	8.62	1.56	1	1.6	0.24	6.5

$|M|^2$ is in units $\hbar = m = c = 1$

(*) These values come from a very rough estimate of the « detailed wave function ».

(*a*) E. BLEULER and W. ZÜNTI: *Helv. Phys. Acta*, **19**, 137 (1946).
(*b*) D. STROMINGER, J. M. HOLLANDER and G. T. SEABORG: *Rev. Mod. Phys.*, **30**, 585 (1958).
(*c*) J. W. COBBLE and R. W. ATTEBERRY: *Phys. Rev.*, **80**, 917 (1950).
(*d*) J. R. PENNING, H. R. MALTRUD, J. C. HOPKINS and F. H. SCHMIDT: *Phys. Rev.*, **104**, 740 (1956).
(*e*) A. R. BROSI, H. ZELDES and B. H. KETELLE: *Phys. Rev.*, **79**, 902 (1950).
(*f*) H. ZELDES, B. H. KETELLE, A. R. BROSI, C. R. FULTZ and R. F. HIBBS: *Phys. Rev.*, **86**, 811 (1952).
(*g*) A. SCHWARTZSCHILD, B. M. RUSTAD and C. S. WU: *Phys. Rev.*, **103**, 1796 (1956).
(*h*) P. R. J. BURCH: *Nature*, **172**, 361 (1953).
(*i*) T. LINDQVIST and A. C. G. MITCHELL: *Phys. Rev.*, **95**, 444 (1954).

(7) J. B. GERHART: *Phys. Rev.*, **109**, 897 (1958).

(8) A. N. SOSNOVSKIJ, P. E. SPIVAK, P. E. PROKOFIEV, A. YU, I. E. KUTIKOV and YU. P. DOBRYNIN: *Contribution to the* 1958 *Annual International Conference on High Energy Physics at CERN*.

(9) J. P. DAVIDSON Jr.: *Phys. Rev.*, **82**, 48 (1951). This reference is inaccurate in its presentation: if the factor

$$|Q_{n+1}(\boldsymbol{\sigma}, \boldsymbol{r})|^2 = (32\,\pi/15)\,|M|^2$$

is removed from the definition of C_n in eq. (9), the definition (8) of f_1 is then the actual one used by DAVIDSON in his computations, and also by us.

who gives an approximate procedure for computing it. We also computed f_1 by numerical integration of the theoretical spectrum, and checked that the approximation of DAVIDSON is accurate within a few percent. f_1 depends on the Q-value for the β transition. Using the experimental values of Q and of the half-life t, we list the experimental values of $f_1 t$, for the transitions of interest, in Table I. The value of ft, where f is that quantity which is currently used for allowed transitions is also listed for the sake of comparison. We then use (3) to determine an « experimental » value for the squared matrix element, $|M|^2_{\text{exp}}$, which is given in Table I.

3. – Calculated β nuclear matrix elements with simple wave functions.

The matrix element for a single particle transition is easily obtained using the definition (2) of $\mathcal{Q}_{2m}(\boldsymbol{\sigma})$. One has for this single particle case ([10]):

$$|M|^2_{\text{S.P.}} = (9/7\pi)\left(\int_0^\infty R_f(r) r R_d(r)\,\mathrm{d}r\right)^2, \tag{4}$$

where $R_f(r)/r$ and $R_d(r)/r$ are the radial wave functions for the f and d states. The integral in (4) cannot be computed without somewhat arbitrary assumptions on these wave functions. However, an estimate of this integral can be easily obtained from some model, for instance oscillator well wave functions. The parameter ν of the well can be adjusted to fit the Coulomb energy differences between mirror nuclei ([11]) in this region of A). In this way we obtain:

$$|M|^2_{\text{S.P.}} = 9/4\,\pi\nu \approx 37\cdot 10^{-6}(\hbar/mc)^2\,. \tag{5}$$

A numerical integration with wave functions for an infinite square well of radius $R = 1.6\cdot 10^{-13}(40)^{\frac{1}{3}}$ cm ([12]) leads to the value:

$$|M|^2_{\text{S.P.}} = (9/7\,\pi)\,0.44\,R^2 \approx 36\cdot 10^{-6}(\hbar/mc)^2\,. \tag{5'}$$

We see that the value of $|M|^2_{\text{S.P.}}$ does not depend too much on the model.

([10]) Cf. R. NATAF: *Journ. Phys. Rad.*, **14**, 72 (1953). There is a misprint in eq. (5) of this reference, which should be read

$$|a_1|^2 = 12\,\frac{L(L-1)}{4L^2-1} \qquad \text{if} \quad J > J'.$$

([11]) B. C. CARLSON and I. TALMI: *Phys. Rev.*, **96**, 436 (1954).

([12]) The radius of the infinite well has to be taken somewhat bigger than the radius of the charge distribution. This value of R leads to a mean square radius of $(3/5)^{\frac{1}{2}}\,1.3\cdot A^{\frac{1}{3}}\cdot 10^{-13}$ cm, which is suggested by Coulomb energies in this region (see ref. ([11])).

But the nuclear radius enters by its square, and the uncertainty on this radius would be reflected in $|M|^2_{\text{S.P.}}$.

This single-particle value should be appropriate to the transition ${}^{37}_{18}\text{Cl}_{17} \to {}^{37}_{17}\text{S}_{16}$. For the other cases, we consider the following « simple » wave functions: the protons (neutrons) in the $d_{\frac{3}{2}}$ ($f_{\frac{7}{2}}$) shell are coupled together to a definite angular momentum J_1 (J_2), equal to 0 if the proton (neutron) is even, to $\frac{3}{2}$ ($\frac{7}{2}$) if the proton (neutron) is odd; J_1 and J_2 are coupled together to give the total angular momentum J. These configurations are given in Table II. The neutrons in the closed $d_{\frac{3}{2}}$ neutron shell play no role in β transitions and can be neglected ([13]). The transitions we consider are therefore of the type:

$$(j)^m_{J_1}(j')^n_{J_2}J' \to (j)^{m+1}_{J_1}(j')^{n-1}_{J_2}J \ .$$

Table II. – *Detailed wave functions.*

${}^{37}_{16}\text{S}_{21}$	$\vert \quad f_{\frac{7}{2}},\ \frac{1}{2}\rangle$
${}^{37}_{17}\text{Cl}_{20}$	$\vert \quad d_{\frac{3}{2}},\ \frac{3}{2}\rangle$
${}^{38}_{17}\text{Cl}_{21}$	$\vert d_{\frac{3}{2}},\ f_{\frac{7}{2}},\ 2\rangle$
${}^{39}_{17}\text{Cl}_{22}$	$0.92\vert d_{\frac{3}{2}},\ (f_{\frac{7}{2}})^2_0,\ \frac{3}{2}\rangle + 0.39\vert d_{\frac{3}{2}},\ (f_{\frac{7}{2}})^2_2,\ \frac{3}{2}\rangle$
${}^{38}_{18}\text{A}_{20}$	$\vert \quad (d_{\frac{3}{2}})^2,\ 0\rangle$
${}^{39}_{18}\text{A}_{21}$	$0.95\vert (d_{\frac{3}{2}})^2_0,\ f_{\frac{7}{2}},\ \frac{7}{2}\rangle + 0.31\vert (d_{\frac{3}{2}})^2_2,\ f_{\frac{7}{2}},\ \frac{7}{2}\rangle$
${}^{41}_{18}\text{A}_{23}$	$\ldots\ \vert (d_{\frac{3}{2}})^2_0,\ (f_{\frac{7}{2}})^3_{\frac{7}{2}},\ \frac{7}{2}\rangle + \ldots$
${}^{39}_{19}\text{K}_{20}$	$\vert (d_{\frac{3}{2}})^3_{\frac{3}{2}},\ \frac{3}{2}\rangle$
${}^{41}_{19}\text{K}_{22}$	$0.92\vert (d_{\frac{3}{2}})^3_{\frac{3}{2}},\ (f_{\frac{7}{2}})^2_0,\ \frac{3}{2}\rangle - 0.38\vert (d_{\frac{3}{2}})^3_{\frac{3}{2}},\ (f_{\frac{7}{2}})^2_2,\ \frac{3}{2}\rangle$
${}^{42}_{19}\text{K}_{23}$	$0.74\vert (d_{\frac{3}{2}})^3_{\frac{3}{2}},\ (f_{\frac{7}{2}})^3_{\frac{7}{2}},\ 2\rangle + 0.65\vert (d_{\frac{3}{2}})^3_{\frac{3}{2}},\ (f_{\frac{7}{2}})^3_{\frac{5}{2}},\ 2\rangle + 0.17\vert (d_{\frac{3}{2}})^3_{\frac{3}{2}},\ (f_{\frac{7}{2}})^3_{\frac{3}{2}},\ 2\rangle$
${}^{43}_{19}\text{K}_{24}$	$0.88\vert (d_{\frac{3}{2}})^3_{\frac{3}{2}},\ (f_{\frac{7}{2}})^4_0,\ \frac{3}{2}\rangle - 0.47\vert (d_{\frac{3}{2}})^3_{\frac{3}{2}} \quad (f_{\frac{7}{2}})^4_2,\ \frac{3}{2}\rangle + \ldots$
${}^{42}_{20}\text{Ca}_{22}$	$\vert (d_{\frac{3}{2}})^4_0,\ (f_{\frac{7}{2}})^2_0,\ 0\rangle$
${}^{43}_{20}\text{Ca}_{23}$	$\vert (d_{\frac{3}{2}})^4_0,\ (f_{\frac{7}{2}})^3_{\frac{7}{2}},\ \frac{7}{2}\rangle$

The simple wave function is the first term of the detailed wave functions.

The matrix elements for such a transition can be related to the single particle value (4) by the straightforward use of tensor algebra ([14]) and of coefficients of fractional parentage ([15]):

$$(6) \qquad M/M_{\text{S.P.}} = (-1)^{j+J_2-J_2'}\sqrt{(m+1)n(2J+1)(2j'+1)(2J_1+1)(2J_2'+1)}\cdot$$

$$\cdot\langle j^{m+1}J_1 \{\!\{ j^m(J_1')jJ_1\rangle \langle j'^nJ_2' \{\!\{ j'^{n-1}(J_2)j'J_2'\rangle \cdot \begin{Bmatrix} J_1 & J_2 & J \\ J_1' & J_2' & J' \\ j & j' & 2 \end{Bmatrix}.$$

([13]) As a check, we also performed the calculations with the $d_{\frac{3}{2}}$ neutrons taken into account, and obtained the same results.

([14]) G. RACAH: *Phys. Rev.*, **62**, 438 (1942).

([15]) G. RACAH: *Phys. Rev.*, **63**, 367 (1943). See eq. (28) of this reference.

The coefficients of fractional parentage for identical particles, $\langle\{\rangle$, are available ([16,17]). The $9-j$ coefficients $\{\}$ ([18]) can also be computed; incidentally, they reduce to Racah coefficients in the cases where one of the j is zero. The resulting value of the ratio:

$$\varrho = |M|^2/|M|^2_{\text{S.P.}} \tag{7}$$

is listed in Table I.

In order to compare the results to experiment, we define an effective single particle matrix element by the relation:

$$|M|^2_{\text{S.P.eff}} = |M|^2_{\text{exp}}/\varrho \,. \tag{8}$$

This procedure allows us to eliminate the uncertain value (5) or (5′). The theory will be satisfactory if $|M|^2_{\text{S.P.eff}}$ is a constant for the different transitions. The values listed in Table I are actually far from constant. Furthermore, the absolute value of $|M|^2_{\text{S.P.eff}}$ is smaller than the estimate (5) or (5′).

4. – Calculated β nuclear matrix elements with more detailed wave functions.

The simple wave functions of the last section gave a poor agreement with experiment, both for the relative and for the absolute values of the matrix elements. It is possible to improve these wave functions by using the freedom on the values of J_1 and J_2. We now choose wave functions of the form:

$$\sum_{J_1 J_2} \alpha_{J_1 J_2} |(d_{\frac{3}{2}})^m_{J_1} (f_{\frac{7}{2}})^n_{J_2} J\rangle \,, \tag{9}$$

where the summation runs over all possible values of J_1 and J_2. The coefficients $\alpha_{J_1 J_2}$ should be determined by the diagonalization of an energy matrix.

In the cases where the proton (neutron) number is even, it was argued ([3]) that the excitation of the proton (neutron) configuration requires much energy, and the admixture of such excited states should be negligible. This argument, however, was made for the calculation of binding energies. The calculation of β transitions requires better wave functions, and we now take into account the admixtures of excited states of the even configurations. Of course, admixtures occur more easily for odd configurations, and these will be also considered.

([16]) A. R. Edmonds and B. H. Flowers: *Proc. Roy. Soc.* (*London*), A **214**, 515 (1952).

([17]) W. C. Grayson Jr. and L. W. Nordheim: *Phys. Rev.*, **102**, 1084 (1956).

([18]) G. Racah and U. Fano: *Irreducible Tensorial Sets* (New York, to be published).

The calculation of the energy matrices closely follows in all cases the techniques which were previously used ([3]) in the odd-odd case of ^{42}K and this calculation will not be described in detail here ([19]). It must however be noted that we do not compute the energy contribution of the forces between identical particles; we rather use the experimental information ([20]) from neighbouring nuclei. For instance, in the case of ^{39}A, the wave function is of the form:

$$\alpha_0 |(d_{\frac{3}{2}})^2_0 f_{\frac{7}{2}}\, 7/2\rangle + \alpha_2 |(d_{\frac{3}{2}})^2_2 f_{\frac{7}{2}}\, 7/2\rangle \,. \tag{10}$$

The proton-proton energy difference between $(d_{\frac{3}{2}})^2_2$ and $(d_{\frac{3}{2}})^2_0$ is then taken as the experimental excitation energy of the first level $(d_{\frac{3}{2}})^2_2$ of ^{38}A relative to its ground state $(d_{\frac{3}{2}})^2_0$. The neutron-proton forces are treated as in ([3]) and expressed in terms of the same parameters V_J. The binding energies which are computed by this procedure are excellent ([21]). The wave functions so obtained are listed in Table II. The energy matrices of interest are given in the Appendix.

Some remarks are necessary: in the case of ^{43}K, there are two possible states with $J_2 = 2$ for the neutron configuration $(f_{\frac{7}{2}})^4$. These states have seniorities 2 and 4. The seniority 4 state is expected to have a higher energy but it cannot be identified in an unique way with a given level of ^{44}Ca; furthermore, there is no element in the energy matrix directly connecting the corresponding unperturbed state of ^{43}K to the unperturbed ground state of ^{43}K. The admixture of this state is thus expected to be small. On the other hand, it can be shown that this seniority 4 component would not directly contribute to the β matrix element: this component therefore does not interfere with the other ones, and would only cause a slight second order modification of the coefficients of the other components. For all these reasons, we neglect the possible admixture of the seniority 4 state.

We have omitted the energy matrix and the detailed wave function for ^{41}A. This is because the energy matrix would be too big, and the various states of the $(f_{\frac{7}{2}})^3$ neutron configuration of ^{41}A cannot be uniquely identified with the levels of ^{43}Ca. Some preliminary calculations however show that ^{41}A is fairly well represented by the simple wave function $|(d_{\frac{3}{2}})^2_0,\ (f_{\frac{7}{2}})^3_{\frac{7}{2}},\ 7/2\rangle$.

It is now possible to compute the β decay matrix elements with the more detailed wave functions (9). Denoting by $M(J_1J_2J'_1J'_2)$ the value computed for M from (6), one immediately sees that:

$$\varrho = |M|^2/|M|^2_{\text{S.P.}} = |\sum_{J_1J_2J'_1J'_2} \alpha_{J'_1J'_2}\alpha_{J_1J_2} M(J_1J_2J'_1J'_2)/M_{\text{S.P.}}|^2 \tag{11}$$

([19]) B. OQUIDAM: *Thesis* (Doctorat de Spécialité de Physique Théorique - Paris), to be published.

([20]) P. M. ENDT and C. M. BRAAMS: *Rev. Mod. Phys.*, **29**, 683 (1957).

([21]) I. TALMI: private communication.

where $\alpha_{J_1'J_2'}$ and $\alpha_{J_1J_2}$ are the coefficients of the wave function (9) for the initial and final states. The values obtained from (11) are listed in Table I. With the value (11) for ϱ, (8) gives new values for $|M|^2_{\text{S.P.eff}}$ which are listed in Table I.

It can be seen that the constancy of $|M|^2_{\text{S.P.eff}}$, is improved by the use of the more detailed wave functions. The progress appears when the last column of Table I is compared with the much more dispersed experimental values $|M|^2_{\text{exp}}$. It must also be remembered that the experimental values are sometimes rather imprecise, and on the other hand that the β matrix elements are sensitive to small changes in the wave function.

5. – Discussion.

The approximate consistency of the values for $|M|^2_{\text{S.P eff}}$ obtained with the detailed wave functions, shows that the shell model, with the refinements of Section **4**, provides a fair account for the relative values of the β matrix elements. Comparison with the results obtained in Section **3** shows that the agreement with experiment is alway improved by the use of the wave functions of Section **4**. It is hoped that the small irregularities which subsist would be removed by further complication of the wave functions, for instance by taking into account the possible admixtures of $f_{\frac{5}{2}}$ orbitals. It must also be remembered that the experimental half-lifes and Q values are often uncertain.

On the other hand, the absolute value of $|M|^2_{\text{S.P.eff}}$ shows a marked departure from the estimates (5) or (5′). It does not seem possible to get entirely rid of this discrepancy by a simple change in the radial wave functions. Everything occurs as if the single particle matrix element was consistently smaller by a factor of about 4 than its estimates (5), (5′). The possible reasons for this apparent « renormalization » could be more easily discussed after a study of some γ transitions.

6. – Comparison with γ transitions.

For all the β transitions which were considered here, the daughter nucleus should have an excited state which is in close correspondence with the initial nucleus in its ground state. The γ transition of this excited state to the ground state is closely related to the corresponding β transition, and it is possible to compare their rates in the few cases when the γ lifetime has been measured, *i.e.* for the decays of the 1.52 MeV level of ^{39}A and of the 1.29 MeV of ^{41}K. The (partial) half-lives are listed in Table III.

TABLE III.

	γ partial half-life	$\lvert M\rvert^2_{exp}$ from γ	Corresponding β transition	$\lvert M\rvert^2_{exp}$ from β
^{39}A (1.52 MeV)	$2.1\cdot10^{-9}$ s	$5.2\cdot10^{-6}$	$^{39}\mathrm{Cl}\rightarrow{}^{39}\mathrm{A}$	$3.3\cdot10^{-6}$
^{41}K (1.29 MeV)	$6.6\cdot10^{-9}$ s	$3.7\cdot10^{-6}$	$^{41}\mathrm{A}\rightarrow{}^{41}\mathrm{K}$	$2.2\cdot10^{-6}$

These γ transitions with a spin change of 2 and a change of parity should be predominantly of M2 character. We assume that the possible E3 contribution is negligible, as indicated by simple estimates ([22]). The γ transition results from the jump of a proton between the $f_{\frac{7}{2}}$ and $d_{\frac{3}{2}}$ orbits. We can take into account some rearrangement of the other particles, using the same model as in Section 3. The important point however is that within this model, *i.e.* with definite orbitals $f_{\frac{7}{2}}$ and $d_{\frac{3}{2}}$ for the proton states, the M2 γ matrix element reduces to the β matrix element ([23]). The γ transition probability per second is then:

$$T=\frac{4\pi}{75}\frac{e^2E^5}{\hbar^4m_p^2c^7}\left(\mu_p-\frac{1}{3}\right)^2\sum\lvert\mathcal{Q}_{2m}(\boldsymbol{\sigma})\rvert^2, \tag{12}$$

where m_p is the proton mass, μ_p the proton magnetic moment in nuclear magneton units, E the γ-ray energy. $\mathcal{Q}_{2m}(\boldsymbol{\sigma})$ is here in cm. This formula is used to compute an experimental squared matrix element $\lvert M\rvert^2_{exp}$, as defined in (1), from the observed γ-transition probability. The value of $\lvert M\rvert^2_{exp}$ which is listed in Table III can be compared with the experimental value for the corresponding β transition matrix element, which is also repeated in Table III. It is seen that the two γ and β determinations are not in bad disagreement.

It thus appears that the γ matrix element is damped by a factor which is roughly the same as for the β matrix element. This fact would tend to prove that most of the « renormalization » of the matrix elements cannot be connected with the field-theoretical nature of the interaction (β or γ) under consideration, since the effect is the same for both interactions, although they are so different in their nature. The « renormalization » should thus mostly be a nuclear structure effect. For instance, if the $d_{\frac{3}{2}}$ and $f_{\frac{7}{2}}$ particles are weakly coupled to collective motions of the core, we expect such « renormalization » effects to occur, although many characters of the spherical shell-model will subsist. This aspect of the question is now being studied in our group.

The difference which subsists between the β and the γ matrix elements could reasonably result form the nuclear model imperfections. For instance, with an admixture of $f_{\frac{5}{2}}$ orbitals, (12) would no longer be valid.

([22]) V. F. WEISSKOPF: *Phys. Rev.*, **83**, 1073 (1951).
([23]) S. A. MOSZKOWSKI: p. 390 of ref. ([6]).

To summarize this work, the conclusion of our study is that the relative values of the β decay matrix elements are fairly accounted for by the shell model. The absolute values are consistently too small by a « renormalization » factor of about 4.

Finally, we see that it cannot be shown here that the effective operator which is responsible for 1st-forbidden unique β transitions is significantly different from $\mathcal{Q}_{2m}(\boldsymbol{\sigma})$. We very tentatively suggest that this is perhaps not a trivial statement, since it has been proposed that the axial β interaction could, like the vector one, be of a more complicated nature than the conventional one. It is indicated by our results that the effective β-decay coupling constant that appears for 1st-forbidden unique transitions does not seem to be actually different by more than 50% from the coupling constant for allowed transitions (which was introduced in (3)). It would be interesting to see, by a more careful knowledge of the nuclear structure, if it is possible to establish more precisely the equality of these constants, or if, conversely, they appear as being definitely different.

* * *

We are indebted to Professor I. TALMI for a stimulating discussion, for his kind interest, and for communication of results that he calculated independently. Thanks are due to Mrs. OQUIDAM who checked some of the calculations. The Centre d'Etudes Nucleaire de Saclay kindly made available 9-j coefficients which were calculated on their electronic computer.

APPENDIX

The energy matrices which do not reduce to a number are the following:

^{39}Cl

J_2	0	2
0	2.03	0.77
2	0.77	0.56

,

^{39}A

J_1	0	2
0	2.03	0.77
2	0.77	— 0.07

,

	J_2	0	2
^{41}K	0	6.08	— 0.71
	2	— 0.71	4.61

,

	J_2	0	2
^{43}K	0	12.17	— 0.82
	2	— 0.82	11.06

,

The energies which are taken into account here are the neutron proton interaction between $d_{\frac{3}{2}}$ and $f_{\frac{7}{2}}$ shells, and the excitation energy of the even group. Minus the energies are given.

The matrix for ^{42}K is given in ([3]). The matrix for ^{41}A is not given here.

RIASSUNTO (*)

Si studiano nel quadro del modello a shell gli elementi di matrice nucleare per le transizioni β proibite del primo ordine, uniche, intorno al numero di massa $A = 40$. L'analisi dei risultati sperimentali permette d'ottenere degli elementi di matrice sperimentali. Poi si calcolano questi elementi di matrice, prima col modello semplice in cui i momenti angolari del gruppo dei protoni e del gruppo dei neutroni sono separatamente buoni numeri quantici; poi con un modello più complicato. I risultati del secondo modello sono in sufficiente buon accordo con l'esperienza per quanto riguarda i valori relativi degli elementi di matrice; pei valori assoluti si ottiene uno scarto sistematico. Lo studio delle analoghe transizioni γ permette di attribuire lo scarto, almeno per la maggior parte, ad effetti della struttura nucleare.

(*) *Traduzione a cura della Redazione.*

NOTE TECNICHE

A Device for Dynamical Measurements of Pressure.

P. Bassi

Istituto di Fisica dell'Università - Padova
Istituto Nazionale di Fisica Nucleare - Sezione di Padova

R. Cano

Istituto di Fisica dell'Università - Trieste
Istituto Nazionale di Fisica Nucleare - Sezione di Trieste

S. Focardi and C. Rubbia (*)

Istituto di Fisica dell'Università - Pisa
Istituto Nazionale di Fisica Nucleare - Sezione di Pisa

A. Michelini

Istituto di Fisica dell'Università - Roma
Istituto Nazionale di Fisica Nucleare - Sezione di Roma

F. Saporetti

Istituto di Fisica dell'Università - Bologna
Istituto Nazionale di Fisica Nucleare - Sezione di Bologna

(ricevuto il 24 Novembre 1958)

Summary. — A device for fast measurements of pressure variations to be used in liquid hydrogen bubble chamber technique, is described. Its characteristic features are speedy and linear response, output signal independence of cable capacity variations, possibility of adjustment at a distance and simplicity of the detecting circuit.

There are several methods in use to transform a fast variation of pressure into an electric signal through capacity variation as well as through resistence variation, piezoelectric effect or e.m. induction.

(*) Now at Columbia University.

The pressure gage which will be described is supposed to work at liquid hydrogen temperature in a bubble chamber. The apparatus should, therefore, have the following characteristics.

a) Work correctly in a magnetic field of the order of 15 000 G.

b) Allow steady pressure calibration and further adjustment at a distance.

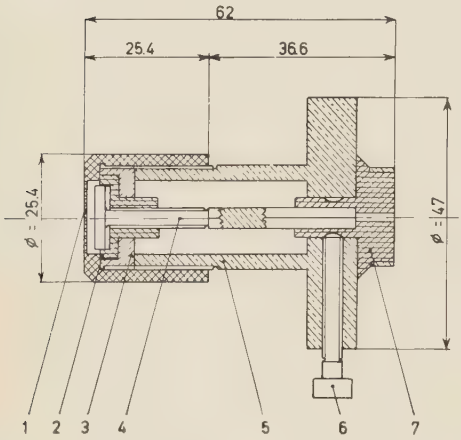

Fig. 1. – *Pressure cell.* During the present measurements the spacing between diaphragm A and the internal electrode was 0.03 mm (at pressure 0 atm) equivalent to an electric capacity of 35 pF.

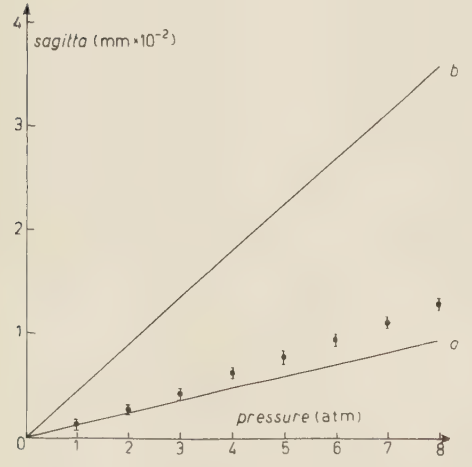

Fig. 2. – Diaphragm A sagittae *vs.* pressure.

c) Have an output signal as independent as possible of capacity variations (due, f.i. to temperature variations) in the coaxial cable connecting the pressure cell to the detecting circuit.

d) Have a response time less than 10^{-4} s to ensure reproduction of pressure transients to a few tenths of a millisecond.

To meet these requirements we have decided to use a system capable of transforming mechanical deformations into electric signals through the capacity variations of a condenser [1-3].

The pressure cell is shown in Fig. 1: diaphragm A is made of stainless steel 0.63 mm thick; the distance of the inner electrode from diaphragm A can be adjusted by means of a screw. The accuracy in the machining of the condenser was 0.01 mm; the two electrodes are parallel within a few hundredths mm. The spacing between the electrodes can be adjusted within 1/360 mm by means of the screw. Fig. 2 shows the measured sagitta diaphragm A as a function of the applied pressure; straight lines c and t are the sagittae evaluated in the two limiting cases of a circular diaphragm clamped, and simply supported at the edges.

As was already pointed out the electric circuit was designed to be insensitive to the capacity variations of the cable. The scheme of the circuit is shown in Fig. 3.

---

(1) T. WRATHALL: *Instrument*, **26**, 736 (1955).
(2) W. I. LINLOR and Q. A. KERN: UCRL-3173.
(3) W. I. LINLOR, Q. A. KERNS and J. W. MARK: *Rev. Sci. Instr.*, **28**, 535 (1957).

A 1.5 mH inductance (not critical) is connected in series with the pressure cell; the LC circuit thus forms the impedance load of a 75 Ω coaxial cable matched on its characteristic impedance.

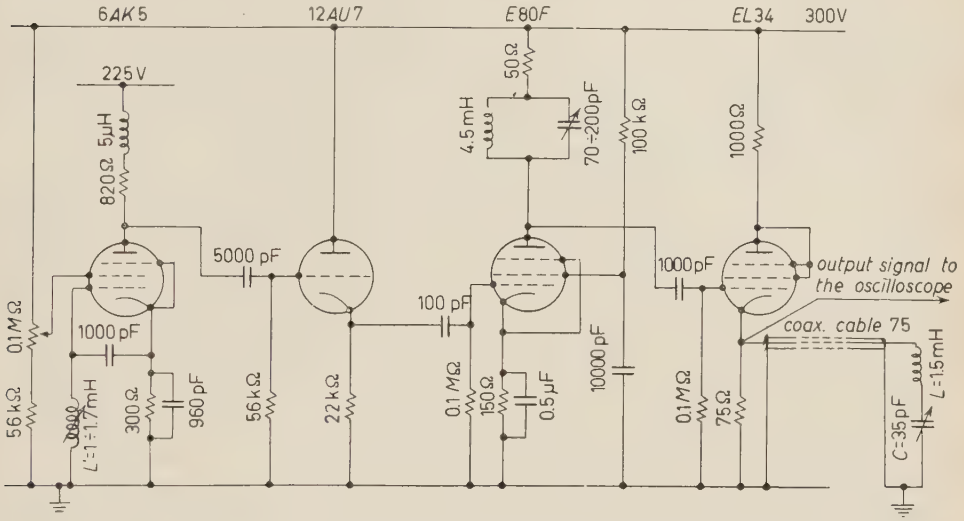

Fig. 3. – *Electric circuit.* The frequency of the 6AK5 oscillator can be modified by varying L' between 630 and 745 MHz.

The first stage consists of an oscillator whose frequency can be adjusted by changing L'. A decoupling and an amplifying stage follow. The EL34 is a low impedance adapter which easily gives an output signal up to 8 V (peak to peak) on 75 Ω.

The cathodic impedance of the EL34 is.

$$(1) \qquad Z_k = \frac{R\sqrt{r^2 + (L\omega - 1/\omega c)^2}}{\sqrt{r^2 + (L\omega - 1/\omega c)^2} + R}.$$

For the case of resonance, Z_k is clearly minimum and is the resultant of the two impedances R ($= 75$ Ω) and r (resistive component of the LC circuit) in parallel.

Variations of C around the resonance may cause an increase in the cathodic impedance.

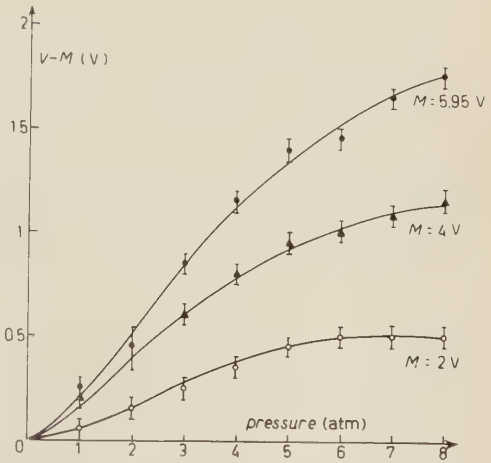

Fig. 4. – *Calibration curves.* The difference between the peak to peak output signal (V) and the signal at resonance (M) *vs.* pressure. Resonance corresponds to 0 atm, the working frequency was 715 MHz.

In Fig. 4 we have plotted the difference between the peak to peak output signal (V) and the signal at resonance (M), measured on the oscilloscopes *vs.* pressure. This was a steady pressure calibration at room temperature.

The frequency of the oscillator was adjusted to coincide with the resonance frequency of the LC circuit at 0 atm.

Fig. 5 shows that, as expected, there is a linear dependence between the modulation and the carrying wave amplitude.

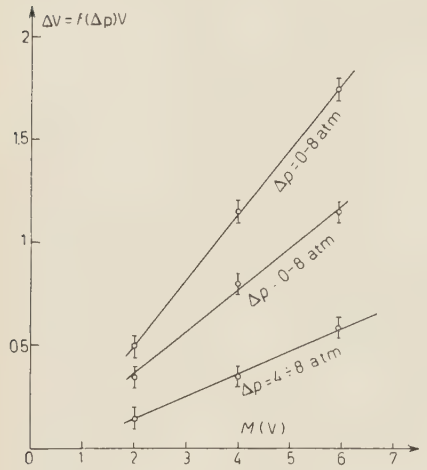

Fig. 5. – Peak to peak modulated signal *vs.* carrying wave amplitude, at resonance (M).

We have investigated the dependence of the instrument characteristics on some parameters with the following results:

— The instrument's sensitivity obviously increases with the decrease of the distance between the two electrodes of the pressure cell. Such an increase in the sensitivity of the system reduces the linearity of the output signal since, with a high value of ΔP, the circuit is working near the saturation of the resonance curve.

— The sensitivity improves with the decrease of r (see [1]). It is then necessary to work with high Q-factor.

— We have found that, by putting 1000 pF in parallel to the cable (10 m cable-70 pF/m), the amplitude of the modulated signal was not modified.

— By varying the working frequency by 15%, the modulated signal proved to be constant within the precision of our measurements (2%).

Furthermore it is possible to perform a readjustment of the frequency up to 15%, if the resonance frequency changes because of thermal effects, without a recalibration of the amplitude.

RIASSUNTO

Viene descritto uno strumento per la misura di variazioni rapide di pressione da usarsi nella tecnica delle camere a bolle a idrogeno liquido. Le sue caratteristiche sono risposta rapida e lineare, indipendenza del segnale d'uscita dalle variazioni di capacità del cavo, possibilità di regolazione a distanza e semplicità nel circuito di rivelazione.

IL NUOVO CIMENTO Vol. XI, N. 4 16 Febbraio 1959

On a 200 keV Radiofrequency Deuteron Accelerator of the Cockcroft and Walton Type.

F. Demanins and G. Poiani

Istituto di Fisica dell'Università - Trieste
Istituto Nazionale di Fisica Nucleare - Sottosezione di Trieste

(ricevuto il 24 Novembre 1958)

Summary. — A description is given of a deuteron accelerator of 200 keV for the production of neutrons through the d-d and d-t reactions. It is pointed out that its principal characteristic is that high tension is obtained by means of a radiofrequency voltage multipliyng circuit.

1. – Introduction.

Recently the improvement of the technique for accelerating deuterons has made it frequently possible to use fast monoenergetical neutron beams obtained from the exothermic reactions $^2H(d, n)^3He$ and $^3H(d, n)^4He$.

The accelerators commonly used for this purposes are of the voltage multiplying type which, as is well known, are based on the original Greinacher circuit [1], successively improved by Cockcroft and Walton [2].

Because of the use to which they are expected to be employed, a strict definition in the energy of the ions and a very small value in the ripple is not important. Therefore they may be constructed with generators of alternating current at industrial frequency.

However, as shown by Lorrain [3], the use of high frequencies to feed the multiplier presents many advantages. First of all a sensible economy can be achieved in the project of the capacitors, then the size can be reduced and furthermore it makes it possible to increase considerably the number

(1) H. Greinacher: *Zeits. f. Phys.*, **4**, 195 (1921).
(2) J. D. Cockcroft and E. T. S. Walton: *Proc. Roy. Soc.*, A **136**, 619 (1932).
(3) P. Lorrain: *Rev. Sci. Instr.*, **20**, 216 (1949).

of stages in the cascade. Another advantage, which has not a negligible practical importance, arises from the fact that the filaments of the rectifying diodes can be fed directly with the radiofrequency itself.

Of course the increase of the working frequency, brings about some disadvantages such as, for instance, the requirement of a somewhat more elaborated generator with respect to the one used in the low frequency set up, but nevertheless similar to the electronic feedings used at low frequency, also because of their easy regulation.

Another disadvantage is the increased influence of stray capacitances among the parts of the multiplier and the consequent occurrence of stray currents along the cascade columns of the multiplier. It has to be remarked that this circumstance practically prevents the use of the conventional multiplying scheme when the number of stages is very large.

However, since it is possible to use parts easily obtained on the ordinary market at a comparatively low price, the use of high frequency becomes advisable for constructing a tube accelerating the ions up to the energy of some hundred keV. Apart from economical reasons, this is indeed possible because a perfect stabilization is obtained with rather simple circuits.

With the aim in view of using a source of monoenergetic neutrons either for research or for teaching purposes, a cheap, small deuteron accelerator has been constructed in this Institute.

2. – The voltage generator.

The usual layout of the voltage multiplying circuit is not very suitable when the feeding frequency is high. This, as already pointed out, is in particular due to the existence of stray currents which bring about a voltage decrease even when one has no load current.

The Everhart and Lorrain theory (4) leads to the following formula for the voltage efficiency F:

$$F = \frac{b}{N} \operatorname{tgh} \frac{N}{b}, \tag{1}$$

where N is the number of stages in the multiplying circuit and b^2 is the ratio between the real capacitance for the stage C_s and the stray capacitance for the stage C, so that the output voltage effectively obtainable is the ideal voltage multiplied by F.

Several methods have been suggested for increasing the factor F. Particularly interesting is the method consisting in load inductances put at the low and high voltage terminals of the multiplying circuit (5). The one at low voltage is nothing but the secondary winding of the input transformer earthed in the middle. Corrispondingly the utilizing current is derived from the middle of the high voltage inductance.

(4) E. EVERHART and P. LORRAIN: *Rev. Sci. Instr.*, **24**, 221 (1953).
(5) See ref. (4).

Such a symmetric method gives two evident advantages: it halves the voltage in the circuit of the input transformer and eliminates the ripple due to stray currents. The ripple due the load can also be reduced by tentatively shifting the high voltage connections to the corresponding inductance. In this case, the voltage efficiency improves and its expression, as calculated by Everhart and Lorrain, is formally equal to eq. (1), provided that b/N is replaced by $2b/N$. In this case the optimum value of the load inductance Q_{opt} is equal to:

$$Q_{opt} = \frac{1}{\omega^2 bC} \operatorname{cotgh} \frac{N}{2b}, \tag{2}$$

where ω represents the angular frequency of the current used.

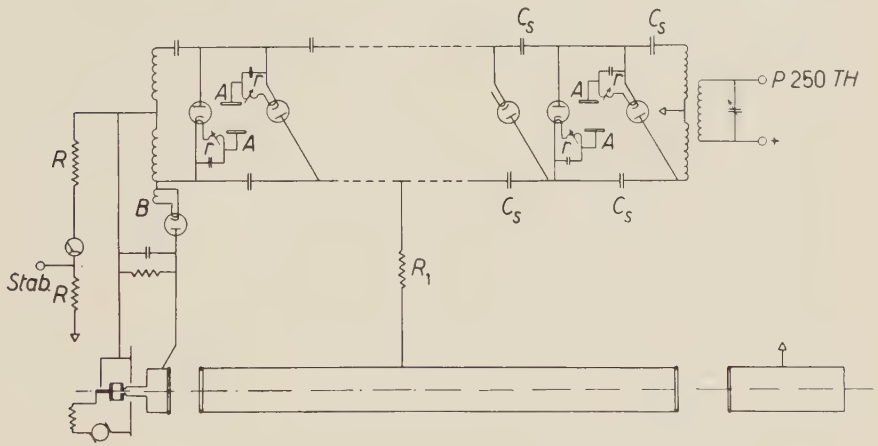

Fig. 1. – Electric scheme of the voltage generator.

The multiplying circuit of our generator, previously discussed, is of the symmetric type. Its layout is given in Fig. 1 and its electrical characteristics are listed in Table I.

TABLE I. – *Electrical characteristics of the multiplier used for the* 200 KeV *deuteron accelerator.*

Number of stages	20
Frequency	480 kHz
Capacitance of stage C_s	500 pF
Capacitance at the base of columns . .	1000 pF
Stray-capacitance for stage	1 pF
Peak input voltage	10 KV
Output voltage	200 KV
b	22.4
Voltage efficiency, F	0.94

The value chosen for the capacitances allows one to employ the normal capacitors used in television, while diodes EY 51 were chosen as rectifiers.

The use of these components gives, at the output, a working current of 0.5 mA, which is sufficient for the requirements of a normal accelerating tube.

The feeding of the multiplying circuit is supplied by a three-stage oscillator, using a 250 TH as output power tube, having the primary winding of the transformer in its anodic circuit.

The use of high frequency allows one to solve in a simple way the problem of feeding the diode filaments. As shown in Fig. 1, each filament is connected to a small resonance circuit (r), having a variable inductance connected to an antenna (A), crudely obtained from an equipotential ring of the multiplier column.

The variation of the inductance enables one to find out the most suitable intensity of the current for the required heating of the filaments.

A coil of a few turns, placed alongside the load inductance, heats an EY 51 diode which rectifies the e.m.f. obtained from suitable connections on the inductance. The rectified e.m.f. is then used for the extraction of the beam from the ion source.

To obtain a greater stability in the working of the multiplier a current of 100 μA is continuously derived by means of an ohmic resistor (R), made up by 200 resistences of 10 Mohm each, and placed in a column of paraffin oil.

Using the decrease of voltage brought about by this resistor, a signal is derived for stabilizing the high voltage of the circuit. A stabilization of the output voltage of the order of 1‰ is possible provided this circuit is carefully constructed.

The feeding voltage for the lenses of the accelerating tube is derived, by means of a 20 Mohm resistance, from a link placed on one of the pulsating columns, in such a way as to give the best focusing of the beam. The RC system consisting of the resistance and the capacitance of the electrode is sufficient to equalize the radiofrequency on the electrode.

3. – The ion source and the accelerating tube.

Several types of ion sources have been carefully examined. The one which offers suitable characteristics as far as simplicity of construction and minimum of power is concerned, is the well known [6] Penning cold cathode type. The source used in the 200 keV deuteron accelerator is shown in Fig. 2. This source possesses aluminium cathodes (c), and a cylindrical anode (a), of graphite. The magnetic field is supplied by a permanent magnet (M), of alnico. The flux of deuterium comes from an electrolytic cell with automatic pressure regulation. The electric voltage for the discharge is supplied by a small converter with $(12 \div 800)$ V d.c., fed by a battery. This battery is used also for the various requirements concerned with a satisfactory working of

[6] D. KAMKE: *Handb. d. Phys.*, Vol. XXXIII (Berlin, Göttingen, Heidelberg, 1956).

the accelerator. The only detail of this source which is somewhat unusual concerns the extraction of the beam which is transversal instead of axial and is performed through a hole in the cylindrical anode.

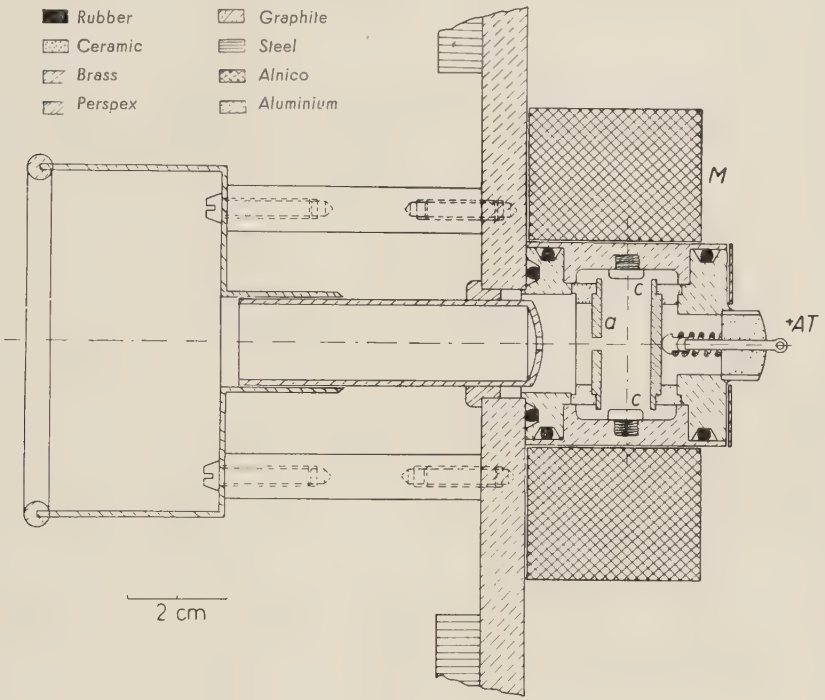

Fig. 2. – Penning ion source. Section parallel to the magnetic field.

The magnetic analysis of the beam, obtained with deuterium containing 0.5% of hydrogen has shown the following percentages for the most abundant components:

H_1^+	0.1%
D_1^+ and H_2^+	18 %
D_2^+ and H_2D^+	12 %
D_3^+	15 %
remainder	54.9%

The extraction was carried out by means of a cylindrical electrode fed with the voltage obtained by rectifying the H.V. existing on the load inductance as previously mentioned. This allows the introduction in the accelerating tube of a thin, cylindrical, slightly divergent beam of ions. The focusing and acceleration of the beam is obtained using two electrostatic and cylindrical

lenses (see Fig. 3) of the same diameter. The distance between the borders is 35 mm for the first lens and 70 mm for the second one. The beam is concentrated on the target having passed through a valve, placed in the accelerating tube in order to interrupt, when needed, the vacuum line, and through a shutter with an electromagnetic remote control.

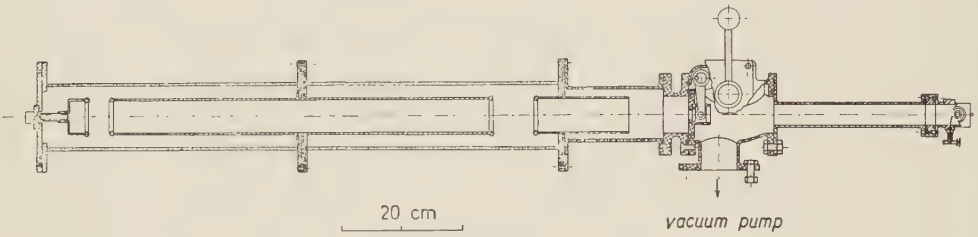

Fig. 3. – Accelerating tube.

The central cylinder of the two lenses is connected to its staff by means of regulating screws. In this way it is possible by subsequent adjustement to obtain the exact alignement of the lenses and the focusing of the beam on the target.

4. – General arrangement and accessories.

Since no sufficient room was available in height, the tube of the accelerator has been placed horizontally. The plan of this arrangement is shown in Fig. 4. The insulating staff columns of the accelerating tube and of the high voltage

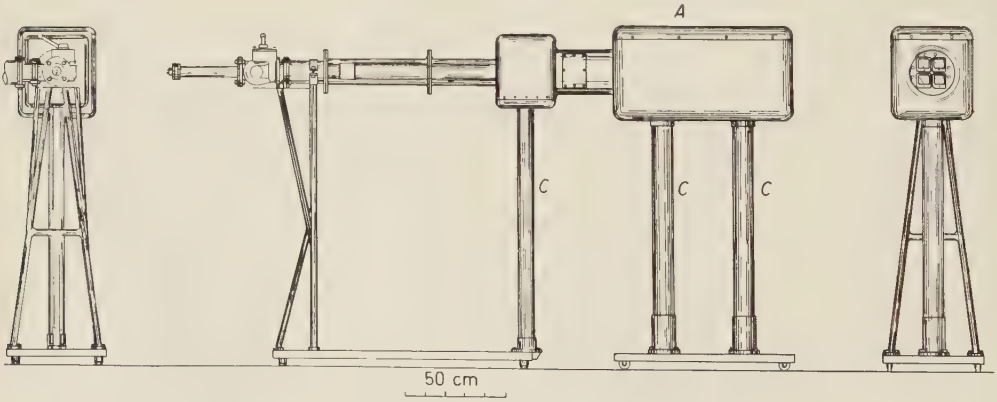

Fig. 4. – General layout of the accelerator.

screen (C) are made of perspex. Controls are carried out by means of perspex bars situated at the rear of the high voltage screen (A). On the same wall, in a suitable board mounted on the plate, are placed the control instruments concerning the source.

The vacuum plant consists in a 900 l oil diffusion pump, with a backing rotary pump. The pumping speed is sufficiently large in order to create within the tube, when the beam is on, a vacuum of $8 \cdot 10^{-6}$ mm Hg.

5. – Operational performances.

Satisfactory performance of the accelerator has been achieved during six months of continuous operation. It has been used essentially as a neutron generator by producing only d-d reactions. For this purpose, various kinds of targets have been examined, namely self targets constructed with different metals, a target of heavy ice and also a target with deuterium absorbed in zirconium. The best yield was found using the last kind of target. The neutron yield as a function of the deuteron accelerating voltage is represented in Fig. 5 (curve B). The absolute value of the yield has been derived by a comparison of a Ra-Be source, and measurements of neutron intensity have been performed with the long counter method.

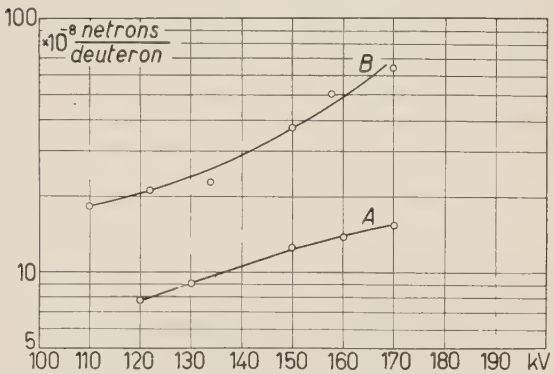

Fig. 5. – Neutron per deuteron yield as a function of the deuteron accelerating voltage. Curve B: our accelerator, deuterium in zirconium target. Curve A: yield of LADENBURG *et al.* [7] with a heavy ice target. Normalization is obtained for a current of 10^{13} deuterons s^{-1}.

In the same figure is reported the yield curve obtained by LADENBURG *et al.* [7] with a heavy ice target. Normalization has been carried out for a current of 10^{13} deuterons per second.

---

[7] R. LADENBURG and M. H. KANNER: *Phys. Rev.*, **52**, 911 (1937).

RIASSUNTO

Viene illustrato un acceleratore di deutoni da 200 keV, impiegato per la produzione di deutoni mediante la reazione d-d e d-t. Si sottolinea la caratteristica principale dell'acceleratore di avere l'alta tensione realizzata con un sistema a moltiplicazione di tensione a radiofrequenza.

IL NUOVO CIMENTO Vol. XI, N. 4 16 Febbraio 1959

A Wave-Length Shifter for Čerenkov Radiation in Water and Aqueous Lead Salt Solution.

K. Saito and K. Suga

Institute for Nuclear Study, University of Tokio - Tanashi, Tokio

(ricevuto il 3 Dicembre 1958)

Summary. — An increase factor of 4.4 in photomultiplier pulse-height was obtained by the use of pure amino G acid as a weve-length shifter for Čerenkov radiation in water. Further attempts were made to use this compound in an concentrated lead salt solution (1 M), and an increase factor of 1.8 was recorded, with the lead ion in the form of its ethylenediamine tetra-acetate (EDTA) complex.

1. – Introduction.

Only little information is available concerning wave-length shifters for Čerenkov radiation emitted in water. Heiberg and Marshal [1] suggested the use of amino G salt (sodium 2-amino-6.8-naphthalenedisulphonate) and recorded a photomultiplier pulse-height increase by a factor 1.3. Porter studied the use of β-methylumbelliferone and recorded an increase factor of 2.0 [2].

The present authors were of the opinion that an improvement of the increase factor would be expected by a closer study with reference to the purity of amino G acid, the optical properties of this solution in water, the pH and the concentration. Therefore, after examination of the optical properties of the solution under various conditions, a test for increase in pulse-height was made with a photomultiplier and an increase factor of 4.4 was obtained under the optimum condition.

Attempts were further made to utilise this compound in a concentrated lead salt solution which is used for a total-absorption Čerenkov detector [3].

---

[1] E. Heiberg and J. Marshal: *Rev. Sci. Instr.*, **27**, 618 (1956).

[2] N. A. Porter: *Nuovo Cimento*, **5**, 526 (1957).

[3] T. Matano, I. Miura, M. Oda, K. Suga, G. Tanahashi and Y. Tanaka: *I.N.S.J.*, **9** (1958) (Institute for Nuclear Study, University of Tokyo).

Although the presence of heavy metal ions decreases the intensity of fluorescence, the effect of the lead ion will be masked to a certain extent by conversion into a suitable complex compound, such as ethylenediaminetetraacetate (EDTA). In this case an increase factor of 1.8 was recorded in a 1 M lead salt solution.

2. – Experimental methods.

2·1. *Materials.* – Commercial amino G acid was recrystallized from an aqueous solution in the presence of activated charcoal. The absorption maximum and the molar extinction coefficient were in good agreement with those in the literature. Further purification did not result in an increase of the intensity of fluorescence (see Fig. 1).

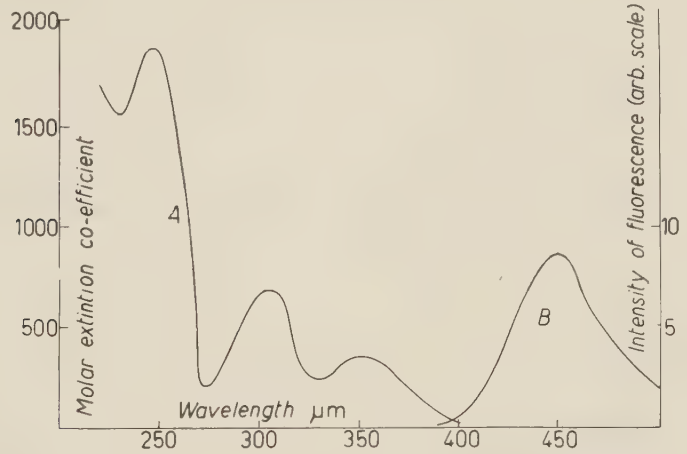

Fig. 1. – Absorption (curve A) and fluorescence (curve B) spectrum of amino G acid in water.

Lead EDTA complex was prepared from known equivalent amounts of lead hydroxide and disodium salt of EDTA. The acid-form complex (H_2PbY, Y = EDTA radical $C_{10}H_{12}O_8N_4$) was precipitated with perchloric acid and acetone, washed with a mixture of acetone and water and then with acetone, and filtered off. The product was dissolved in sodium hydroxide or aqueous ammonia solution to produce the 1 M solution (*e.g.* 250 ml) of its disodium or diammonium salt. It was essential to prepare as pure a compound as possible for a good result to be obtained.

For the fundamental test of optical properties of the amino G acid solution, the pH value was adjusted with an acetate buffer (0.2 M) and the ionic strength with sodium nitrate.

2·2. *Measurements.* – The pH value was measured with a glass-electrode pH-meter. The absorption and the fluorescence spectra were measured with

a Beckmann-type spectrophotometer (made by Hitachi Co.) with appropriate accessories.

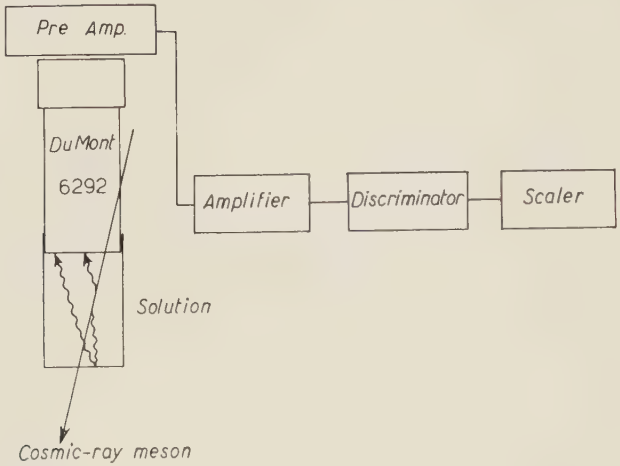

Fig. 2. – Arrangement for the measurement of the photomultiplier pulse-height.

The increase factor of the light output was measured with the aid of cosmic-ray mesons, by the use of an arrangement shown in Fig. 2. The aqueous solution of amino G acid with or without lead EDTA complex was placed in cylinder

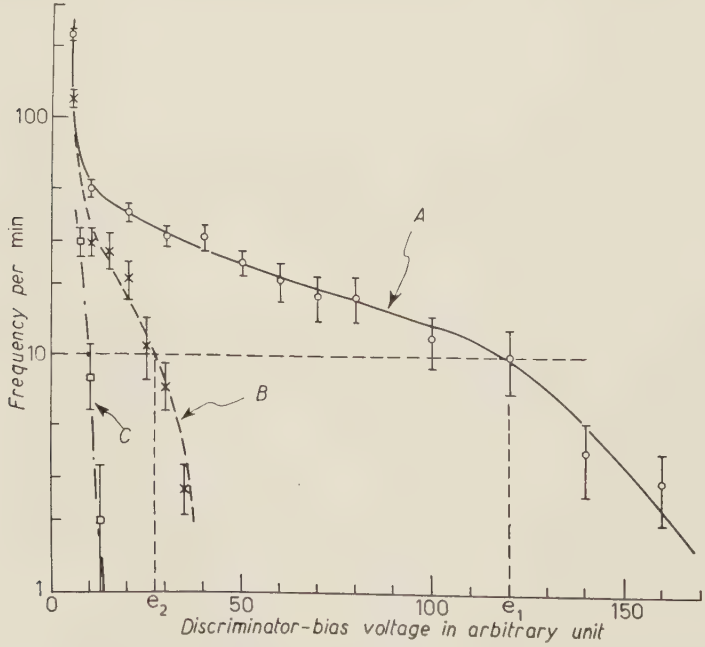

Fig. 3. – Frequency *vs.* discriminator-bias diagram. Curve *A* for aqueous solution of pure amino G acid; *B* for distilled water; *C*, noise of the photomultiplier.

(diameter 5.5 cm, length 7.5 cm) lined with titanium-white reflective paint, to optically couple with the photomultiplier (DuMont 6292). The photomultiplier output voltage pulse, with a time constant of 10 μs, was amplified by a conventional amplifier, and the pulse-height was analysed with a discriminator. Fig. 3 shows the frequency *vs.* discriminator-bias diagram. Curve *A* was obtained with aqueous solution of amino-G-acid and curve *B* with pure water, the increase factor being represented by the ratio e_1/e_2.

3. – Results and discussion.

3·1. *Use of amino-G-acid in water.* – The intensity of fluorescence of this acid markedly decreases at a pH more than nine and less than unity, the shape of the spectrum remaining unchanged. The intensity also decreases with increasing ionic strength, as shown in Fig. 4. The intensity depends on the concentration of this acid, the optimum concentration varying with the ionic strength as shown in Fig. 5.

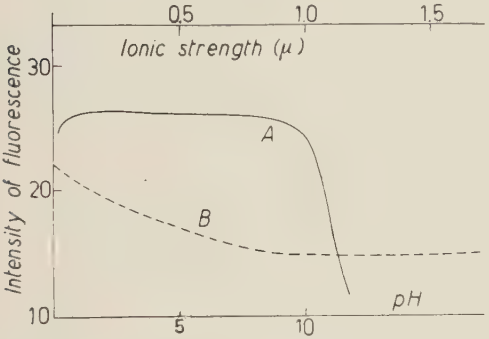

Fig. 4. – Change in intensity (arbitrary scale) of fluorescence with the pH (curve *A*) and the ionic strength (curve *B*) of the aqueous solution.

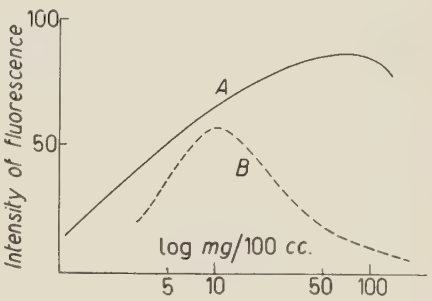

Fig. 5. – Change in intensity (arbitrary scale) of the fluorescence with the concentration of amino G acid in water (curve *A*) and in an aqueous solution of $\mu = 1$ (curve *B*).

Aqueous solution of amino-G-acid (a few hundred milligrams per litre) has a pH value near 3 and can be used as wave-length shifter without buffer. The maximum increase factor amounts to 4.4 in the absence of dissolved oxygen; the extent to which the pulse-height increases is largely affected by oxygen. The results are summarized in Table I. The pulse-height decreases on prolonged storage, presumably owing to dissolution of atmospheric oxygen; the deteriorated solution does not recover the initial activity even after the removal of dissolved oxygen. When kept sealed, however, the solution maintains its activity for months.

3·2. *Use of amino-G-acid in the presence of a large amount of lead.* – For the aqueous amino-G-acid solution to be used as a total-absorption Čerenkov detector, a large amount of lead should be present in water to increase the

radiation length of the material. Although the lead ion quenches the fluorescence of this acid to a marked extent, this action is suppressed by converting the lead ion into stable lead EDTA complex. Since the degree of dissociation of the complex decreases with increasing pH, the aqueous solution is made at pH 8 (with aqueous ammonia or sodium hydroxide), where amino-

TABLE I. – *Increase factor under various conditions.*

Solution	Increase factor	Condition
water + amino G acid	4.4	with nitrogen bubbling
water + amino G acid	1.7	after 3 months' storage
water + amino G acid	2.3	without nitrogen bubbling
water + amino G acid + $(NH_4)_2PbY$	1.8	with nitrogen bubbling
water + amino G acid + Na_2PbY	1.5	with nitrogen bubbling
water + amino G acid + Na_2PbY	1.2	without nitrogen bubbling
water (standard)	1.0	distilled water

Concentration of amino G acid, 200 mg per litre; concentration of the lead salt, ca. 1 M; Y stands for ethylenediaminetetraacetate radical.

G-acid still exhibits an intense fluorescence (see Fig. 4). The results shown in Table I indicate that the increase factor (1.8 with ammonium salt and 1.5 with sodium salt) is not so great as in the absence of lead, but it is quite significant and very useful for practical purposes.

3·3. *The verification of the role of amino-G-acid as a wave-length shifter and the decay time.* – Although the amount of the direct fluorescence is expected to be very small from the slight amount of this acid in water, its participation was measured in the following procedure. A very intense source of ^{210}Po, free from its parent activity (*), was added to the solution and the light emitted by this solution was similarly measured. It was found that the amount of direct scintillation light is less than a few percent of the total light from the

(*) Carrier-free ^{210}Po was distilled from 0.1 N nitric acid solution of RaD in the presence of diphenylcarbazide ([4]), into 1 N hydrochloric acid, which was, after distillation, evaporated with a small amount of hydrogen peroxide.

([4]) K. KIMURA and H. MABUCHI: *Bull. Chem. Soc. Japan*, **28**, 535 (1955).

solution. Therefore, though the detector involving the use of amino-G-acid loses the directional property, it preserves the role of a velocity discriminator.

Further examination was made to find whether such a detector is suitable for fast detection of particles. The current pulse of the photomultiplier which received the light from the solution was displayed on a Tektronics 545 synchroscope. The decay time was estimated to be less than $2 \cdot 10^{-8}$ s. The real value of the decay time was not determined from the above procedure, but the solution is suitable for fast detection of particles.

RIASSUNTO (*)

Usando G-aminoacido puro per spostare la lunghezza d'onda si è ottenuto l'aumento per un fattore di 4.4 della radiazione Čerenkov nell'acqua. In ulteriori tentativi di usare detto composto sotto forma di una soluzione concentrata del suo sale di piombo (1 M) si è registrato un aumento per un fattore 1.8, collo ione piombo in forma del suo complesso etilendiamminatetracetato (EDTA).

(*) *Traduzione a cura della Redazione.*

LETTERE ALLA REDAZIONE

(La responsabilità scientifica degli scritti inseriti in questa rubrica è completamente lasciata dalla Direzione del periodico ai singoli autori)

Associated Production by Non-Local Interaction.

S. N. Biswas (*)

Department of Theoretical Physics,
Indian Association for the Cultivation of Science - Calcutta

(ricevuto il 14 Luglio 1958)

The observed associated production of the K-mesons and Λ-hyperons from the meson-nucleon interaction in $T=\frac{1}{2}$ state may be obtained from the following two Feynman diagrams.

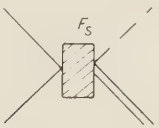

Fig. 1

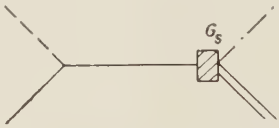

Fig. 2

——— nucleon line. —·—·— K-meson line.
····· meson line. ═══ hyperon line.

In the above diagrams the shaded area G_s in Fig. 1 denotes the 3-body non-local (N-K-Λ) interaction and F_s in Fig. 2 indicates a direct 4-body non-local (π-N-K-Λ) interaction.

One way of introducing the above 3 and 4-body non-local interaction is to assume a compound hypothesis for K-mesons and Λ-hyperons and accordingly suggest that the K-meson may be an excited bound state of two pions and the Λ-hyperon is composed of a nucleon and a pion. In a recent paper [1] the present author has introduced such a composite model for K-mesons and on the basis of the solution all the observed phenomena including that of associated production could well be explained. Similar conclusions were also obtained from the meson-nucleon compound system for the hyperon introduced first by Fermi, Feynman, Green and from detailed

(*) Now at Tata Institute for Fundamental Research, Bombay.
(1) S. N. Biswas: *Nuovo Cimento*, **7**, 577 (1958).

calculations by MacCarthy (2). The nature of the wave function for the composite model suggests that one may also assume the particle as elementary, having a structural co-ordinate as suggested by Yukawa (3) for other elementary particles. It should be mentioned that the model suggested here is not the only one of its kind; one can also use Sakata's interesting compound model (4).

Assuming pure pseudoscalar meson-nucleon interaction we will find the nature of the interaction G_s and F_s and it turns out that G_s and F_s are non-local but covariant depending upon the four-momenta of the interacting particles and are also spin dependent. The existence of a spin-dependent term shows that the K-particle may be produced in parity-mixture states. In the extreme relativistic region, however, the spin-dependent term disappears but the interaction still remains non-local.

In the following we will calculate G_s from the following simplest Feynman diagram assuming strangeness conservation as well as charge conservation.

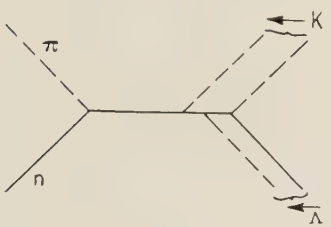

Fig. 3

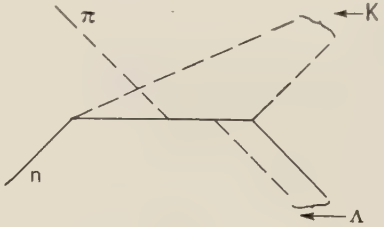

Fig. 4

It should be pointed out that the explicit determination of G_s requires a knowledge of the internal structure of both the K and Λ-particle. As a trial function we introduce the momentum distribution of the form

$$N\theta(l) = N'\Lambda(l) = \{l^4 - \mu^4\}^{-1},$$

for θ-and Λ-particles; l is the variable four-momentum of the particle concerned, μ is the meson mass, and N, N' are the normalization constants. Following Feynman we have from Fig. 3 for G_s.

$$(1) \qquad G_s = G^3\{(2\pi)^4 i\}^2 \iint \tau_j\gamma_5 S(2p - q - p_1)\tau_k\gamma_5 S(p - p_1 - r)\tau_1\gamma_5\theta(2p_1)\Lambda(2r)\,\mathrm{d}^4p_1\,\mathrm{d}^4r\,,$$

where G is the ordinary pion-nucleon coupling constant, τ's are as usual the isotopic spin-matrices and $S(p)$ stands for the nucleon propagator $2p - k$, $2p - 2q$, k and $2q$ are the four-momenta of the nucleon, hyperon, pion and K-meson respectively.

The determination of the normalization constants N and N' can be effected by noting that the equation satisfied by (1) has the form

$$\varphi(k) = \lambda' \int K(k, l)\varphi(l)\,\mathrm{d}^4l\,,$$

(2) I. E. MacCarthy: *Ph. D. Thesis* (Adelaide University, 1955; unpublished).
(3) H. Yukawa: *Phys. Rev.*, **77**, 219 (1956).
(4) S. Sakata: *Progr. Theor. Phys.*, **16**, 686 (1950).

with

$$K(k, l) = (k^4 - \mu^4)^{-1}(l^4 - \mu^4)^{-1} \qquad \text{and} \qquad \frac{i\lambda'}{(2\pi)^4}\int (l^4 - \mu^4)^{-2}\, \mathrm{d}^4 l = 1\,,$$

and using the normalization condition ([1]) for the wave equation, we have from (1)

$$G_s \to f\gamma_5(A + Bp_\mu\gamma^\mu)\,, \tag{2}$$

with

$$f = \tau_j\tau_k\tau_l(2M_\theta M_\Lambda G^3)/(2\pi)(r_1 r_2)^2; \qquad r_1 = M_\theta/\mu, \qquad r_2 = M_\Lambda/\mu\,,$$

M_θ and M_Λ are the K-meson and Λ-hyperon mass respectively.

$$A = \{p\cdot q - 5p^2/4\}/(2p)^4 + \tfrac{1}{4}m(M_\Lambda - m)/(2p)^4, \qquad \text{and} \qquad B = \tfrac{1}{4}M_\Lambda(2p)^{-4}\,.$$

The result (2) shows that the interaction G_s is non-local depending on the momentum of the interacting particles. The interaction is thus in general a mixture of (ps) scalar and (pv) vector-type fields. If, however, we make an extreme relativistic approximation by neglecting the masses of the nucleon and hyperon compared to the high incident energy of the meson the interaction is purely pseudoscalar but non-local. The appearance of the scalar and the spin-dependent terms shows that the K-meson may be produced with even or odd integer spin. That is to say that the K-meson is produced in a parity-mixture state. The same may be true of the Λ-particle. We have at the extreme relativistic energy the production cross section of the θ-particle using the diagram of Fig. 1 having a pure pseudoscalar interaction of the type $fA\gamma_5$:

$$\sigma = \frac{2r_0^2 G^8}{\pi\omega_1^2}\left\{\frac{4}{3}\left(\frac{\omega_2}{\omega_1}\right)^4 - \frac{5}{2}\left(\frac{\omega_2}{\omega_1}\right)^3 + \frac{25}{16}\left(\frac{\omega_2}{\omega_1}\right)^2\right\}, \tag{3}$$

where $r_0 = (M_\theta M_\Lambda)/\omega_1^2 r_1^2 r_2^2$.

ω_1 and ω_2 are the incident pion and final K-meson energies respectively. For a 1.4 GeV incident pion and using the pseudoscalar pion-nucleon coupling constant $G^2 \approx 12$ we have the total production cross section,

$$\sigma = .7264 \cdot 10^{-27}\ \mathrm{cm}^2\,.$$

the experimentally determined value being ≈ 1 mb.

A similar calculation can be made for F_s from the Feynman diagram Fig. 4: the conclusions are on similar lines. A detailed calculation involving all possible Feynman diagrams for the associated production of the strange particles will soon be reported.

* * *

The author is grateful to Prof. Basu for giving him the opportunity to work in his department and for discussion from time to time. He is also grateful to Prof. H. S. Green for a stimulating discussion on strange particles while the author was a Research Fellow of the Adelaide University during 1956-57.

Neutron Capture Gamma-Rays of Iodine, Iridium and Cerium.

R. Balzer, H. Knoepfel, J. Lang, R. Müller and P. Stoll
Federal Institute of Technology - Zürich

(ricevuto il 10 Novembre 1958)

We have investigated (n, γ)-spectra of several elements at the Swimmingpool-Reactor « Saphir » in Würenlingen [1]. For the energy range above 3 MeV a pair-spectrometer of high intensity was used [2]. The γ-rays below 3 MeV were determined by a gray wedge spectrometer [3].

1. – Measurements with the pair-spectrometer.

1·1. *Iodine.* – The upper part of the measured spectrum (deduced background and random coincidences) of the reaction $^{127}I(n, \gamma)^{128}I$ is shown in Fig. 1. The

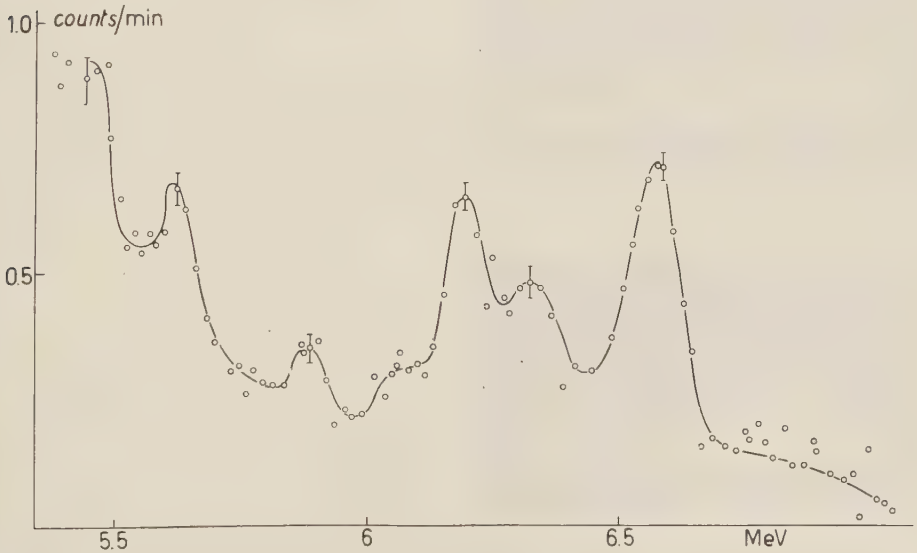

Fig. 1.

[1] H. Knoepfel, Ch. Menoud and P. Stoll: *Helv. Phys. Acta*, **31**, 330 (1958).
[2] R. Balzer, H. Knoepfel, P. Stoll and W. Wölfli: *Helv. Phys. Acta*, **31**, 328 (1958).
[3] D. Maeder: *Nucl. Instr.*, **2**, 299 (1958).

ordinates are reduced to « weight one », that means, that depending on the counting channel, we actually have measured 5 to 9 times more counts per minutes as given in the figure. The target consisted of 1.5 kg of pure Iodine enclosed in a polyethylene container. The spectrum was evaluated by resolving it to single lines ([4]), the shape of which has been determined experimentally with Fe, Ti and Ni-lines. We found γ-rays with following energies:

a) (6.71 $\pm$ 0.02) MeV (neutron binding energy);
b) (6.45 $\pm$ 0.03) MeV; *c*) (6.29 $\pm$ 0.03) MeV;
d) (6.16 $\pm$ 0.04) MeV (?); *e*) (5.99 $\pm$ 0.03) MeV;
f) (5.75 $\pm$ 0.03) MeV; *g*) (5.57 $\pm$ 0.03) MeV.

1·2. *Iridium.* – The measurement was performed with 40 g of pure Iridium (Isotopes: ^{191}Ir and ^{193}Ir). The counting rate was higher than for the Iodine probe and therefore the statistic better. The mean width of the lines is 110 keV. For the natural isotope mixture we have measured the following γ-ray energies of ^{192}Ir and ^{191}Ir:

a) (6.085 $\pm$ 0.015) MeV; *b*) (5.98 $\pm$ 0.02) MeV; *c*) (5.92 $\pm$ 0.03) MeV;
d) (5.77 $\pm$ 0.03) MeV; *e*) (5.67 $\pm$ 0.03) MeV; *f*) (5.59 $\pm$ 0.04) MeV (?);
g) (5.48 $\pm$ 0.04) MeV (?); *h*) (5.34 $\pm$ 0.03) MeV.

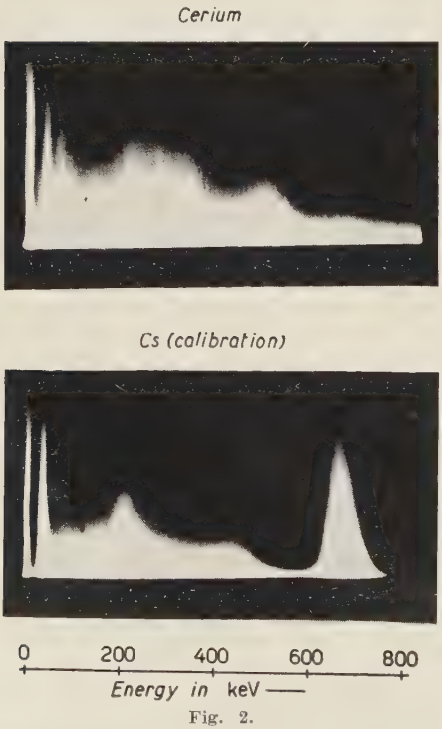

Fig. 2.

2. – Measurements with the gray wedge spectrometer.

2·1. *Cerium.* – Fig. 2 shows a photograph of the Ce(n, γ)-spectrum, as it was taken with our crystal-spectrometer. For comparison and calibration the Cesium spectrum is also shown. Our results are:

(1170 $\pm$ 20) keV,
(940 $\pm$ 20) keV,
(671 $\pm$ 10) keV,
(504 $\pm$ 10) keV (annihilation),
(344 $\pm$ 8) keV,
(277 $\pm$ 8) keV,
(217 $\pm$ 6) keV,
(88 $\pm$ 6) keV,
(72 $\pm$ 4) keV (Pb+Bi, X-ray?),
(38 $\pm$ 3) keV (Ce, X-ray?).

([4]) B. B. KINSEY, and G. A. BARTHOLOMEV: *Can. Journ. of Phys.*, **31**, 537 (1953).

2·2. *Iodine.* – This element has been measured for low energies by other authors ([5,6]), but their results are contradictory. We found the following γ-rays:

(652±20) keV,	(501±10) keV (annihilation),
(435±15) keV,	(260±15) keV,
(130±10) keV,	(75± 8) keV (Pb+Bi, X-rays).

We confirm the 130 keV line, but concerning the intensity, this line is not stronger as the one of 260 keV, in contradiction with ([6]). We can not find the 85 keV γ-ray ([5]), because it is covered by the X-ray of Pb and Bi (from the collimator). The new lines at 435 keV and 652 keV are probably due to inelastic neutron scattering, as measured by ([7]), because of the still high epithermal neutron flux in the target region (cfr. ([1])).

The discussion about the measured spectra and the absolute intensities of the different lines follows together with the description of the γ pair-spectrometer in a later publication.

([5]) M. Reier and M. G. Shamos: *Phys. Rev.*, **100**, 1302 (1955).

([6]) I. V. Estulin, L. F. Kalinkin and A. S. Melioransky: *Nucl. Phys.*, **4**, 91 (1957), *Soviet Phys. Journ. Exp. Theor. Phys.*, **4**, 752 (1957).

([7]) D. A. Lind, R. B. Day and R. M. Kloepper: *Bull. Am. Phys. Soc.*, **2**, no. 6, 309, H 5.

IL NUOVO CIMENTO Vol. XI, N. 4 16 Febbraio 1959

A Possible Parity Assignment for Strange Particles and a New Kind of Heavy Meson.

H. Katsumori

Department of Physics, Osaka Gakugei University - Osaka

(ricevuto il 14 Gennaio 1959)

The possibility was suggested, in our previous report [1], that the observed level ordering of baryon masses can be explained in the lowest order approximation, assigning the opposite parities between N and Ξ (case (*a*)), or the opposite parities between Λ and Σ as well as between N and Ξ (case (*b*)). It was assumed that the baryons are Dirac particles and the K-meson is a spinless particle, and the interaction Lagrangian is given by d'Espagnat and Prentki's charge independent interaction [2] with common coupling constants g_{K} and g_{π} for K- and π-couplings respectively.

It goes without saying that there is another possibility to explain the baryon mass levels apart from such a parity assignment, assuming different coupling constants for the different interaction terms instead of the common g_{K} and the common g_{π}. Since only the first approximation starting with an hypothetical world, where the strong interactions are absent, has been considered in our previous and the present reports, all the K- and π-coupling constants are assumed to be equal to the unrenormalized g_{K} and g_{π} respectively, and moreover the masses of all baryons appearing in the real and virtual states are assumed to equal the unrenormalized (degenerate) baryon mass.

It has been further shown [3] that the numerical estimate, of the baryon mass levels according to our proposal, is not inconsistent with the observation, when the reasonable magnitudes of coupling constant g_{K} and of cut-off momentum are used. It should be noted that the correct direction of level splittings $\Xi - (\Sigma, \Lambda) - \mathrm{N}$ and the approximately correct interval ratio $[M(\Xi) - M(\Sigma, \Lambda)]/[M(\Sigma, \Lambda) - M(\mathrm{N})] = 1$ are obtained from only the K-coupling assuming the above parity assignment (*a*) or (*b*), and these features are independent of the magnitude of cut-off momentum. However, as to the numerical estimate of the Σ-Λ mass difference for case (*b*), the consistency is not so good and therefore it is difficult to know whether the Σ-Λ mass

(1) H. Katsumori: *Memoirs of the Osaka Gakugei Univ.*, B, no. 6, 48 (1957); *Progr. Theor. Phys.* (*Japan*), **19**, 342 (1958).

(2) B. d'Espagnat and J. Prentki: *Nucl. Phys.*, **1**, 33 (1956).

(3) H. Katsumori and K. Shimoura: *Progr. Theor. Phys.* (*Japan*), **20**, 578 (1958).

difference comes mainly from the lowest order effect of π-coupling or from the higher order effect of K-coupling or from both. In spite of such ambiguousness, the assignment (*b*) seems to be favorable, because the lowest order self energies for the case (*b*) give the level splittings $M(\Sigma) - M(\Lambda)$ as well as $M(\Xi) - M(\mathrm{N})$ with the correct directions. This calculation has been carried out using the d'Espagnat and Prentki interactions for the case (*b*),

$$(1) \qquad L_{\mathrm{K}} = g_{\mathrm{K}}[\bar{\mathrm{N}}\boldsymbol{\tau}\cdot\boldsymbol{\Sigma}\mathrm{K} + \bar{\mathrm{N}}(i\gamma_5)\Lambda\mathrm{K} + \bar{\Xi}(i\gamma_5)\tau_2\boldsymbol{\tau}\cdot\boldsymbol{\Sigma}\mathrm{K}^* + \bar{\Xi}\tau_2\Lambda\mathrm{K}^*] + \mathrm{H.C.},$$

$$(2) \qquad L_{\pi} = g_{\pi}[\bar{\mathrm{N}}(i\gamma_5)\boldsymbol{\tau}\cdot\boldsymbol{\pi}\mathrm{N} + \bar{\Xi}(i\gamma_5)\boldsymbol{\tau}\cdot\boldsymbol{\pi}\Xi + (i\boldsymbol{\Sigma}(i\gamma_5)\times\boldsymbol{\Sigma})\cdot\boldsymbol{\pi} + (\bar{\Lambda}\boldsymbol{\Sigma}\cdot\boldsymbol{\pi} + \mathrm{H.C.})].$$

The validity of this type of interactions, especially L_{K}, ought to be experimentally tested in the future by the baryon-K scattering or the hyperon production (*).

Now it should be interesting to conjecture why both the relative parity between N and Ξ and that between Λ and Σ happen to be odd. As has been pointed out by Tiomno and Yang [4], there are four kinds of spinor transformation under space reflection,

$$(3) \qquad \psi \to \eta_R\gamma_4\psi\,, \qquad \eta_R = \pm i\,, \qquad \pm 1\,.$$

Then it seems tempting to speculate that each type of the spinor fields should have an equal right for existence in the natural world and that the four kinds η_R's ($\pm i$, ± 1) just correspond to the « four » kinds of existing baryons which would degenerate in the limit of vanishing strong interaction. According to this conjecture, the following is the desired parity assignment,

$$(4) \qquad \begin{cases} \eta_R = \pm i & \text{for } (\mathrm{N}, \Xi)\,, & \pm i & \text{for } (\mathrm{N}^C, \Xi^C) \\ \eta_R = \pm 1 & \text{for } (\Lambda, \Sigma)\,, & \mp 1 & \text{for } (\Lambda^C, \Sigma^C) \end{cases}$$

or

$$(4') \qquad \begin{cases} \eta_R = \pm 1 & \text{for } (\mathrm{N}, \Xi)\,, & \mp 1 & \text{for } (\mathrm{N}^C, \Xi^C) \\ \eta_R = \pm i & \text{for } (\Lambda, \Sigma)\,, & \pm i & \text{for } (\Lambda^C, \Sigma^C) \end{cases}$$

where a superscript C indicates the charge conjugate of the corresponding baryon. In the interaction Lagrangian L_{K}, (1), it was assumed that all the baryon fields have either $\eta_R = \pm 1$ or $\pm i$, and therefore the K-meson field transforms as $\mathrm{K} \to \pm\,\mathrm{K}$ under space reflection. On the contrary, if the parity assignment (4) or (4′) is taken, the transformation $\mathrm{K} \to \pm\, i\mathrm{K}$ under space reflection must be assumed. When this parity assignment is used, one has to introduce a new kind of heavy meson field, which is called as K′ hereafter, in order that our previous argument on the mass level splitting similarly applies. The K′ field is introduced as a second kind isospinor and couples with Ξ (but not with N), while the K field is a first kind isospinor and couples with N (but not with Ξ). The assumption is made that $\mathrm{K}'^{(-,0)}$ and $\mathrm{K}^{C(-,0)}$ (therefore $\mathrm{K}'^{C(+,0)}$ and $\mathrm{K}^{(+,0)}$) are not the same particles but have opposite parities.

---

(4) C. N. Yang and J. Tiomno: *Phys. Rev.*, **79**, 495 (1950).

(*) After this report has been written, S. Barshay's recent article [*Phys. Rev. Lett.*, **1**, 97 (1958)] has reached us. He points out that the analysis of hyperon production and K-N scattering experiments may give an indirect support not only for the opposite parities between Λ and Σ but also for the coupling types of (ΛNK), (ΣNK) and ($\Sigma\Lambda\pi$) interactions in our equations (1) and (2).

In the following the assignment (4) is chosen instead of (4′), since (4′) leads to the same space parity (η_R) and the same isospace parity (η_I) [5] for N and Ξ^C (therefore also for N^C and Ξ). As it is a matter of convention whether $\eta_R = \pm 1$ or ∓ 1 is chosen for Σ and Λ (therefore $\eta_R = \pm i$ or $\mp i$ for K, K′ and K^C, K'^C), the former one is chosen here. η_R for bosons is defined by the transformation $\varphi \to \eta_R \varphi$ under space reflection. The thus specified parities for all the baryons and all the mesons are listed in Table I (*). For the sake of comparison, the isoparity η_I which is defined by the transformations $\psi \to \eta_I \psi$ and $\varphi \to \eta_I \varphi$ under isospace reflection is also added in the table. This table seems to suggest a close connection between ordinary space parity and isoparity. Furthermore the charge singlet pion field (π') is included in the table, which was never detected experimentally but its existence was proposed by several authors [6-8]. It seems interesting to note that, if a scalar π' is introduced, the four kinds of mesons π, π', K and K'^C correspond to the four possible η_R's (± 1, $\pm i$) for the bosons just like for the baryons.

TABLE I.

	η_R	η_I		η_R	η_I
$N^{(+,0)}$	i	i	$N^{C(-,0)}$	i	$-i$
$\Xi^{(-,0)}$	$-i$	$-i$	$\Xi^{C(+,0)}$	$-i$	i
$\Sigma^{(+,0,-)}$	1	1	$\Xi^{C(-,0,+)}$	-1	1
$\Lambda^{(0)}$	-1	1	$\Lambda^{C(0)}$	1	1
$\pi^{(+,0,-)}$	-1	1	$\pi^{C(-,0,+)}$	-1	1
$(\pi'^{(0)})$	(1)	(1)	$(\pi'^{C(0)})$	(1)	(1)
$K^{(+,0)}$	i	i	$K^{C(-,0)}$	$-i$	$-i$
$K'^{(-,0)}$	i	$-i$	$K'^{C(+,0)}$	$-i$	i

Now the parity conserving interaction Lagrangian L_K is written as

$$L_K = g_K[\bar{N}\boldsymbol{\tau}\cdot\boldsymbol{\Sigma}K + \bar{N}(i\gamma_5)\Lambda K + \bar{\Xi}(i\gamma_5)\boldsymbol{\tau}\cdot\boldsymbol{\Sigma}K' + \bar{\Xi}\Lambda K'] + \text{H. C.}, \tag{5}$$

which also gives us a similar mass splitting as before. Within the Yukawa type baryon-meson direct interaction, the charge independence and parity conservation would lead to additional interaction terms like

$$g_K[\bar{N}\tau_2\Lambda K'^* + \bar{N}(i\gamma_5)\tau_i\boldsymbol{\tau}\cdot\boldsymbol{\Sigma}K'^* + \bar{\Xi}(i\gamma_5)\tau_2\Lambda K^* + \bar{\Xi}\tau_2\boldsymbol{\tau}\cdot\boldsymbol{\Sigma}K^*] + \text{H. C.}.$$

---

[5] G. RACAH: *Nucl. Phys.*, **1**, 302 (1956).

(*) After this report has been written, F. GÜRSEY's recent article [*Phys. Rev. Lett.*, **1**, 98 (1958)] has reached us. He has discussed a connection between strangeness and parity, assuming a parity assignment similar to that we have used here. The coupling type of his Lagrangian L_K is, however, different from ours at the ($\Xi\Sigma K$) and ($\Xi\Lambda K$) terms, and it does not lead to the N-Ξ mass splitting as far as the common g_K is used and unless the K' field is introduced.

[6] M. GELL-MANN: *Phys. Rev.*, **106**, 1296 (1957).

[7] Y. NAMBU: *Phys. Rev.*, **103**, 1366 (1957).

[8] J. SCHWINGER: *Ann. of Phys.*, **2**, 407 (1957).

These terms, however, contradict the foregoing assumption that N does not couple with K', and Ξ does not couple with K. The above description may be written as a symmetrical form of a 4-dimensional isospace. If 4-isospinors and 4-isovectors are defined by

$$\Psi = \begin{pmatrix} N^+ \\ N^0 \\ i\gamma_5 \Xi^0 \\ i\gamma_5 \Xi^- \end{pmatrix}, \qquad \mathcal{K} = \begin{pmatrix} K^+ \\ K^0 \\ K'^0 \\ K'^- \end{pmatrix}, \tag{6}$$

and

$$\Sigma_\mu = (\boldsymbol{\Sigma}, i\gamma_5 \Lambda), \qquad T_\mu = (\boldsymbol{\tau}, 1),$$

the K-interaction Lagrangian L_K, which is invariant with respect to rotations in a 4-isospace, is given below:

$$L_K = g_K \overline{\Psi} T_\mu \Sigma_\mu \mathcal{K} + \text{H. C.}. \tag{7}$$

Similarly the π-interaction Lagrangian L_π may be written in a 4-isospace invariant form, if a 4-isovector Π_μ and a tensor $\Pi_{\mu\nu}$ which consist of $\boldsymbol{\pi}$ (and π' if necessary) are introduced. These Lagrangians are essentially equivalent to those of (5) and (2), and lead to the same self energies. It is clear that L_K, (7), is invariant for the simultaneous substitution, $N \leftrightarrow i\gamma_5 \Xi$ and $K \leftrightarrow K'$, but has no symmetry either between N and Ξ or between K and K', so it gives not only the N-Ξ mass splitting but also the K-K' mass splitting. The K-K' mass difference will be discussed below. L_K is also invariant for the substitution $i\gamma_5 \Lambda \leftrightarrow \boldsymbol{\tau} \cdot \boldsymbol{\Sigma}$, but has no symmetry between Λ and $\boldsymbol{\tau} \cdot \boldsymbol{\Sigma}$, and then it gives the Λ-Σ mass splitting to the higher orders, although the lowest order splitting turns out to vanish. On the other hand, L_π is invariant for the substitution $N \leftrightarrow i\gamma_5 \Xi$ and also has a symmetry between N and Ξ, so the L_π gives no mass splitting between them even to the higher orders. This L_π has no symmetry between $\delta_{\alpha\beta}\Lambda$ and $(\boldsymbol{\tau} \cdot \boldsymbol{\Sigma})_{\alpha\beta}$, and gives the Λ-Σ mass splitting even to the lowest order. As a matter of fact, the contributions arising from the cross terms of L_K and L_π might have a complicated effect on the mass splitting in the higher order approximation.

It seems that at present there is no experimental objection against the introduction of the K' field, since so far most of the experimental evidence has been concerned with K and K^0 (but not with K' and K'^0). If a Ξ-production experiment, such as

$$N + \pi \rightarrow (\Lambda \text{ or } \Sigma) + K \rightarrow \Xi + K + K',$$

is done with better statistics in the future, it will be possible to test the existence of the K' meson. Using the above L_K, the lowest order self energies of K and K' can be calculated as has been done for the baryons,

$$\begin{cases} \Delta M(K) = g_K^2 (F_{ps} + 3F_s), \\ \Delta M(K') = g_K^2 (F_s + 3F_{ps}), \end{cases} \tag{8}$$

where F_{ps} and F_s stand for the contributions from the pseudoscalar and scalar couplings respectively. Then the mass difference of K and K', which would dege-

nerate in the limit of vanishing K-baryon interaction, becomes

$$(9) \qquad M(\mathrm{K}) - M(\mathrm{K}') = 2g_{\mathrm{K}}^2 (F_{\mathrm{s}} - F_{\mathrm{ps}}) =$$

$$= \left(\frac{g_{\mathrm{K}}^2}{4\pi}\right) \frac{M}{\lambda} \frac{2}{\pi} \int_0^1 \mathrm{d}u[1 - (1-u)\lambda] \left\{ \log \frac{\varkappa + \sqrt{\varkappa^2 + 1 - u(1-u)\lambda^2}}{\sqrt{1 - u(1-u)\lambda^2}} - \frac{\varkappa}{\sqrt{\varkappa^2 + 1 - u(1-u)\lambda^2}} \right\},$$

where the straight cut-off technique has been adopted, and M is the degenerate baryon mass, $\lambda =$ (the degenerate heavy meson mass m_{K})$/M$, and $\varkappa =$ (the cut-off momentum)$/M$. Although both F_{s} and F_{ps} are quadratically divergent, the difference $F_{\mathrm{s}} - F_{\mathrm{ps}}$ is only logarithmically divergent, because coefficients of the quadratically divergent terms for both expressions are equal. Moreover, as $F_{\mathrm{s}} - F_{\mathrm{ps}}$ is always positive irrespective of the cut-off momentum, the K′ meson happens to be lighter than the K meson as far as the lowest order is concerned. Table II shows how the mass difference $M(\mathrm{K}) - M(\mathrm{K}')$ depends on the magnitude of the cut-off parameter $\varkappa$, assuming $M = 2\,000\ \mathrm{m_e}$, $m_{\mathrm{K}} = 1000\ \mathrm{m_e}$ and $g_{\mathrm{K}}^2/4\pi = 1$. If $M(\mathrm{K}')$ is smaller than $\sim 810\ \mathrm{m_e}$, K′ cannot decay into three pions. Besides the mass difference, the K and K′ mesons would show different behaviors for the scattering by nucleons and for the absorption by nuclei, etc. According to our assumption, K and K′ do not strongly couple either directly with each other or indirectly through baryons, and so γ-decay of K into K′ through strong interactions cannot take place.

TABLE II.

Cut-off parameter $\varkappa$	0.5	0.75	1.0
Mass difference: $M(\mathrm{K}) - M(\mathrm{K}')$	$67\ m_{\mathrm{e}}$	$188\ m_{\mathrm{e}}$	$346\ m_{\mathrm{e}}$
Mass of K′ meson: $M(\mathrm{K}')$	$900\ m_{\mathrm{e}}$	$779\ m_{\mathrm{e}}$	$621\ m_{\mathrm{e}}$

* * *

The author wishes to thank Dr. T. NAKANO (Osaka City University) for valuable discussions.

Direttore responsabile: G. POLVANI Tipografia Compositori - Bologna

Questo Fascicolo è stato licenziato dai torchi il 28-III-1959